Ph.D. Program in Civil, Chemical and Environmental Engineering

Curriculum in Fluid Dynamics and Environmental Engineering

Department of Civil, Chemical and Environmental Engineering

Polytechnic School, University of Genoa, Italy.

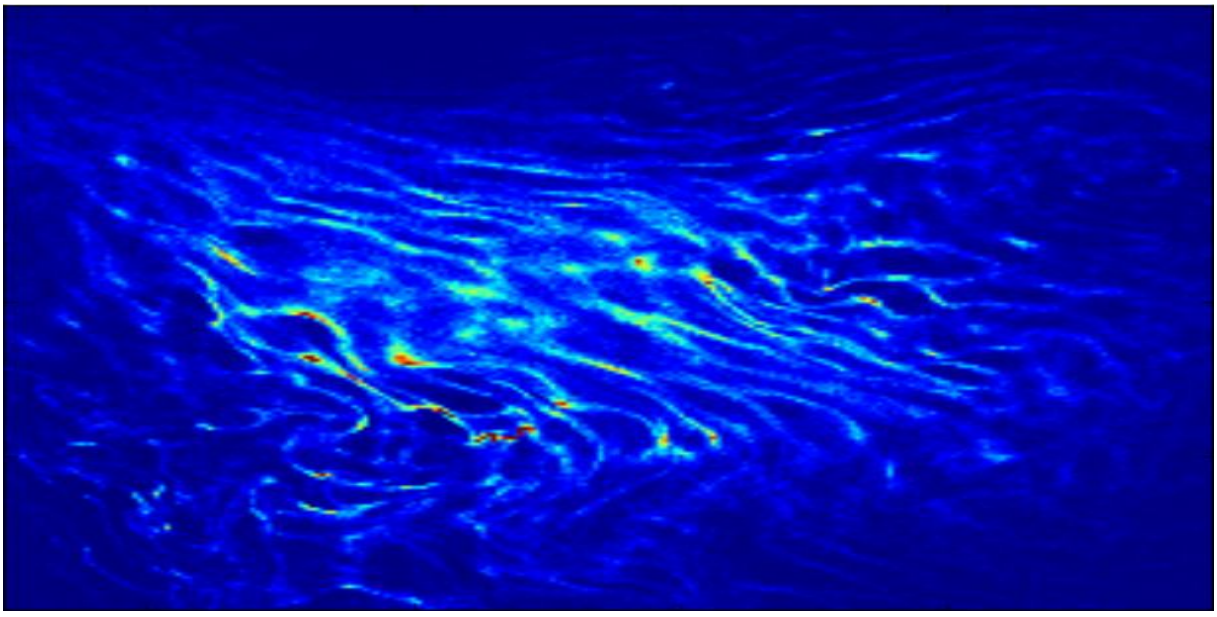

Study of statistical properties associated to transport of inertial particles and tracers

Simone Boi

STUDY OF STATISTICAL PROPERTIES

ASSOCIATED TO TRANSPORT OF

INERTIAL PARTICLES AND TRACERS

BY

SIMONE BOI

Dissertation discussed in partial fulfillment of
the requirements for the Degree of

DOCTOR OF PHILOSOPHY

Civil, Chemical and Environmental Engineering
curriculum in Fluid Dynamics and Environmental Engineering,
Department of Civil, Chemical and Environmental Engineering, University of Genoa, Italy

March, 2017

Adviser:
Prof. Andrea Mazzino – DICCA, University of Genoa

External Reviewers:
Prof. Luca Biferale – Department of Physics, University of Rome "Tor Vergata"
Prof. Mauro Sbragaglia – Department of Physics, University of Rome "Tor Vergata"

Examination Committee:
Prof. Marco Colombini – DICCA, University of Genoa
Prof. Alessandro Stocchino – DICCA, University of Genoa
Prof. Ambrogio Manzino – DIATI, Polytechnic University of Turin

Ph.D. program in Civil, Chemical and Environmental Engineering

Curriculum in Fluid Dynamics and Environmental Engineering

Cycle XXIX

ABSTRACT

A collection of results about diffusion of tracers and inertial particles in different fluid flows is proposed, by using both analytical and numerical approaches. From a numerical point of view, it is explained how to generate numerical kinetic models of turbulence. They are then exploited to prove the presence of resummation terms in the perturbation expansion at small Stokes numbers for the eddy diffusivity of inertial particles. This evidence contradicts a conjecture about an anomalous diffusion effect published in literature. Synthetic fields are also used to investigate the important issue of eddy diffusivity and its possible deterioration in the presence of a “non ideal” scale separation. Clear potential applications and implications might be in the realm of Large Eddy Simulations (LES) for atmospheric sciences. Finally, diffusion of inertial particles is tackled from an analytical point of view. Results about that include the derivation of explicit expressions for the eddy diffusivity tensor field in quasi-shear flows or at low Péclet number, as well as the generalisaton of Taylor's formula for inertial particles.

LIST OF PUBLICATIONS

[1] S. Boi, M. Martins Afonso, and A. Mazzino, Anomalous diffusion of inertial particles in random parallel flows: theory and numerics face to face, *J. Stat. Mech.: Theory and Experiment* **10**, P10023, 2015.

[2] S. Boi, A. Mazzino, G. Lacorata, Explicit expressions for eddy-diffusivity fields and effective large-scale advection in turbulent transport, *J. Fluid Mech.* **795**, 524, 2016.

[3] S. Boi, A. Mazzino, P. Muratore-Ginanneschi, Eddy diffusivities of inertial particles in random Gaussian flows, *Phys. Rev Fluids* **2**, 014602, 2017.

Contents

Introduction

The problem of stochastic/chaotic diffusion is intimately related to the problem of a particle following a random path or, equivalently, a *random walk*. Although, as we will see, it appears in many research fields concerning transport or dispersal problems, its origins were almost purely mathematical. They can be traced back to K. Pearson (Nature, 1905)[1], who posed the problem for the first time:

> *Can any of you readers refer me to a work wherein I should find a solution of the following problem, or failing the knowledge of any existing solution provide me with an original one? I should be extremely grateful for the aid in the matter. A man starts from the point 0 and walks L yards in a straight line; he then turns through any angle whatever and walks another L yards in a second straight line. He repeats this process n times. Inquire the probability that after n stretches he is at a distance between D and D +δD from his starting point 0.*

A random walk turns out to be basically a mathematical object describing a path which consists of a succession of random steps (Fig.1). The previous model, despite its clear simplicity, has got anything but trivial properties. For instance, the man (or, alternatively, the particle) will return at the starting point 0 almost surely (i. e. with probability 1) in 1 and 2 dimensions, whereas only with probability around 34% in three dimensions [2].

Examples of random walks are present in several context inlcuding Matter Physics, Chemistry, Economics, Statistical Mechanics, Fluid Dynamics and Biology: the path of a molecule travelling in a liquid or a gas, the search path of a foraging animal, stock prices and the financial status of a gambler can all be approximated by random walk models. These processes can be unbiased - that is, the proabilities of any direction are the same - or biased in the opposite situation. Bias corresponds spatially to the possibility of having an anisotropic probability distribution of the particle positions. Random walks explain the observed behaviors of those processes in those fields, providing fundamental model for the recorded stochastic activity. Notwithstanding, it is important to notice that such phenomena can actually not be stochastic in reality. We will return on this fundamental point.

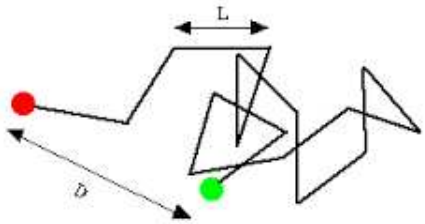

Figure 1: An example of random walk with free path L and final distance D. Image taken from www2.ess.ucla.edu

Figure 2: A Wiener process (Brownian motion) in the 2D plane. Image taken from www.reddit.com.

Once we have a well-posed definition of random walk, the parameters of the steps, such as their lengths or duration, can also be manipulated. In the simplest context the walk is in discrete time, that is a sequence of random variables $(X_1, X_2, ...)$ indexed by the natural numbers. If we let random walks take their steps at random times, the position X_t has to be defined for all times $t \in [0, +\infty]$. Specifically, these limits of random walks include the Lévy flight and diffusion models like the *Wiener process*, which corresponds to a random walk whose increments are a zero-mean Gaussian process with variance proportional to the time step itself, and then the limit for a vanishing time step is considered. Wiener process represents the corresponding mathematical model for Brownian motion (Fig. 2).

The latter will play a central role in the whole of this thesis. That constitutes – under certain conditions – the random motion of very small particles in a fluid, as a consequence of their collision with the fast-moving atoms or molecules in it. It is a transport phenomenon the botanist Robert Brown observed in 1827 for the first time. He looked through a microscope at pollen grains in water, and noted that the particles moved continuously in random directions (Fig.3).

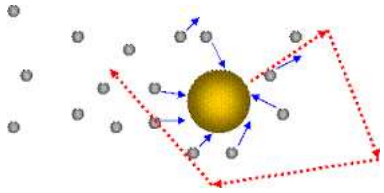

Figure 3: Sketch of the Brownian motion of a particle in a flow. Image taken from http://web2.clarkson.edu.

A first important contribution to the comprehension of this phenomenon was Albert Einstein's credit. In 1905 he explained in an article the motion that Brown had observed was ultimately a result of the collision of pollen particles with water molecules. Thanks to his work, there had been provided a simple explanation connecting the microscopic mean free path of the molecules to the macroscopic molecular diffusivity which enters into the Fick law and in the diffusion equation. The solution of the latter is the very distribution function of the Wiener process we have mentioned, that is a Gaussian distribution whose variance grows *linearly* in time. The same physical interpretation arises when we consider a *large number* - say, more than Avogadro's number - of particles in the fluid, in order to have a thermodynamic limit. In this case, indeed, the probability distribution of particles corresponds to their concentration. It is also important to notice that the diffusion equation for particles is the same as Fourier's equation, the simplest model for heat conduction. This explains well how the mathematical models for transport are ubiquitous in physics, engineering and applications.

As we have already said, the Wiener process is a model for a large number of particles in a system which is not actually a stochastic one. The importance of the stochastic models to mimick *small-scale chaos* statistics has been stated in several other results though. By way of example, a rigorous result in climate models showed that if one has a *slow system* coupled with a *sufficiently fast chaotic system*, then slow climate dynamic statistics tends to converge *in distribution* to a process whose dynamics is governed by a stochastic differential equation endowed with a white noise mimicking the fast scales [4]. It turns out thus that Wiener process and Brownian motion can be used to model not only microscopic collisions, but in general the statistics of many chaotic systems whose fast and slow dynamics are well separated.

Einstein model for Brownian motion was however too simple, and many other factors have to be taken into consideration in the majority of the situations. First of all, one has to consider that the flow itself could be not at rest on average with respect to the diffusing particles - at least, at

wavelengths comparable to the sizes of the particles. In such a situation, in a sense one has to sum the Lagrangian dynamics of the flow particles and the random contribution given by molecular collisions - or, in general, *fast dynamics*. This implies one has to solve equations like $d\boldsymbol{\mathcal{X}}(t) = \boldsymbol{v}(\boldsymbol{\mathcal{X}}, t) + \sqrt{2D_0}d\boldsymbol{W}(t)$, where $\boldsymbol{\mathcal{X}}$ is the coordinate of the particle, $\boldsymbol{v}$ the diffusing flow and the other term is the Brownian motion coupled to Einstein's molecular diffusivity. The corresponding equation for the probability density function is the well-known *advection-diffusion equation* [57]. Once again, this equation, which is called *passive scalar equation* too, is the same for dynamics in a flow of pollutant concentration or temperature.

Another element to take into consideration is the *inertia* of the diffusing particles. In principle, if one tries to interpret the above described equations as second Newton's law $\boldsymbol{F} = m\boldsymbol{a}$ for a generic particle, one notices immediately no mass term appears. This is equivalent to consider a particle with a vanishing *Stokes number* St. A more complete study of these phenomena should then start off by the second Newton law, where one eventually can insert the stochastic Brownian contribution from molecular collision or small-scale fast dynamics. This complicates the topic a lot, and a complete theory for the dynamical equation of a particle in a flow is still an open problem. Under strong assumptions, including small sizes in comparison to the minimal wavelengths of the flow, Maxey-Riley equation [30] helps us towards this direction. Many forces in this equation appear, and most of them depend strongly on the density of the particle with respect to the fluid. Due to their very complicated structure, further simplifing hypotheses can be considered. They allow one to handle them effectively and with a full control of the physical interpretation of the interaction between the several terms.

The last hypothesis from initial Einstein theory one can loosen is the Gaussian character of the dispersal process. Indeed, as we already mentioned, when the Central Limit Theorem applies, variance grows linearly in time. This regime is called *normal diffusion*. However, many time in experiments one finds a variance growing like t^α, where α can be greater than 1 (superdiffusion), or lesser than 1 (subdiffusion). In those cases, diffusion is said to be *anomalous*. Ultraslow scenarios with a behaviour of the position variance like $\propto \ln^\beta t$ are also possible. When diffusion becomes anomalous, it can mean that the infintesimal increments for each time step are not independent, which implicates a memory effect, their probability density being time dependent. Another possibility can be that their distribution functions have longer tales than a Gaussian distribution. An example in nature of this behaviour would be the trajectories albatrosses follow during their flights [5]. As to fluid dynamics, superdiffusion emerges when large-scale structures (eddies, jets or convection rolls) are predominant in the transport [6]. Subdiffusive regimes of charge carriers in disordered solids under an electric field

are also worthy to be mentioned [7].

All of the points we illustrated heretofore will be the subject of the study in this PhD thesis. In Chapter 1 we will study the possibility of an effect of inertia to have anomalous diffusion in flows where molecular diffusivity is not negligible. To do that, we will exploit synthetic kinematic flow models for statistic properties of tubulence. This choice is made to have a full control on the energy spectrum shape, which is more difficult to have in DNS data. In Chapter 2, we will utilise this synthetic flow to present a model where small-scale chaos in turbulence can be statistically substituted by suitable Wiener processes. This model represents a closure one could use in LES for atmosphere physics or oceanography. In Chapter 3, finally, we will present other quite general results of diffusion in flows with inertia, provided that particles fullfill some hypotheses for simplified Maxey-Riley equation. These results, again, could potentially have strong implications due to their analytical character. After any chapter, appendices with mathematical tools to understand the main text are provided.

Chapter 1

Anomalous diffusion of inertial particles in random parallel flows: numerics vs perturbation results

1.1 Introduction

The large-scale transport of inertial particles is a problem attracting much attention in different situations, both practical and theoretical, in different fields of Sciences. For the sake of example, it is known that elemental carbon (also known as black carbon) in the terrestrial atmosphere includes strongly light-absorbing material and is thought to yield large positive radiative forcing, thus potentially affecting Earth climate dynamics [3]. From a theoretical point of view, a quantity of particular interest is the rate at which particles are transported by an incompressible flow [14, 15, 16, 17]. For inertialess particles (i.e. fluid particles), the large-scale dynamics is fully controlled by enhanced (effective) diffusion coefficients [18], the so-called eddy diffusivities. These latter include all the (often nontrivial) effects played by the advecting velocity. Inertialess particles thus behave in this case as Brownian particles but with an enhanced mean-free path.
Although the above scenario is the typical one, there exist situations where the standard diffusion regime is replaced by anomalous diffusion [19]. It is practically impossible to cite the huge literature on anomalous diffusion of tracer particles in incompressible velocity fields. Here we only report Majda and Avellaneda [20] for random shear flow, del Castillo Negrete for non-Gaussian statistics of passive scalars in vortices in shear [21], the experimental study of Solomon et al. [22] on superdiffusion in an annular tank, and the study by Andersen et al. [23] on simple stochastic models able to capture the very origin of strong anomalous diffusion.

Anomalous diffusion of tracer particles is observed when at least one of the two following conditions is not satisfied for the Lagrangian velocity auto-correlation function: convergence of its integral for $t \to 0$; fast enough decay for $t \to \infty$. The above conditions follow from simple considerations carried out on the so-called Taylor relation [24] relating the eddy-diffusivity tensor, D_{ij}, to the velocity auto-correlation function[1]:

$$D_{ij} = \lim_{t\to\infty} \frac{1}{2}\frac{\mathrm{d}}{\mathrm{d}t} \int_0^t \mathrm{d}s \int_0^t \mathrm{d}s' \ \langle \dot{\mathcal{X}}_i(t+s)\dot{\mathcal{X}}_j(t+s')\rangle \ . \tag{1.1}$$

Here, $\mathcal{X}_i(t)$ is the i-th coordinate of tracer position obeying the evolution equation $\dot{\mathcal{X}}_i(t) = u_i(\boldsymbol{\mathcal{X}}(t), t)$ and $\boldsymbol{u}$ is the prescribed carrier flow.
In the presence of non-negligible inertia with respect to the surrounding flow, diffusivity is nomore just the integral of the Lagrangian correlation of the flow velocity, and the problem of finding out the conditions at the origin of anomalous diffusion becomes very challenging. A first attempt along this direction has been done in [25] for the case of random shear flow. The strategy in [25] exploited the results obtained by means of a formal multiple-scale expansion [27, 26], through which an explicit expression for the eddy diffusivity in parallel flows was obtained in [26] in the limit of small inertia. In this limit, a possible source of anomalous diffusion was identified in [25] as a consequence of long-range correlations in both the spatial and the temporal domains. The emergence of anomalous diffusion was traced back to the study of the behavior of the integral defining the eddy diffusivity in the infra-red limit. The same method was successfully exploited in [14] to identify the infra-red properties of the flow spectrum at the origin of anomalous diffusion for tracer particles. Although the method of analysis in [25] is thus similar to that exploited in [14], the main difference is that the expression for the eddy-diffusivity in [14] is exact, while the one in [25] is a first-order small-inertia expansion. The subtle point to investigate is thus on whether or not possible resummations occurring in the presence of secular terms might invalidate the perturbative results and, consequently, the predictions for the emergence of anomalous diffusion. The investigation of the present point is the main concern of the present study.
This chapter is organized as follows. In Sec. 1.2 we recall the main perturbative results obtained in [25] in relation to the conditions for the emergence of anomalous diffusion of inertial particles in parallel flows. Consequently, in Sec. 1.3 we present some first clues about a possible breakdown of the perturbative techniques which have motivated the present work. In Sec. 1.4 we derive a generalization of Taylor's formula valid for generic density ratio (between particles and fluids). This formula, although formal, will help us to formulate heuristic arguments in favor of the possible emergence of resummations in the small-inertia perturbative approach. The numerical strategy

[1] For an introduction to the concept of eddy diffusivity, see the Appendix of this Chapter

to search for possible resummations is introduced in Sec. 1.5, where it is also tested against situations known to produce anomalous diffusion in the tracer limit. In Sec. 1.6 the results of our numerical analysis are presented and discussed. Conclusions are finally reserved to Sec. 1.7.

1.2 Known results for the anomalous diffusion of inertial particles

Let us briefly recall known perturbative results on bounds for the presence or absence of anomalous diffusion of inertial particles recently obtained in [25].
Let us start our analysis by recalling the equations ruling the evolution of inertial particles in a given (random) carrier flow $\boldsymbol{u}(\boldsymbol{x},t)$. Taking into account the added-mass effect in a simplified way — as in [29] — and neglecting any feedback on the carrier fluid, the Lagrangian evolution of inertial particles obeys the following set of stochastic differential equations[2] for particle position, $\boldsymbol{\mathcal{X}}(t)$, and co-velocity, $\boldsymbol{\mathcal{V}}(t)$ [30, 31]:

$$\begin{cases} \dot{\boldsymbol{\mathcal{X}}}(t) = \boldsymbol{\mathcal{V}}(t) + \beta \boldsymbol{u}(\boldsymbol{\mathcal{X}}(t),t) \\ \dot{\boldsymbol{\mathcal{V}}}(t) = -\dfrac{\boldsymbol{\mathcal{V}}(t) - (1-\beta)\boldsymbol{u}(\boldsymbol{\mathcal{X}}(t),t)}{\tau} + \dfrac{\sqrt{2\,D_0}}{\tau}\boldsymbol{\eta}(t)\ . \end{cases} \tag{1.2}$$

Here, the term $\boldsymbol{\eta}(t)$ is a white-noise process coupled with a constant Brownian diffusivity D_0 [32], and the dimensionless coefficient $\beta \equiv 3\rho_{\rm f}/(\rho_{\rm f}+2\rho_{\rm p})$ is defined through the mass densities of the fluid $\rho_{\rm f}$ and of the particles $\rho_{\rm p}$. Non-vanishing values of this added-mass factor β, i.e. particles not much heavier than the fluid, induce a discrepancy between the particle velocity, $\dot{\boldsymbol{\mathcal{X}}}(t)$, and co-velocity, $\boldsymbol{\mathcal{V}}(t)$ [33]. For small spherical inertial particles of radius R, the Stokes time τ (expressing the typical response delay of particles to flow variations) is related to the kinematic viscosity ν of the carrier fluid by $\tau = R^2/(3\nu\beta)$. For $\tau = 0$ the tracer limit is obtained independently of β. From [27, 26] it is known that the evolution of the physical-space probability density function of inertial particles carried by an incompressible flow obeys a diffusion equation, if the problem is investigated – by means of multiple-scale techniques – in the frame of reference moving with the particle effective terminal velocity, and at spatial/temporal scales much larger/longer than the ones typical of the carrier flow, say $\gg L$ and $\gg T$, respectively. In the limit of vanishing Stokes number ($\mathrm{St} \equiv \tau/T$) one obviously recovers the expression of the eddy diffusivity for tracer particles given in [14], where an explicit formula was more specifically presented for the case of parallel flows. The fact that an explicit formula for the eddy diffusivity can be obtained in

[2] For an exhaustive enough introduction for SDEs and equations of motion for inertial particles, see the Appendix of this chapter.

that case is due to vanishing convolutions in Fourier space as a result of the specific geometry of the parallel flow. When considering particles endowed with small but finite inertia in this class of bi-dimensional parallel flows, $u_j(\boldsymbol{x},t) = \delta_{j1}u(y,t)$, an expansion in St gives the following expressions for the zeroth and first orders of the effective-diffusivity tensor[3] [25]:

$$D_{ij}^{(0)} = D_0\left[\delta_{ij} + \delta_{i1}\delta_{j1}\int \mathrm{d}k \int \mathrm{d}\omega\, \mathcal{E}(k,\omega)\frac{k^2}{\omega^2 + D_0^2k^4}\right] , \tag{1.3}$$

$$D_{ij}^{(1)} = \delta_{i1}\delta_{j1}\frac{L}{U}\int \mathrm{d}k \int \mathrm{d}\omega\, \mathcal{E}(k,\omega)\frac{(1-\beta)\omega^2 + (3-\beta)D_0^2k^4}{2(\omega^2 + D_0^2k^4)} , \tag{1.4}$$

$$D_{ij} = D_{ij}^{(0)} + \mathrm{St}D_{ij}^{(1)} + O(\mathrm{St}^2) . \tag{1.5}$$

Here $\mathcal{E}(k,\omega)$ stands for the Fourier transform of the velocity correlation function, in both time and the y direction perpendicular to the flow. (It is worth noticing that in three-dimensional parallel flows the expressions (1.3)–(1.4) change only for the presence of the Jacobian $\mathrm{d}^2\boldsymbol{k}$ instead of $\mathrm{d}k$, and for the fact that the Fourier transform must be performed in both the directions orthogonal to the flow. However, in this chapter we are going to deal only with two-dimensional flows.) Note that, although not explicitly stated, Eqs. (1.3) and (1.4) naturally contain endpoints (ultra-violet and infra-red cutoffs) in the integration interval.

These general results were applied in [25] to parallel flows having spectra with power-law forms (while in [26] they were more specifically substantiated for the Kolmogorov sinusoidal flow), in the spatial variable and possibly also in the temporal one. The analysis of possible anomalies there relied on the presence of a spatial velocity spectrum unbounded in the infra-red region, i.e. with wave lengths extending to infinity. This poses two problems, namely the impossibility of defining an observation length much larger than any spatial scale possessed by the velocity field (a necessary condition for a multi-scale approach), and the definite non-periodicity of the fluid flow under investigation. The first point requires the use of a regularization procedure, as explained in [14] and as implemented in the numerical procedure we are going to introduce in next sections. The second difficulty can be overcome by recalling that the results of [14, 26] also apply for random (stationary and homogeneous) ergodic velocity fields, by appropriately reformulating the space-time integrals as statistical averages.

With these provisos, and imposing a velocity spectrum of the type

$$\mathcal{E}(k,\omega) \sim |k|^{\alpha}|\omega|^{\zeta} , \tag{1.6}$$

[3] According to the "big-O notation", $f(x) \sim O(g(x))$ when$x \to x_0$ iff $\exists\epsilon$, $A \ni x_0$: $|f(x)| < \epsilon|g(x)|\ \forall x \in A - \{x_0\}$. If g is non-zero in a punctured neighbourhood of x_0, this is equivalent to $\limsup_{x\to x_0}|f(x)/g(x)| < \infty$.

the role of the exponents α and ζ was investigated in [25]. Physically, the possibility of having different exponents α and ζ is a consequence of the well-known lack of universal behavior occurring in the infra-red region of a turbulent flow. This region is indeed dominated by forcing mechanisms which can be very different.
Intuitively, smaller and smaller values (i.e. more and more negative) of these exponents are associated with the presence of long-range correlations, and are thus more and more likely to induce anomalies. The effective diffusivity of tracers is exactly given by the integral in (1.3), which converges for

$$\alpha > -3 \quad \cap \quad \zeta > -1 \quad \cap \quad \alpha + 2\zeta > -1 \, . \tag{1.7}$$

When inertial particles are investigated, this result might be modified by the presence of additive contributions in (1.5), where the leading correction is given by (1.4). If $\beta \neq 1$ and $\beta \neq 3$, the latter integral converges for

$$\alpha > -1 \quad \cap \quad \zeta > -1 \quad \cap \quad \alpha + 2\zeta > -3 \, . \tag{1.8}$$

In the plane case, four different regions can thus be identified. I) Zone A: $\alpha > -1 \ \cap \ \zeta > -1 \ \cap \ \alpha + 2\zeta > -1$: diffusion is definitely normal because both the tracer contribution and the leading correction converge. II) Zone B: $\alpha > -1 \ \cap \ \zeta > -1 \ \cap \ \alpha + 2\zeta < -1$: anomaly is likely because the zeroth order diverges while the first one converges. III) Zone C: $-3 < \alpha < -1 \ \cap \ \alpha + 2\zeta > -1$: anomaly is possible because the zeroth order converges but the first one diverges. IV) Rest of the plane: both the tracer contribution and the leading correction diverge, again anomaly is likely. These four regions are represented in an overlap in Fig. 1.1.
What is remarkable in these considerations from a physical point of view, is that inertia seems to be able to change the tracer regime, in particular to create anomalous diffusion under certain conditions. This situation is the one associated to the aforementioned region C. Different bounds emerge when $\beta = 1$ or $= 3$, because the inertial contribution in the integrating function in (1.4) changes. However, when $\beta = 3$, what varies is just the ζ bound, that is the integral converges if $\zeta > -3$. This means that in fact nothing changes in the global situations represented in Fig. 1.1, because in the region $-3 < \zeta < -1$ the tracer contribution is still divergent. On the other hand, for $\beta = 1$, the first bound in (1.8) becomes $\alpha > -5$. As a result of this, the regime of zone C disappears and the situation remains unchanged in comparison to the pure tracer.
The main limitation of these results lays in the fact that their perturbative spirit makes it impossible to understand what happens when, in the small-inertia expansion truncated at the first order, either or both integrals diverge. Indeed, subleading terms may induce spurious divergences or renormalizing summations which cannot be accounted for by a perturbative scheme, e.g. in region C one cannot exclude the possibility that the sum of the neglected

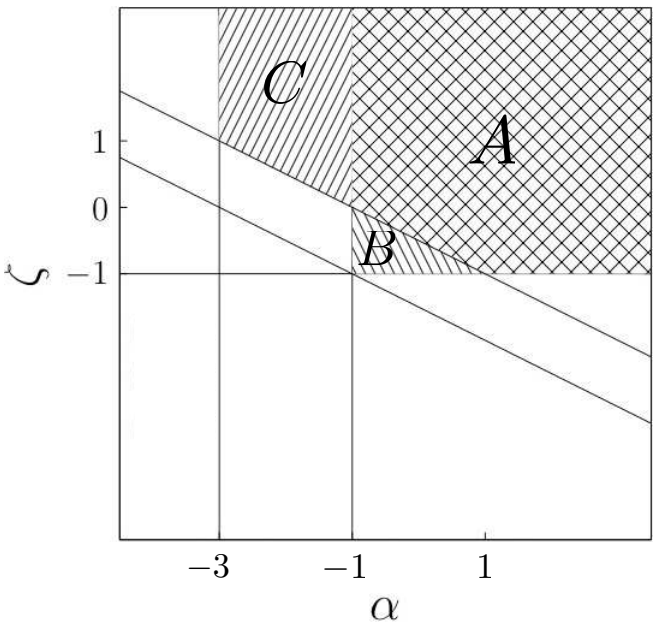

Figure 1.1: Sketch of diffusion anomaly for inertial particles and tracers [see (1.7) coupled with (1.8)]. Diffusion is definitely normal only in the meshed area A. In zone B only the inertial correction converges and anomaly is likely, whereas in zone C only the tracer contribution converges and an inertia-driven anomaly is possible. In the fourth zone, the white one, both the tracer and the $O(\mathrm{St})$ contributions diverge.

orders (St^2 and higher) may exactly cancel the divergence at $O(\mathrm{St})$.
In order to investigate this subtle point one has to resort to numerical simulations. This is one of the main aim of the present chapter which will be carried out in the next sections.

1.3 Subtle points: clues for the possible emergence of resummations

Before carrying out a systematic numerical analysis to investigate the genuine/spurious character of anomalous diffusion identified in [25], let us first discuss some clues that seem to point towards the possible emergence of resummations. These latter might invalidate the above-mentioned bounds for the emergence of anomalous diffusion. In doing that, it is convenient to recast (1.4) in the form

$$\delta_{i1}\delta_{j1}\frac{L}{U}\int \mathrm{d}k \int \mathrm{d}\omega\, \mathcal{E}(k,\omega)\left[\frac{1-\beta}{2}+\frac{D_0^2k^4}{\omega^2+D_0^2k^4}\right] . \tag{1.9}$$

When $\beta > 1$, the first addend in (1.9) becomes negative, and if diverging it can give rise to negative infinities which are hard to justify, the eddy diffusivity being a positive definite quantity. To be more specific, this can happen for $\alpha = -5/3$ and $\zeta = 1$, with any ultra-violet cutoff (i.e. in the region C where only the tracer contribution converges and an inertia-driven anomaly is inferred by the perturbative strategy).
To gather more insights on the emergence of possible resummations, let us evaluate explicitly the correction $O(\mathrm{St})$ in the simple case $\zeta = 0$, corresponding to a white-in-time flow field. When doing that, assuming a flat spectrum in frequencies (i.e. $\zeta = 0$), an integration immediately leads to the expression:

$$\delta_{i1}\delta_{j1}\frac{L}{U}\int \mathrm{d}k\, |k|^{\alpha}\left[(1-\beta)\omega_{\max}+2D_0k^2\arctan\frac{\omega_{\max}}{D_0k^2}\right] . \tag{1.10}$$

Here, $\omega_{\max}$ is a possible ultra-violet cutoff frequency which goes to infinity in the white-noise case, whereas the infra-red cutoff frequency is set to 0 because no divergence occurs in that region. Our remark is that when $\beta \neq 1$ and $\omega_{\max}$ is sufficiently large, we have a $O(\mathrm{St})$ correction having a magnitude comparable with the one of the $O(1)$ correction. This clearly signals a secular behavior, to deal with which renormalized perturbative approaches have to be exploited [28]. In the limit $\omega_{\max} \to \infty$ the correction diverges, and then one could state that δ-correlated flows are associated to anomalous diffusion. Conversely, for $\beta = 1$ the correction is limited and nonzero. An explicit dependence on β thus appears from the perturbative analysis. As we are going to see in the next section, these conclusions are actually an artifact of the perturbation strategy.

1.4 Lagrangian view for the eddy-diffusivity of inertial particles

For passive tracers, there are well-established results on the relation between diffusion phenomena and velocity correlation functions. The most famous one is Taylor's formula [24]. In this section we generalize such a formula for the case of inertial particles of arbitrary inertia. For this purpose, let us start from the dynamical equations (1.2).
Due to the presence of Brownian noise on the right-hand side of (1.2), our flows are fully mixing (i.e. ergodic in statistical terms) and particles tend to visit every point of the space as $t \to \infty$. This means that the Eulerian and Lagrangian averages coincide after a sufficiently long time, i.e. $\langle \boldsymbol{u}(\boldsymbol{x},t)\rangle = \langle \boldsymbol{u}(\boldsymbol{\mathcal{X}}(t),t)\rangle$. It is thus convenient for the successive analysis to choose as a reference frame the one such that $\langle \boldsymbol{u}(\boldsymbol{x},t)\rangle = \langle \boldsymbol{u}(\boldsymbol{\mathcal{X}}(t),t)\rangle = 0$ (and thus the mean co-velocity is equal to the mean velocity). Here, brackets denote ensemble average over both $\boldsymbol{u}(\boldsymbol{x},t)$ and $\boldsymbol{\eta}$.
By taking the average of both sides of (1.2) and integrating, one obtains:

$$\left\{ \begin{array}{rcl} \langle \boldsymbol{\mathcal{X}}(t)\rangle &=& \boldsymbol{\mathcal{X}}(0) + \tau \boldsymbol{\mathcal{V}}(0)[1-\mathrm{e}^{-t/\tau}] \\ \langle \boldsymbol{\mathcal{V}}(t)\rangle &=& \boldsymbol{\mathcal{V}}(0)\mathrm{e}^{-t/\tau}\ . \end{array} \right. \tag{1.11}$$

For $t \gg \tau$ a stationary state sets in, for which $\langle \boldsymbol{\mathcal{X}}(t)\rangle = \boldsymbol{\mathcal{X}}(0) + \tau\boldsymbol{\mathcal{V}}(0)$ and $\langle \boldsymbol{\mathcal{V}}(t)\rangle = 0$. Because of the fact that our attention in the following will be paid on large-scale/long-time transport, without loss of generality we can assume $\boldsymbol{\mathcal{V}}(0) = 0$ from the very beginning. To describe asymptotic transport, the eddy diffusivity can be introduced according to the usual definition:

$$D_{ij} \equiv \lim_{t\to\infty} \frac{1}{2}\frac{\mathrm{d}}{\mathrm{d}t} R_{ij}(t) \tag{1.12}$$

where $R_{ij}(t) \equiv \langle \mathcal{X}_i(t)\mathcal{X}_j(t)\rangle - \langle \mathcal{X}_i(t)\rangle\langle \mathcal{X}_j(t)\rangle$. By simple integration, the expression for the eddy diffusivity can be finally recast in the following form:

$$D_{ij} = \lim_{t\to\infty} \frac{1}{2}\frac{\mathrm{d}}{\mathrm{d}t} \int_0^t \mathrm{d}s \int_0^t \mathrm{d}s'\ \langle \dot{\mathcal{X}}_i(t+s)\dot{\mathcal{X}}_j(t+s')\rangle\ . \tag{1.13}$$

Exploiting the Green function method, we can convert (1.2) into a system of integral equations. Namely, the solution of the equation for the co-velocity reads:

$$\boldsymbol{\mathcal{V}}(t) = \frac{1-\beta}{\tau}\int_0^t \mathrm{d}s\ \mathrm{e}^{-(t-s)/\tau}\boldsymbol{u}(\boldsymbol{\mathcal{X}}(s),s) + \frac{\sqrt{2D_0}}{\tau}\int_0^t \mathrm{d}s\ \mathrm{e}^{-(t-s)/\tau}\boldsymbol{\eta}(s)\ , \tag{1.14}$$

while the velocity turns out to be:

$$\begin{array}{rcl} \dot{\boldsymbol{\mathcal{X}}}(t) &=& \dfrac{1-\beta}{\tau}\displaystyle\int_0^t \mathrm{d}s\ \mathrm{e}^{-(t-s)/\tau}\boldsymbol{u}(\boldsymbol{\mathcal{X}}(s),s) \\ &+& \dfrac{\sqrt{2D_0}}{\tau}\displaystyle\int_0^t \mathrm{d}s\ \mathrm{e}^{-(t-s)/\tau}\boldsymbol{\eta}(s) + \beta\boldsymbol{u}(\boldsymbol{\mathcal{X}}(t),t)\ . \end{array} \tag{1.15}$$

Note that, if $\boldsymbol{\mathcal{V}}(0) \neq 0$, some constant terms and exponentially decaying contributions do appear in the above expressions, without any effect in the final form of the eddy diffusivity. This is because of the time derivative involved in its definition, and also because of the long-time limit considered. By plugging the previous expression for $\dot{\boldsymbol{\mathcal{X}}}(t)$ into (1.13), one obtains:

$$
\begin{aligned}
D_{ij} = D_0\delta_{ij} + \lim_{t\to+\infty}\frac{1}{2}\Bigg\{ & \frac{(1-\beta)^2}{\tau^2}\int_0^t \mathrm{d}s \int_0^s \mathrm{d}s' \int_0^t \mathrm{d}s'' \\
& \times \mathrm{e}^{-(t+s-s'-s'')/\tau}\langle u_i(\boldsymbol{\mathcal{X}}(t+s'),t+s')u_j(\boldsymbol{\mathcal{X}}(t+s''),t+s'')\rangle \\
& + \frac{(1-\beta)\beta}{\tau}\int_0^t \mathrm{d}s \int_0^t \mathrm{d}s'\ \mathrm{e}^{-(t-s)/\tau}\langle u_i(\boldsymbol{\mathcal{X}}(t+s),t+s)u_j(\boldsymbol{\mathcal{X}}(t+s'),t+s')\rangle \\
& + \frac{(1-\beta)\beta}{\tau}\int_0^t \mathrm{d}s \int_0^s \mathrm{d}s'\ \mathrm{e}^{-(s-s')/\tau}\langle u_i(\boldsymbol{\mathcal{X}}(t+s'),t+s')u_j(\boldsymbol{\mathcal{X}}(2t),2t)\rangle \\
& + \beta^2\int_0^t \mathrm{d}s\ \langle u_i(\boldsymbol{\mathcal{X}}(t+s),t+s)u_j(\boldsymbol{\mathcal{X}}(2t),2t)\rangle + (i\leftrightarrow j)\Bigg\}\ ,
\end{aligned}
\tag{1.16}
$$

where the symbol $+(i\leftrightarrow j)$ means that the same expression has to be added with interchanged indices (i.e. symmetrization). Note that the Lagrangian correlation functions have to be computed in the stationary regime due to the considered long-time limit and to the definition (1.12) of the eddy diffusivity. This happens because the system is fully mixing, with the consequence that the stationarity of the Eulerian correlations is inherited by the Lagrangian ones as $t\to\infty$ [56].
We have also used the fact that $\langle \eta_i(s)\eta_j(s')\rangle = \delta_{ij}\delta(s-s')$, the independence of the two processes $\boldsymbol{u}(\boldsymbol{x},t)$ and $\boldsymbol{\eta}(t)$, i.e. $\langle u_i(\boldsymbol{\mathcal{X}}(t),t)\eta_j(t)\rangle = 0$, and:

$$
\lim_{t\to+\infty}\frac{2D_0}{\tau^2}\int_0^t \mathrm{d}t' \int_0^{t'} \mathrm{d}s\ \mathrm{e}^{-(t+t'-2s)/\tau} = D_0\ . \tag{1.17}
$$

The explicit contribution of Brownian diffusivity to the effective diffusivity is encoded in the term $D_0\delta_{ij}$. We are saying "explicit" because, obviously, also the other integrals depend upon D_0, since they are implicitly evaluated on the particle trajectories which, in turn, depend on the white-noise component. The trajectories will statistically tend to the noiseless ones as $D_0\to 0$.

1.4.1 Discussion of some relevant limits and heuristics

Very heavy particles Let us now focus on the limit of very heavy particles, i.e. $\beta = 0$. In this case (1.16) reduces to the white-noise contribution plus the first triple integral in the curly brackets. This latter can be simplified as done in [56]. The final expression is:

$$
\begin{aligned}
D_{ij} \;=\; & D_0\delta_{ij} + \lim_{t\to+\infty}\frac{1}{4\tau}\int_0^t \mathrm{d}s \int_{-\infty}^{+\infty} \mathrm{d}s' \\
& \times \mathrm{e}^{-|s-s'|/\tau}\left[\langle u_i(\boldsymbol{\mathcal{X}}(t+s'),t+s')u_j(\boldsymbol{\mathcal{X}}(2t),2t)\rangle + (i\leftrightarrow j)\right]\ .
\end{aligned}
$$

From this formula, it is immediately verified that for $\tau \to 0$ the usual Taylor's expression for tracer particles is obtained, by virtue of the fact that $\exp(-|s-s'|/\tau)/(2\tau)$ approaches the Dirac delta as τ goes to zero.
Although the above expression is valid at a formal level (indeed, the particle trajectories involved in the integration are unknown), some physical considerations highlighting the role of inertia on the large-scale transport (possibly anomalous) can be provided. To do that, let us define the time-weighted average (on a windows of size τ) of the velocity field at time s as:

$$\overline{u}_i(\boldsymbol{\mathcal{X}}(s), s) = \int_{-\infty}^{+\infty} \mathrm{d}s' \, \frac{\mathrm{e}^{-|s-s'|/\tau}}{2\tau} u_i(\boldsymbol{\mathcal{X}}(s'), s') \; , \tag{1.18}$$

in terms of which expression (1.18) becomes:

$$D_{ij} = D_0 \delta_{ij} + \lim_{t \to +\infty} \frac{1}{2} \int_0^t \mathrm{d}s \, \left[\langle \overline{u}_i(\boldsymbol{\mathcal{X}}(t+s), t+s) u_j(\boldsymbol{\mathcal{X}}(2t), 2t) \rangle + (i \leftrightarrow j) \right] .$$

It thus has the form of a "standard" Taylor formula with two major differences: fluid velocities are evaluated along inertial-particle trajectories, and the filtered velocity does appear instead of the punctual velocity. These two points are likely to act in competition: the first indeed plays to reduce the auto-correlation function (thus depleting large-scale transport), while the opposite is expected from the second. Even more interestingly, the second effect might cause an exceptionally slow decrease of the auto-correlation function, so slow as to render the integral divergent. This should be the fingerprint of anomalous diffusion. It is however difficult to isolate the two contributions in a way to control, a priori, who is the winner between the two competing mechanisms.

Inertialess particles Let us now consider the limit $\tau \to 0$. From (1.16) one recovers the tracer limit, regardless of β. Indeed, denoting by $H(x)$ the Heaviside function, Eq. (1.16) contains the following expressions:

$$\frac{1}{\tau} H(x) \mathrm{e}^{-x/\tau} \to \delta(x) \; , \qquad \frac{1}{\tau} \mathrm{e}^{-|x|/\tau} \to 2\delta(x) \; .$$

The Heaviside function indeed arises from the replacement of $\int_0^t \mathrm{d}s$ with $\int_0^{+\infty} \mathrm{d}s \; H(t-s)$ (or of $\int_0^s \mathrm{d}s'$ with $\int_0^{+\infty} \mathrm{d}s' \, H(s-s')$ when $s' \in [0, s]$). After the above substitutions, the tracer limit easily follows.

Delta-correlated flows Let us now pass to discuss the relevant limit of homogeneous δ-correlated-in-time velocity field in (1.16). The analysis of this limit will provide a further clue in favor of the emergence of resummation in the perturbative expansion (1.5). A Gaussian, zero-mean, δ-correlated-in-time random velocity is defined in terms of the two-point correlation function

$$\langle u_i(\boldsymbol{x}, t) u_j(\boldsymbol{x}', t') \rangle = 4\pi F_{ij}(\boldsymbol{x} - \boldsymbol{x}') \delta(t - t') \; . \tag{1.19}$$

If we evaluate this function along the Lagrangian trajectories, i.e. on the points $\boldsymbol{\mathcal{X}}(s)$ and $\boldsymbol{\mathcal{X}}(s')$, it is easy to conclude that the flow is δ-correlated in time also from a Lagrangian point of view. Let us plug $\langle u_i(\boldsymbol{\mathcal{X}}(s'),s')u_j(\boldsymbol{\mathcal{X}}(s),s)\rangle = 4\pi F_{ij}(0)\delta(s-s')$ into (1.16), and proceed with simple manipulations exploiting the symmetry of $F_{ij}(0)$. To obtain the final result, let us proceed with a term-by-term analysis of the four integrals appearing in (1.16). The first and second integrals are:

$$(1-\beta)^2\frac{2\pi F_{ij}(0)}{2\tau}\int_0^{+\infty}\mathrm{d}s\int_{-\infty}^{+\infty}\mathrm{d}s'\,\mathrm{e}^{-|s-s'|/\tau}\delta(s')+(i\leftrightarrow j) = (1-\beta)^2 2\pi F_{ij}(0)$$

and

$$\begin{aligned}&\lim_{t\to+\infty}(1-\beta)\beta\frac{2\pi F_{ij}(0)}{\tau}\int_0^t\mathrm{d}s\int_0^t\mathrm{d}s'\;\mathrm{e}^{-(t-s)/\tau}\delta(s-s')+(i\leftrightarrow j)\\ =\;& 4\pi(1-\beta)\beta F_{ij}(0)\;.\end{aligned} \tag{1.20}$$

As far as the third term is concerned, by exploiting the formal identity $\int_t^{t'}\mathrm{d}s\;f(s)\delta(t'-s) = f(t')/2$, the inner integral yields a function whose values are $2\pi(1-\beta)\beta F_{ij}(0)$ if $s=t$ and 0 elsewhere. When one integrates that function in s, the result is obviously 0 because the function is zero almost everywhere. Finally, the fourth integral is:

$$2\pi\beta^2 F_{ij}(0)\int_0^t\mathrm{d}s\;\delta(t-s)+(i\leftrightarrow j) = 2\pi\beta^2F_{ij}(0)\;.$$

Summing up all the contributions, one finds

$$D_{ij} = D_0\delta_{ij} + 2\pi F_{ij}(0)\;, \tag{1.21}$$

that corresponds to the result for the tracer eddy diffusivity in δ-correlated flows (see, e.g., [14]). Note that such an expression holds for all τ and β. This remark casts in a bad light the perturbative result (1.5). This latter contains indeed an explicit dependence on both τ and β and, as we have already discussed, Eq. (1.4) is a divergent correction when $\omega_{\max}\to\infty$, because the integrating function does not vanish at infinity. This means that resummations are surely present in the ultra-violet region of the spectrum. It is quite hard to imagine a mechanism of resummation which acts on the sole ultra-violet divergences and preserves the infra-red ones.

1.5 The numerical strategy

Our aim here is to carry out a systematic analysis to check the reliability of the bounds reported in [25] on the emergence of anomalous diffusion for

inertial particles. The flows we are going to consider are parallel, incompressible, random (stationary and homogeneous), and are characterized by different spectral power-law behaviors (see Eq. (1.6)). These parallel flows will have a dependence on the sole coordinate, say, y: $\boldsymbol{u}(\boldsymbol{x},t) = (u(y,t),0)$. The definition of the one-dimensional Fourier transform we use here is of the form

$$\mathfrak{F}_t[f(t)](\omega) \equiv \frac{1}{2\pi}\int_{\mathbb{R}} f(t)\mathrm{e}^{\mathrm{i}\omega t}\mathrm{d}t$$

and similarly for the y dependence (with $t \mapsto y$ and $\omega \mapsto k$).
The Fourier transform of velocity correlations is denoted by $\mathcal{E}(k,\omega)$
$= \mathfrak{F}_{y,t}\left[\langle \boldsymbol{u}(y,t)\cdot\boldsymbol{u}(0,0)\rangle\right]$.

1.5.1 The kinematic model

In order to build a parallel flow with the desired aforementioned properties, let us consider a superposition of N independent spatial sinusoidal modes, with time-dependent amplitudes, and different wave numbers. Namely,

$$\left\{\begin{array}{lcl} u_x(x,y,t) &=& \sum_{i=1}^{N} A_i(t)\cos[k_i(y+\tilde{\theta}_i)] \\ u_y(x,y,t) &=& 0\,, \end{array}\right. \tag{1.22}$$

where x and y are the spatial coordinates of a tracer particle, $A_i(t)$ is the mode amplitude, k_i is the wave number of the spatial mode i, N is the number of modes and $\tilde{\theta}_i$ are static random phases uniformly distributed in the interval $[0,2\pi[$. These phases are fixed in each realization of the flow, but they are in general different for each particle. This is an example of quenched random process. The role of the random phases is simply to have a homogeneous process and to allow efficient particle mixing along x. Mixing along the transverse direction y is guaranteed by the presence of the Brownian contribution in (1.2).
We have distributed the spatial modes according to a given density factor, here of the form $k_{i+1} = \varrho k_i$ with $\varrho = \sqrt{2}$. The amplitudes can be conveniently factorized as $A_i(t) = CK_i a_i(t)$, where K_i will give the sought spatial spectrum, $a_i(t)$ will mimic the sought temporal statistical behavior, and C is a constant having dimensions $[L]^{(\alpha+3)/2}[T]^{(\zeta-1)/2}$, so that the field in (1.22) is dimensionally a velocity.
The velocity field defined in (1.22) is a variation of a well-known strategy to mimic unresolved small-scale motion, and its effect, on particle dispersion (both absolute and relative). For examples of applications see, e.g., [34, 35, 36] and references therein.
The next step is to create a stochastic process for velocity amplitudes able to generate a zero-mean flow with the sought spectral behavior in frequency and wave numbers. To do that, let us start from a Gaussian white-noise

process for each component i:

$$\eta_i(t) \equiv \lim_{\delta t \to 0} \frac{G_i(0,1)}{\sqrt{\delta t}}$$

where $G_i(0,1)$ is a Gaussian zero-mean (vector) process having unit variance for each component. Here δt is the infinitesimal time step that we are going to use in our numerical algorithm. It is easy to see that such a process mimics a δ-correlated-in-time process (i.e. its temporal spectrum is flat). Then, once this process is numerically generated, one can take its (discrete) Fourier transform $\hat{\eta}_i(\omega)$ and define the following new quantity:

$$\hat{\eta}_i(\omega) \to \hat{\eta}_i(\omega)\sqrt{2\pi\Omega(\omega)} \; .$$

In doing that, what we have now is a process in the frequency domain with a generic (even) frequency spectrum $\Omega(\omega)$ that, in the present study, will be a power law $|\omega|^{\zeta}$. The sought $a_i(t)$ can be immediately obtained by Fourier anti-transform, and as a direct consequence

$$\langle a_i(t) a_j(t') \rangle = \delta_{ij} \int \mathrm{d}\omega \; \mathrm{e}^{\mathrm{i}\omega(t-t')} \Omega(\omega) \; ,$$

where the relation $\langle a_i(t) a_j(t') \rangle \propto \delta_{ij}$ has been used explicitly. It is easy to see that the process is stationary (and thus, in particular, mean value and variance are time independent).
As far as the behavior in the wave-number space is concerned, the following relation is obtained from (1.22):

$$\langle u_x(y,t) u_x(y,t) \rangle = C^2 \langle a_i^2 \rangle \sum_{i=1}^{N} \frac{K_i^2}{2} \; , \tag{1.23}$$

with $\langle a_i^2 \rangle$ independent of i by construction.
For the sake of example, a classical Kolmogorov spectrum can be obtained by setting $K_i^2 = k_i^{-5/3} \delta k_i$ (if the spectrum is approximated from above) or $k_{i+1}^{-5/3} \delta k_i$ (from below), δk_i being $k_{i+1} - k_i$.

1.5.2 Some benchmark cases

We are now going to perform three tests to check the behavior of the proposed kinematic model. In this way one can gather information on its precision to reproduce the sought flow field and the order of magnitude of the statistical samples one needs to consider to achieve statistical convergence. The first two tests are relative to tracer particles described by the equation

$$\dot{\boldsymbol{\mathcal{X}}}(t) = \boldsymbol{u}(\boldsymbol{\mathcal{X}}(t), t) + \sqrt{2D_0}\boldsymbol{\eta}(t) \; , \tag{1.24}$$

for which the mean velocity is zero if we choose the reference frame such that $\langle u(\boldsymbol{x},t)\rangle = 0$. Since our flow is fully mixing, particles tend to visit every point of the space as $t \to \infty$. As already observed, this means that Eulerian and Lagrangian averages coincide after a sufficiently long time, i.e. $\langle \boldsymbol{u}(\boldsymbol{x},t)\rangle = \langle \boldsymbol{u}(\boldsymbol{\mathcal{X}}(t),t)\rangle = 0$.
The third example will concern a pure kinematic property of a flow with a non-flat frequency spectrum. As it will be explained, simple dimensional considerations (i.e. power-counting arguments) can be done in that case, and will be used to check the correctness of our algorithm to properly generate the sought dependence of spectrum on frequency.

Eddy diffusivity for δ-correlated velocity fields

In order to test the absolute dispersion of tracer particles in a velocity field generated by our kinematic model, we have focused our attention on a two-dimensional, parallel, δ-correlated velocity field given by (1.22). This latter case is known to produce an exact expression for the eddy diffusivity [14]. More specifically, here the velocity field is a Gaussian, zero-mean, random process with auto-correlation function given by

$$\langle u_x(\boldsymbol{x},t)u_x(\boldsymbol{x},t')\rangle = 4\pi W\delta(t-t') \;, \tag{1.25}$$

with, in our case,

$$W = \frac{1}{2}\int \mathrm{d}k\; \mathcal{E}(k,\omega) \propto \int \mathrm{d}k\; |k|^{\alpha}|\omega|^{0} \;. \tag{1.26}$$

In our discrete model, (1.26) becomes $W = \sum_{i=1}^{N} W_i$, where $W_i = C^2|k_i|^{\alpha}\delta k_i/4$. To achieve the desired velocity field, it is sufficient to consider (1.22) with amplitudes $A_i(t)$ given by:

$$A_i(t) = \sqrt{8\pi W_i}\eta_i(t) \;. \tag{1.27}$$

(Note that here i is not a contracted index.) Once the velocity field is generated at each time step, we carried out numerical simulations of particle dispersion by uniformly distributing $N = 1600$ particles in a square box, whose side corresponds to the maximum wavelength (here 2048). The problem is made dimensionless by assuming as a characteristic length scale the minimal wave length appearing in our kinematic model, i.e. $L_{\min} = 2\pi/k_{\max}$ (for the sake of notation, $k_{\max} \equiv k_{N+1}$), and the bare molecular diffusivity D_0. The typical time scale follows accordingly.
The numerical integration of the particle equation (1.25) was performed by a Runge–Kutta algorithm adapted to deal with additive white noises [37]. The integration step was $\delta t = 0.1$ and the total number of integration steps was 8000. The measured observable is the mean-square particle displacement (with respect to particle initial condition):

$$\sigma^2(t) \equiv \langle |\boldsymbol{\mathcal{X}}(t) - \boldsymbol{\mathcal{X}}(0)|^2\rangle \;. \tag{1.28}$$

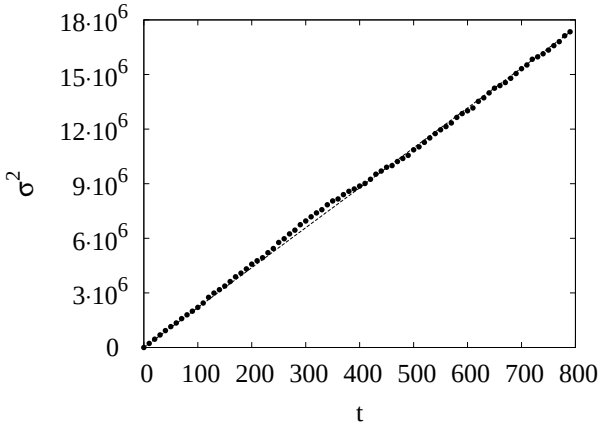

Figure 1.2: Absolute dispersion in a δ-correlated flow. The dashed line represents the best-fit slope calculated on the whole time interval shown in the figure. Here $k_{\max} = 2\pi$, $C^2 = 10$ and $k_{\min} = \pi/\sqrt{2}$.

From [14] we know that such a quantity undergoes a diffusive behavior with a diffusion coefficient given by $2(2+2\pi W)$. In Fig. 1.2 we show the behavior of $\sigma^2(t)$ as a function of time ($\alpha = -5/3$). In the present case, $2\pi W = 9.01$ and the expected diffusion coefficient is thus 22.02. The best fit slope from Fig. 1.2 is ~ 21.94 and thus agrees with the theory with a relative error of about 0.4%.

Behavior of eddy diffusivities with different infra-red cutoffs

Our attention is now focused on the dependence of eddy diffusivities with respect to an infra-red cutoff implicitly assumed inside the integral (1.26). This is the main ingredient to access the emergence of possible anomalous-diffusion behavior. The main aim here is to test our method to assess anomaly in situations under control where the existence of anomalous/normal diffusion is a well-established result.
For this purpose, let us suppose to have two flows δ-correlated in time and having spectral power laws $\propto k^{-5/3}$ and $\propto k^{-1/3}$ respectively, with $|k| \in [k_{\min}, k_{\max}]$. Here, $C^2 = 10$ in the first case and $C^2 = 1$ in the second one. Keeping $k_{\max} = 2\pi$ fixed, both situations have an eddy diffusivity with a dependence on the infra-red cutoff of the form $ak_{\min}^b + c$, b being $-2/3$ in the first case and $2/3$ in the second one. This trivially follows from (1.26). The first case with a $-5/3$ slope thus induces anomalous diffusion since the eddy diffusivity diverges as $k_{\min} \to 0$. The resulting curves are shown in Fig. 1.3, as functions of $k_{\min}$. For each $k_{\min}$, eddy diffusivities are obtained as described in the previous section, by uniformly distributing one million particles in a square box, the side of which corresponds to the max-

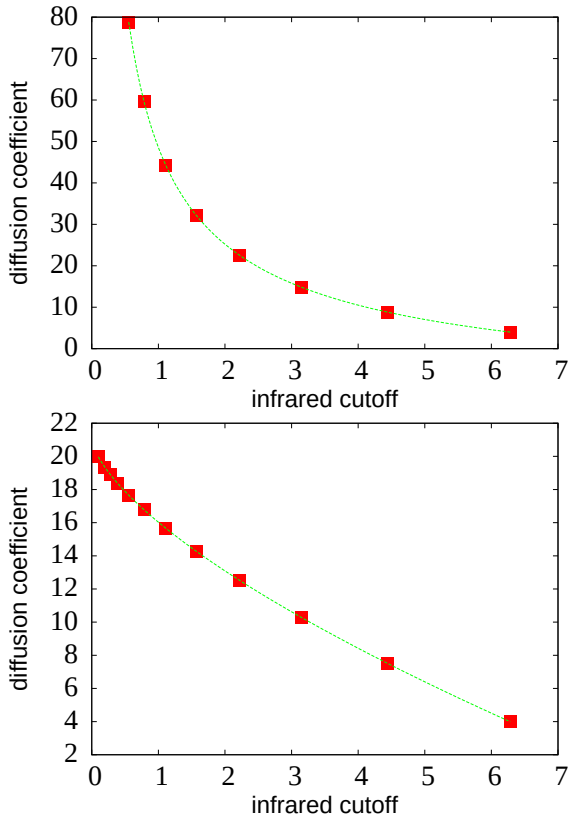

Figure 1.3: Diffusion coefficient for different infra-red cutoffs $k_{\min}$ in two δ-correlated flows having different spectral power-law behavior: $\propto k^{-5/3}$ (upper panel) and $\propto k^{-1/3}$ (lower panel). Squares indicate numerical results, while continuous lines are the resulting best-fit curves (of the form $ak_{\min}^b + c$).

imum wave length of the flow, and then averaging over particle positions. The best fit, assuming the law $ak_{\min}^b + c$, yields $a = 63.0787 \pm 5 \cdot 10^{-4}$, $b = -0.666646 \pm 7 \cdot 10^{-6}$, $c = -14.5347 \pm 5 \cdot 10^{-4}$ for the $-5/3$ spectrum, and $a = -5.00650 \pm 4 \cdot 10^{-5}$, $b = 0.666664 \pm 3 \cdot 10^{-6}$, $c = 21.03860 \pm 3 \cdot 10^{-5}$ for the $-1/3$ law. The meaning of the resulting error is statistical: it has to be multiplied by a factor 3 to obtain the corresponding maximum error, according to the 3σ criterion.

What clearly stands out is that the two exponents arising from best fit are fully compatible with the theoretical results. One could also note in Fig. 1.3 that plotted data are closer to zero in the normal-diffusion case than in the anomalous one. This is due to the fact that, in order to see a good diffusive regime, it is necessary to wait longer and longer times as $L_{\max}$ increases.

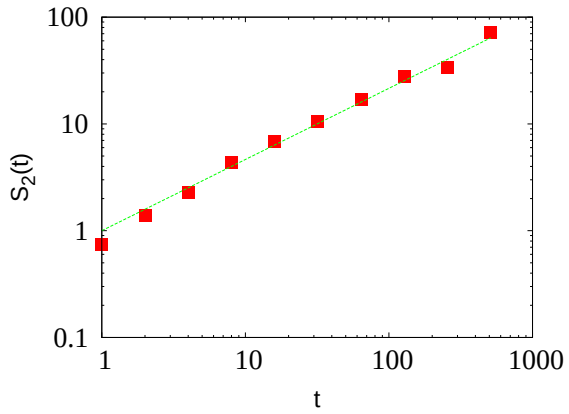

Figure 1.4: Analytical (continuous line) vs. numerical (square) results for the two-time velocity structure function $S_2(t)$ for a spectral law $\omega^{-5/3}$. The continuous line has the slope 2/3, as expected by simple power-counting. It has been sufficient to take averages over only 5 frames to obtain such a good agreement with the theoretical slope.

A flow with a power-law frequency spectrum

We now aim at assessing the validity of our kinematic model in the time domain. To do that, we build an energy spectrum $\mathcal{E}(k,\omega)$ with a prescribed behavior in ω (here of the form $\mathcal{E}(k,\omega) \propto \omega^{-5/3}$), and numerically test the corresponding expected form for the flow two-time correlation function $S_2(t) \equiv \langle |\boldsymbol{u}(\boldsymbol{x},t) - \boldsymbol{u}(\boldsymbol{x},0)|^2 \rangle$ By simple power counting, the resulting time behavior is $t^{2/3}$. The validity of this behavior can be detected in Fig. 1.4, where the $S_2(t)$ is reported as a function of t.

1.6 Infra-red resummation: numerical results and analysis

Having verified the accuracy of our kinematic model to reproduce the desired spectral properties of a given carrier flow, we are now ready to exploit it to verify the perturbative predictions of [25] on the emergence of anomalous diffusion of inertial particles in random parallel flows.
We thus need to solve (1.2), $\boldsymbol{u}(\boldsymbol{x},t)$ being a two-dimensional random parallel flow described by (1.22) with a given power-law spectrum (1.6) ($|k| \in [k_{\min}, k_{\max}]$ and $|\omega| \in [\omega_{\min}, \omega_{\max}]$). The two ultra-violet cutoffs provide, respectively, a minimal spatial length $L = 2\pi/k_{\max}$ and time $T = 2\pi/\omega_{\max}$ through which we made our system dimensionless. Our velocity spectra will thus always have ultra-violet cutoffs equal to 2π.
What we are going to do is to move the infra-red regularizing cutoffs closer

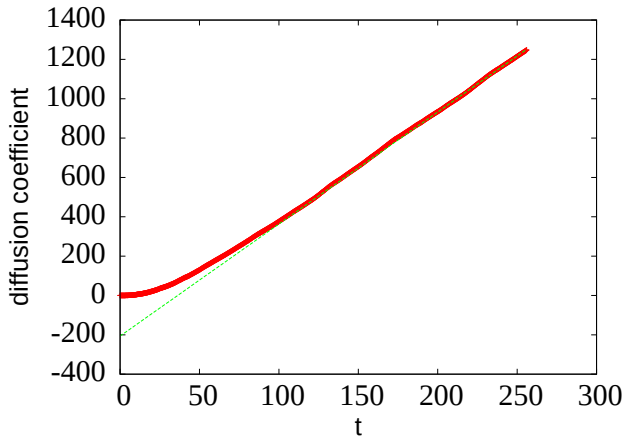

Figure 1.5: An example of best fit of the form $\sigma^2(t) = at + b$ for the diffusion coefficient. Here St = 20.

and closer to zero in every numerical simulation and measure the diffusion coefficient. This is exactly the procedure we followed for the benchmark cases discussed in the previous section. Note that, to obtain a diffusive regime, one needs to wait longer and longer time (and/or a larger statistics) as the cutoffs approach zero. By virtue of what stated in the previous sections, we will set for every particle $\boldsymbol{\mathcal{V}}(0) = 0$. With respect to what we did in Sec. 1.5.2, best-fit curves are obtained with the fitting function $\sigma^2(t) = at + b$ on an interval $t \gtrsim 5\text{St}$, in order to neglect any offset or other transient residuals (see Fig. 1.5). Also, measures have been obtained by averaging the results arising from a discrete spectrum approximating the continuous one from above and below, respectively.

Defining the Péclet number as $\text{Pe} \equiv L^2/(D_0 T)$ (with $L = 2\pi/k_{\max}$ and $T = 2\pi/\omega_{\max}$), we set it equal to 1. The parallel flow we consider is flowing along the x axis, and only two components (xx and yy) of the eddy diffusivity are non-zero. Moreover, we consider the limit $\beta = 0$, which means diffusing particles much heavier than fluid particles.

As a representative sampling point of the zone C in Fig. 1.1, we choose the point corresponding to $\alpha = -5/3$, $\zeta = 1$. In this case, we can set $\omega_{\min} = 0$ because no divergence is present in the frequency part of the spectrum, and we only have to move the spatial infra-red cutoff towards zero. For such a flow, we can exploit (1.3) and integrate over the frequencies to obtain an analytical expression for the zeroth-order contribution (i.e. the tracer case). By setting $\langle A_i^2 \rangle \propto k_i^{-5/3}$ (or $k_{i+1}^{-5/3}$ with an approximation from below) in (1.22), one obtains:

$$D_{ij} = \delta_{ij} + \delta_{i1}\delta_{j1} \int_{k_{\min}}^{2\pi} \mathrm{d}k \; \frac{k^{1/3}}{2} \ln\left[1 + \frac{(2\pi)^2}{k^4}\right] . \tag{1.29}$$

From our Lagrangian simulations we can compute the mean-square particle displacement, $\sigma^2(t)$, given by (1.28), from which the trace of the eddy-diffusivity tensor is easily obtained via best fit. The resulting value has to be compared with the double of the trace of (1.29), which reads:

$$4 + \int_{k_{\min}}^{2\pi} \mathrm{d}k \; k^{1/3} \ln\left[1 + \frac{(2\pi)^2}{k^4}\right] \; . \tag{1.30}$$

In Fig. 1.6 the continuous line represents the above integral function, whilst the squares are our numerical results. The integration step was $\delta t = 0.0625$, the number of particles was 40000 (uniformly distributed on the entire box) and the integration was carried out for 8192 time steps. As expected, this case shows convergence as the infra-red cutoff goes to zero. Moreover, we can observe a change of concavity when $k_{\min} \lesssim 0.5$. There, the graph of (1.30) tends to a straight line and in the neighborhood of zero it has a sort of knee. This did not happen in the benchmark cases with the white noise, because no ultra-violet frequency cutoff was present and the eddy diffusivity had a pure power-law expression with respect to $k_{\min}$. Here, on the contrary, the integrating function in (1.30) has a logarithm, whose argument depends on the ratio between the ultra-violet cutoff frequency (2π in the present case) and k^2. The loss of self-similarity is thus a consequence of finite-size effects (i.e. a non zero ultra-violet cutoff).
A similar feature is present in Fig. 1.7. It corresponds to the same case analyzed in Fig. 1.6, but now the Stokes number is $\mathrm{St} = 0.5$, a representative value sufficiently small for the perturbative results to hold and, at the same time, to guarantee a sufficiently large effect of inertia on the diffusion process. In this figure, the change of concavity tells us that the diffusion coefficient definitely crosses the vertical axis. Consequently, the eddy diffusivity tends to a finite value even though $k_{\min} \to 0$. This contrasts the divergence predicted by the first-order perturbative correction given in (1.4). Infra-red resummations at higher orders in St are thus very likely to appear in the low-inertia perturbative expansion.

The fact that the behavior of the eddy diffusivity vs. the infra-red cutoff crosses the vertical axis is not peculiar of the chosen small Stokes number, the same behavior being observed for larger Stokes numbers as well, also far away from the perturbative region. To be more specific, we have fixed the infra-red cutoff $k_{\min}$ to the smallest value of Figs. 1.6–1.7, $k_{\min} \sim 0.098$, and computed the resulting eddy diffusivity for different Stokes numbers. The resulting curve is reported in Fig. 1.8. As one can see, a decreasing behavior clearly emerges from the simulations. Again, this seems to contradict the perturbative results: a diverging first-order correction in St for $k_{\min} \to 0$ should be associated (at least in the perturbative region of small St) to eddy diffusivities increasing with the Stokes number. This fact is clearly ruled out by our numerical results.
To conclude this section, it is worth observing that the monotonic character

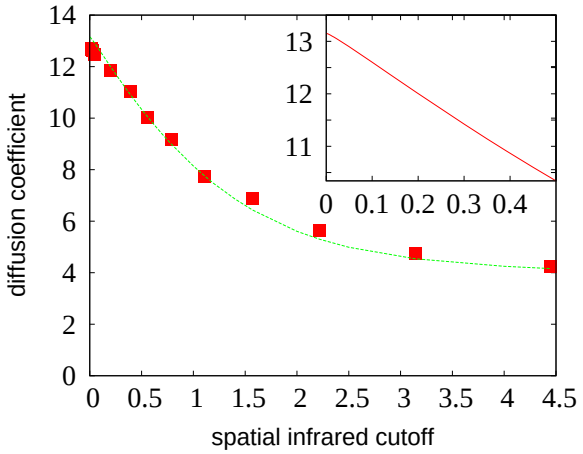

Figure 1.6: Diffusion coefficient as a function of the infra-red cutoff, $k_{\min}$, for $\mathrm{St} = 0$ (tracer case). The continuous line is the analytical result from (1.30), while the numerical results are denoted by squares. The velocity spectrum is a power law with exponents $\alpha = -5/3$, $\zeta = 1$. The inset is a zoom in the interval $k_{\min} \in [0, 0.5]$, showing the change of concavity and a knee close to 0.

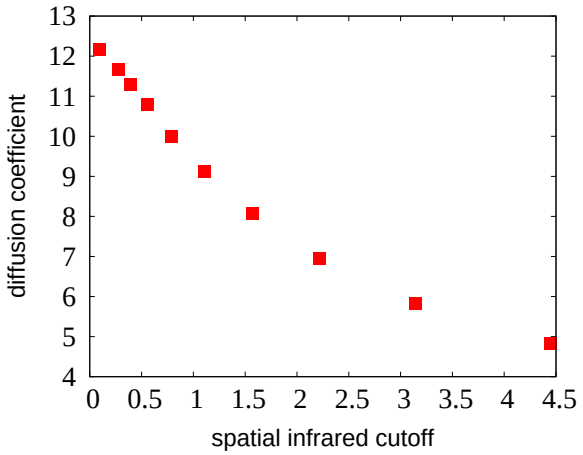

Figure 1.7: The measured eddy diffusivity as a function of the infra-red cutoff, $k_{\min}$, for $\mathrm{St} = 0.5$ (case with inertia). The curve clearly crosses the vertical axis, a fingerprint of standard diffusion, and shows a change of curvature similar to the one in the tracer case reported in Fig. 1.6 when the infra-red cutoff is $\lesssim 0.5$.

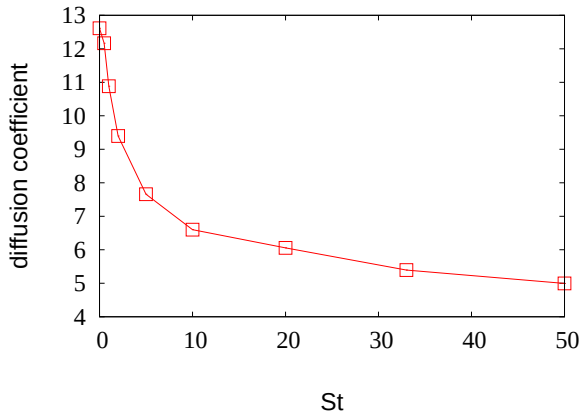

Figure 1.8: Diffusion coefficient for different Stokes numbers. The velocity spectrum is a power law with exponents $\alpha = -5/3$, $\zeta = 1$. The infra-red cutoffs are fixed to the values $k_{\min} \sim 0.098$ and $\omega_{\min} = 0$.

of the eddy diffusivity in St tells us that, among the two possible mechanisms discussed in relation to (1.18), the winner here is the one associated to decorrelation due to the mismatch between inertial and fluid trajectories.

1.7 Conclusions

In this chapter we have investigated the transport of inertial particles in the limit of large scales, where the diffusive limit sets in. The main aim of the present chapter was the investigation of anomalous diffusion for random parallel flows. In the presence of inertia, and the problem of identifying which properties of the carrier flow may cause anomalous diffusion becomes very challenging.

A first attempt to try to provide an answer in this direction was proposed in [25] for the case of random shear flow, using the same strategy exploited in [14] for inertialess particles in parallel flows. In this latter case the expression for the eddy diffusivity follows from a formal multiple-scale expansion. The same asymptotic method led to differential equations for the eddy diffusivity of inertial particles in the same parallel flow. An explicit expression follows after a second (regular) perturbative expansion in the Stokes number. Exploiting such an explicit expression, statistical properties of the infra-red part of the velocity spectrum were identified as a possible cause of anomalous diffusion.

By means of accurate Lagrangian simulations, we have verified that the small-Stokes expansion is affected by higher-order resummations that invalidate the conclusions based on the analysis of the sole first-order contribution. The mechanisms for the resummation of higher-order terms however remain

elusive, and call for a deep theoretical analysis on the complete structure of the perturbative expansion in the limit of small inertia. This will be indeed the aim of the chapter 3, where we will show that an explicit espression for eddy diffusivity in parallel flows is possible for inertial particle. However, the numerical approach adopted here it is instructive for the numerical method on a kinematic flow model we are going to use in the next chapter. That will be basically a sort of evolution of the model we presented here.

Appendix

In this Appendix we will treat the basic theory of the stochastic differential equations, in order to give a sense to expressions such as Eq.(1.2). Also, we will understand the origin of that very equation, which derives from the Maxey-Riley equation after many simplifications. These are however very reasonable in the majority of the applications for small particles, especially for the ones being much denser than the fluid. Eventually, we will introduce the concept of eddy diffusivity, and why the multiple-scale approach ought to be a good approach to deal with large-scale diffusion.

1.A Stochastic differential equations

Let us consider for simplicity a function $f : \mathbb{R} \to \mathbb{R}$. Generalization to the case $\mathbb{R} \to \mathbb{R}^n$ is trivial and well stated in [11].

Definition 1.A.1. Let us consider a function $f : \mathbb{R} \to \mathbb{R}$. Let Π be the set of all finite subdivision π of an interval $[0, T]$, with $0 = t_0 < t_1 < \cdots < t_n = T$. Its *total variation* is:

$$V_f(T) = \sup_{\pi \in \Pi} \sum_{i=0}^{n-1} |f(t_{i+1}) - f(t_i)| \tag{1.31}$$

If $V_f(T) < +\infty \, \forall T$, the function f is of *finite (total) variation.*

We recall that $f \in C^1[a, b]$ if $f \in C[a, b]$, f is differentiable on (a, b) and there exists another function $g \in C[a, b]$ which is equal to f' over the whole (a, b). For continuous functions, the supremum in Eq. (1.31) is obtained when the mesh size $|\pi| \equiv \sup_i |t_{i+1} - t_i| \to 0$ and $n \to \infty$. For $f \in C^1[a, b]$, the total variation is finite and equal to $\int_a^b |f'(t)|dt$ [12]. Finite variation functions which are also right continuous are a category of *càdlàg* functions – i. e., functions being continuous on the right side and with a limit on the left side at any point [11].

Definition 1.A.2. The *quadratic variation* of f is:

$$V_f^2(T) = \lim_{\substack{n \to \infty \\ |\pi| \to 0}} \sum_{i=0}^{n-1} (f(t_{i+1}) - f(t_i))^2 \tag{1.32}$$

A finite variation function has a quadratic variation equal to zero. Besides, when the total variation is bounded, the usual Lebesgue-Stjeltjes integrals is well-defined and independent of the mesh.

There can exist functions with infinite total variation and finite nonzero quadratic variations. An example is the paths of the Brownian motion. Stochastic calculus focuses on this kind of functions, especially by means of Ito and Stratonovich analysis. Extensions to locally jumping càdlàg functions having non-continuous quadratic variations are possible [11], although they are not of interest for us.

Theorem 1.A.1 (Ito's formula in $\mathbb{R}$)**.** If $X : [0, \infty) \to \mathbb{R}$ is a continuous function with continuous quadratic variation, and $F \in C^2(\mathbb{R})$ a twice continuously differentiable real function, then for $T \geq 0$:

$$F(X(T)) = F(X(0)) + \int_0^T F'(X)|_{X(s)} dX(s) + \frac{1}{2} \int_0^t F''(X)|_{X(s)} dV_X^2(s) \tag{1.33}$$

where $dV_X^2(s)$ is the measure induced by the quadratic variation, which is an isotone function, and the Ito integral of F' with respect to X is defined:

$$\int_0^T F'(X)|_{X(s)} dX(s) := \lim_{\substack{n\to\infty \\ |\pi|\to 0}} \sum_{n=0}^{n-1} F'(X)|_{X(t_i)} (X(t_{i+1}) - X(t_i))$$

Proof. By Taylor's theorem with Lagrange's remainder:

$$F(X(t_{i+1})) - F(X(t_i)) = F'(X)|_{X(t_i)} \Delta X_i + \frac{1}{2} F''(X)|_{X(\tilde{t_i})} (\Delta X_i)^2 \tag{1.34}$$

where $\Delta X_i = X(t_{i+1}) - X(t_i)$ and $\tilde{t_i} \in (t_i, t_{i+1})$. Eq. (1.34) can also be written as:

$$F(X(t_{i+1})) - F(X(t_i)) = F'(X)|_{X(t_i)} \Delta X_i + \frac{1}{2} F''(X)|_{X(t_i)} (\Delta X_i)^2 + R(t_i) \tag{1.35}$$

where $R(t_i) = \frac{1}{2} \left[F''(X)|_{X(\tilde{t_i})} - F''(X)|_{X(t_i)} \right] (\Delta X_i)^2$. It follows that:

$$|R(t_i)| \leq \frac{1}{2} (\Delta X_i)^2 \max_{0 \leq i \leq n-1} \max_{x_i, y_i \in \Delta X_i} \left| F''(X)|_{x_i} - F''(X)|_{y_i} \right|$$

We recall that $\forall i \; \exists \max_{x_i, y_i \in \Delta X_i} |F''(X)|_{x_i} - F''(X)|_{y_i}|$ due to Weierstrass theorem applied to the continuous second derivative $F''(X)$ on the subintervals $[t_i, t_{i+1}]$. By taking the biggest one of all of these n values, we will obtain a certain ϵ_π, and as a consequence:

$$|R(t_i)| \leq \epsilon_\pi (\Delta X_i)^2$$

If we now sum every term of Eq. (1.35) from $i = 0$ to $n-1$ and take the limit of the mesh size to 0:

$$\lim_{\substack{n\to\infty \\ |\pi|\to 0}} \left| \sum_{i=0}^{n-1} R(t_i) \right| \leq \lim_{\substack{n\to\infty \\ |\pi|\to 0}} \epsilon_\pi \sum_{i=0}^{n-1} (\Delta X_i)^2 = 0 \tag{1.36}$$

since $\sum_{i=0}^{n-1}(\Delta X_i)^2$ is bounded by the finite quadratic variation, whereas $\epsilon_\pi \to 0$ as $|\pi| \to 0$ because $\max_{x_i, y_i \in \Delta X_i} |F''(X)|_{x_i} - F''(X)|_{y_i}| \to 0$ due to the continuity of F"(X) in every sub-interval. Thus we end up with:

$$F(X(T)) - F(X(0)) = \lim_{\substack{n\to\infty \\ |\pi|\to 0}} \sum_{i=0}^{n-1} F'(X)|_{X(t_i)} \Delta X_i + \frac{1}{2} \lim_{\substack{n\to\infty \\ |\pi|\to 0}} \sum_{i=0}^{n-1} F''(X)|_{X(t_i)} (\Delta X_i)^2 \tag{1.37}$$

whence the claim. □

The Ito formula is often written in differential form, that is, as a Stochastic Differential Equation, that is a relationship between (Ito) differentials:

$$dF(X(t)) = F'(X)|_{X(t)} dX(t) + \frac{1}{2} F''(X)|_{X(t)} dV_X^2(t)$$

This must be meant as:

$$F(X(t_{i+1})) - F(X(t_i)) \to F'(X)|_{X(t_i)} \Delta X_i + \frac{1}{2} F''(X)|_{X(t_i)} (\Delta X_i)^2$$

up to other terms which tend to 0 when the sum and the mesh zero-size limit are taken. SDEs indeed are not differential equations proper, but relationships between differentials which constitute the infinitesimal limit of the increments of integral equations.

Another often used discretization is:

Theorem 1.A.2 (Stratonovich's formula in $\mathbb{R}$)**.** If $X : [0, \infty) \to \mathbb{R}$ is a continuous function with continuous quadratic variation, and $F \in C^2(\mathbb{R})$ a twice continuously differentiable real function, then for $T \geq 0$:

$$F(X(T)) = F(X(0)) + \int_0^T F'(X)|_{X(s)} \circ dX(s) \tag{1.38}$$

where the Stratonovich integral of F' with respect to X is defined:

$$\int_0^T F'(X)|_{X(s)} \circ dX(s) := \lim_{\substack{n\to\infty \\ |\pi|\to 0}} \sum_{n=0}^{n-1} \frac{F'(X)|_{X(t_{i+1})} + F'(X)|_{X(t_i)}}{2} (X(t_{i+1}) - X(t_i))$$

Proof. We start from Eq. (1.35), where we can plug the Taylor-Peano formula[4]:

$$F'(X)|_{X(t_{i+1})} = F'(X)|_{X(t_i)} + F''(X)|_{X(t_i)}(\Delta X_i) + o(\Delta X_i)$$

If we substitute the second derivative in Eq. (1.35) from the previous one, it takes this form:

$$F(X(t_{i+1}))-F(X(t_i)) = \frac{F'(X)|_{X(t_{i+1})} + F'(X)|_{X(t_i)}}{2}\Delta X_i - o(\Delta X_i)^2 + R(t_i) \tag{1.39}$$

bearing in mind that we could write $o(\Delta X_i) = o_i(1)\Delta X_i$, where $o_i(1)$ is a generic quantity tending to 0 when $\Delta X_i \to 0$. If we now sum every term of Eq. (1.39) from $i = 0$ to $n-1$ and take the limit of the mesh size to 0, again $R(t_i) \to 0$. Moreover,

$$\lim_{\substack{n\to\infty \\ |\pi|\to 0}} \left| \sum_{n=0}^{n-1} o_i(1)(\Delta X_i)^2 \right| \leq \lim_{\substack{n\to\infty \\ |\pi|\to 0}} \left| \max_{0\leq i\leq n-1} o_i(1) \right| \sum_{n=0}^{n-1} (\Delta X_i)^2 = 0$$

due to the boundedness of the quadratic variation. We conclude then:

$$F(X(T)) - F(X(0)) = \lim_{\substack{n\to\infty \\ |\pi|\to 0}} \sum_{i=0}^{n-1} \frac{F'(X)|_{X(t_{i+1})} + F'(X)|_{X(t_i)}}{2}\Delta X_i \tag{1.40}$$

whence the claim. □

Stratonovich formula is more convenient owing to its formally equivalent form to the classical Torricelli-Barrow fundamental integral formula. This makes it useful for stochastic differential geometry, because the usual differentiation rules still hold true [13]. Stratonovich formula is often written in differential form:

$$dF(X(t)) = F'(X)|_{X(t)} \circ dX(t)$$

which must be meant:

$$F(X(t_{i+1})) - F(X(t_i)) \to \frac{F'(X)|_{X(t_{i+1})} + F'(X)|_{X(t_i)}}{2}\Delta X_i$$

Sometimes it is useful to pass from Ito to Stratonovich differential to apply ordinary calculus rules to SDEs, namely when there are multiplicative noises.

[4]According to the "little-o notation", $f(x) \sim o(g(x))$ when$x \to x_0$ iff $\forall\epsilon\,\exists A \ni x_0 : |f(x)| < \epsilon|g(x)|\ \forall x \in A - \{x_0\}$. If g is non-zero in a punctured neighbourhood of x_0, this is equivalent to $\lim_{x\to x_0} f(x)/g(x) = 0$.

Example 1.A.1. Consider the Ito SDE:

$$d\xi(t) = 2W(t)dW(t) + dt$$

In order to solve it, we will convert it in a Stratonovich representation:

$$\begin{aligned}\Delta\xi(t_i) &= 2W(t_i)\Delta W(t_i) + \Delta t_i = \\ &\quad 2\left[\frac{W(t_i) + W(t_{i+1})}{2} - \frac{\Delta W(t_i)}{2}\right]\Delta W(t_i) + \Delta t_i\end{aligned} \tag{1.41}$$

If we now sum all of the terms from $i = 0$ to $n - 1$ and take the limit of the mesh size to 0:

$$\lim_{\substack{n\to\infty \\ |\pi|\to 0}} \sum_{n=0}^{n-1} \left[(W(t_i) + W(t_{i+1}))\Delta W(t_i) - (\Delta W(t_i))^2 + \Delta t_i\right]$$

Remembering that $\lim_{\substack{n\to\infty \\ |\pi|\to 0}} \sum_{n=0}^{n-1}(\Delta W(t_i))^2 = T$, we obtain:

$$\xi(T) - \xi(0) = \int_0^T W(t) \circ dW(t) - \not{T} + \not{T} \tag{1.42}$$

or, in differential form:

$$d\xi(t) = W(t) \circ dW(t)$$

Eq. (1.42) can be promptly solved in the "usual" manner to arrive at:

$$\xi(t) = \xi(0) + \frac{1}{2}[W(t)]^2$$

Example 1.A.2. We want to compute:

$$\int_0^t W(t')dW(t')$$

We can write in differential form:

$$dx = W(t)dW(t)$$

$$\begin{aligned}&\Delta x(t_i) = W(t_i)\Delta W(t_i) = W(t_i)\frac{W(t_i) + W(t_{i+1}) + W(t_i) - W(t_{i+1})}{2}\Delta W_i \\ &= W(t_i)\frac{W(t_i) + W(t_{i+1})}{2} - \frac{1}{2}(\Delta W_i)^2\end{aligned} \tag{1.43}$$

After we take the sum and the zero-size limit of the mesh:

$$x(t) = \int_0^t W(t') \circ dW(t') - \frac{1}{2}\int_0^t dt'$$

and, by integrating both members, we finally achieve the strange result:

$$\int_0^t W(t')dW(t') = \frac{W^2(t)}{2} - \frac{t}{2}$$

We now consider the following Ito SDE:

$$dX(t) = b(X(t),t)dt + A(X(t),t)dW(t) \tag{1.44}$$

For $F(X,t) \in C^2(\mathbb{R})$ with respect to X and $C^1(\mathbb{R})$ with respect to t, we have:

$$\begin{aligned}
& F(X(t),t) - F(X(0),0) \\
= & \sum_{n=0}^{n-1}\left[\frac{\partial F}{\partial X}|_{X(t_i),t_i}\Delta X_i + \frac{1}{2}\frac{\partial^2 F}{\partial X^2}|_{X(t_i),t_i}(\Delta X_i)^2 + \frac{\partial F}{\partial t}|_{X(t_i),t_i}\Delta t_i\right. \\
+ & \left. o(\Delta t_i) + o(\Delta X_i)^2\right] \\
= & \sum_{n=0}^{n-1}\left[\left(\frac{\partial F}{\partial X}|_{X(t_i),t_i} b(X(t_i),t_i) + \frac{\partial F}{\partial t}|_{X(t_i),t_i}\right)\Delta t_i\right. \\
+ & \frac{\partial F}{\partial X}|_{X(t_i),t_i} A(X(t_i),t_i)\Delta W_i \\
+ & \left.\frac{1}{2}\frac{\partial^2 F}{\partial X^2}|_{X(t_i),t_i} A^2(X(t_i),t_i)(\Delta W_i)^2\right] + \sum_{n=0}^{n-1}\left[o(\Delta t_i) + o(\Delta W_i \Delta t_i)\right]
\end{aligned} \tag{1.45}$$

Now, $o(\Delta W_i \Delta t_i) \sim o(\Delta t_i)$ due to the boundedness of the Wiener process, which is a continuous function, over the closed interval [0,T]. Once again:

- $\lim\limits_{\substack{n\to\infty \\ |\pi|\to 0}} \left|\sum_{n=0}^{n-1}\left[o(\Delta t_i) + o(\Delta W_i \Delta t_i)\right]\right| \leq \lim\limits_{\substack{n\to\infty \\ |\pi|\to 0}} \left|\max_i o_i(1)\right| T = 0;$

- $\lim\limits_{\substack{n\to\infty \\ |\pi|\to 0}} \sum_{n=0}^{n-1} \frac{1}{2}\frac{\partial^2 F}{\partial X^2}|_{X(t_i),t_i} A^2(X(t_i),t_i)(\Delta W_i)^2$

$$= \int_0^T \frac{1}{2}\frac{\partial^2 F}{\partial X^2}|_{X(t),t} A^2(X(t),t)dV_W^2(t) = \int_0^T \frac{1}{2}\frac{\partial^2 F}{\partial X^2}|_{X(t),t} A^2(X(t),t)dt$$

by having used the well-known properties of the quadratic variation of the Wiener process. Thus we obtain the following relationship between Ito differentials:

Theorem 1.A.3.

$$\begin{aligned} & dF(X(t),t) \\ = & \left(\frac{\partial F}{\partial X}|_{X(t),t} b(X(t),t) + \frac{\partial F}{\partial t}|_{X(t),t} + \frac{1}{2}\frac{\partial^2 F}{\partial X^2}|_{X(t),t} A^2(X(t),t)\right) dt \\ + & \frac{\partial F}{\partial X}|_{X(t),t} A(X(t),t) dW(t) \end{aligned} \tag{1.46}$$

Likewise, by means of Taylor-Peano expansions plugged into Eq. (1.46), one could prove Stratonovich's version:

Theorem 1.A.4.

$$\begin{aligned} & dF(X(t),t) \\ = & \left[\left(b(X(t),t) - \frac{1}{2}A(X(t),t)\frac{\partial A}{\partial X}|_{X(t),t}\right)\frac{\partial F}{\partial X}|_{X(t),t} + \frac{\partial F}{\partial t}|_{X(t),t}\right] dt \\ + & \left[\frac{\partial F}{\partial X}|_{X(t),t} A(X(t),t)\right] \circ dW(t) \end{aligned} \tag{1.47}$$

Corollary 1.A.1.

$$\begin{aligned} & dX(t) = b(X(t),t)dt + A(X(t),t)dW(t) \\ = & \left[b(X(t),t) - \frac{1}{2}A(X(t),t)\frac{\partial A}{\partial X}|_{X(t),t}\right] dt + A(X(t),t) \circ dW(t) \end{aligned}$$

Proof. Apply the theorems 1.46-1.47 with F(X)=X. □

Analogous results are attainable for vector stochastic fields $\boldsymbol{X}(t)$.

Example 1.A.3. To solve Ito's SDE:

$$dx = x\ dW(t) \quad ,$$

we apply the previous corollary with $A = x$, $b = 0$:

$$dx = -\frac{1}{2}x dt + x \circ dW(t)$$

We now devide both members by x and integrate both of the members with the standard integral theorem:

$$\ln \frac{x(t)}{x(0)} = \frac{-t}{2} + W(t)$$

whence the general integral follows:

$$x(t) = x(0)e^{-\frac{t}{2}+W(t)}$$

1.B Small particles in a flow: Maxey-Riley equation an its simplified versions

The study of the dispersed phase is done through a Lagrangian description. We are going to start with the Maxey-Riley model [30] which is valid for point-like particles. The trajectory of each particle in the flow is tracked by evaluating its position at a certain time, $\mathcal{X}(t)$, from:

$$\frac{\mathrm{d}\boldsymbol{\mathcal{X}}}{\mathrm{d}t} = \mathbf{V}(t) \tag{1.48}$$

The particle velocity obeys the following equation:

$$\begin{aligned} m_\mathrm{p}\frac{\mathrm{d}\mathbf{V}}{\mathrm{d}t} = 6\pi r_\mathrm{p}\mu[\mathbf{u}(\boldsymbol{\mathcal{X}}(t),t) - \mathbf{V}(t) + \frac{1}{6}r_\mathrm{p}^2\nabla^2\mathbf{u}|_{\boldsymbol{\mathcal{X}}(t)}] + m_\mathrm{f}\frac{\mathrm{D}\mathbf{u}}{\mathrm{D}t}\bigg|_{\boldsymbol{\mathcal{X}}(t)} + (m_\mathrm{p} - m_\mathrm{f})\mathbf{g} + \\ + \frac{1}{2}m_\mathrm{f}\left[\frac{\mathrm{D}\mathbf{u}}{\mathrm{D}t}\bigg|_{\boldsymbol{\mathcal{X}}(t)} - \frac{\mathrm{d}\mathbf{V}}{\mathrm{d}t} + \frac{1}{10}r_\mathrm{p}^2\frac{\mathrm{d}}{\mathrm{d}t}(\nabla^2\mathbf{u})\bigg|_{\boldsymbol{\mathcal{X}}(t)}\right] + \\ + 6r_\mathrm{p}^2\rho_\mathrm{f}\sqrt{\pi\nu}\int_0^t \frac{1}{\sqrt{t-\tau}}\frac{\mathrm{d}}{\mathrm{d}\tau}[\mathbf{u}(\boldsymbol{\mathcal{X}}(t),t) - \mathbf{V}(t) + \frac{1}{6}r_\mathrm{p}^2\nabla^2\mathbf{u}|_{\boldsymbol{\mathcal{X}}(t)}]\,\mathrm{d}\tau\ , \end{aligned} \tag{1.49}$$

where, $\mathbf{u}(\boldsymbol{\mathcal{X}}(t),t)$ is the flow velocity evaluated at the particle position, ρ_f is the fluid density, ρ_p is the particle density, r_p is the particle radius, μ and ν are respectively the dynamic and kinematic viscosities of the fluid, $m_\mathrm{p} = \frac{4}{3}\pi r_\mathrm{p}^3\rho_\mathrm{p}$ is the particle mass, $m_\mathrm{f} = \frac{4}{3}\pi r_\mathrm{p}^3\rho_\mathrm{f}$ is the mass of the fluid element of same volume and $\mathbf{g}$ is the gravitational acceleration vector.

Maxey-Riley equation comes from handling the equation for the flow around the sphere perturbatively. Indeed, in [30] the authors firstly introduced the flow including the feedback given by the sphere, $\mathbf{v}(\mathbf{x},t)$, and the undisturbed flow field $\mathbf{u}(\mathbf{x},t)$. Then, they started by writing the Navier Stokes equation for the flow in the frame reference of the sphere, by introducing $\mathbf{w}(\mathbf{x},t) = \mathbf{v}(\mathbf{x},t) - \mathbf{V}(t)$:

$$\begin{aligned} \frac{d\mathbf{w}}{dt} + \mathbf{w}\cdot\nabla\mathbf{w} &= \mathbf{g} - \frac{d\mathbf{V}}{dt} - \frac{1}{\rho}\nabla p + \nu\nabla^2\mathbf{w} \\ \nabla\cdot\mathbf{w} &= 0 \end{aligned} \tag{1.50}$$

with the limt condition that $\mathbf{w} \to \mathbf{u} - \mathbf{V}$ as $|\mathbf{x}| \to \infty$. They supposed the particle radius r_p is very small in comparison to the minimal undisturbed flow length L, thus they could split w in $\mathbf{w}^{(0)} = \mathbf{u} - \mathbf{V}$ and the perturbation $\mathbf{w}^{(1)} = \mathbf{w} - \mathbf{w}^{(0)}$ and solve the Navier-Stokes equation perturbatively. The

equation for the perturbation is:

$$\begin{aligned}\frac{d\mathbf{w}^{(1)}}{dt}+\mathbf{w}^{(1)}\cdot\nabla\mathbf{w}^{(0)}+\mathbf{w}^{(0)}\cdot\nabla\mathbf{w}^{(1)}+\mathbf{w}^{(1)}\cdot\nabla\mathbf{w}^{(1)} &= -\frac{1}{\rho}\nabla p^{(1)}+\nu\nabla^2\mathbf{w}^{(0)}\\ \nabla\cdot\mathbf{w}^{(1)} &= 0\end{aligned} \tag{1.51}$$

We now consider the typical values $W^{(0)}$, $W^{(1)}, T^{(1)}, P^{(1)}, r_p$ and L to evaluate the order of magnitude of all of the addends as to have any element of the equation order O(1). We recall that $\nabla\mathbf{w}^{(0)}{=}\nabla\mathbf{u} = U/L$, and that $W^{(0)} \gg W^{(1)}$.

$$\begin{aligned}&\frac{W^{(1)}}{T}\frac{d\hat{\mathbf{w}}^{(\mathbf{1})}}{dt}+\frac{W^{(1)}U}{L}\hat{\mathbf{w}}^{(\mathbf{1})}\cdot\nabla\mathbf{w}^{(0)}+\frac{W^{(1)}W^{(0)}}{r_p}\mathbf{w}^{(0)}\cdot\nabla\hat{\mathbf{w}}^{(\mathbf{1})}\\ &+\frac{W^{(1)\,2}}{r_p}\hat{\mathbf{w}}^{(\mathbf{1})}\cdot\nabla\hat{\mathbf{w}}^{(\mathbf{1})}=-\frac{P^{(1)}}{r_p\rho}\nabla\hat{p}^{(1)}+\frac{\nu W^{(1)}}{r_p^2}\nabla^2\mathbf{w}^{(1)}\\ &\nabla\cdot\mathbf{w}^{(1)}=0\end{aligned} \tag{1.52}$$

or, equivalently:

$$\begin{aligned}&\frac{r_p^2}{\nu T}\frac{d\hat{\mathbf{w}}^{(\mathbf{1})}}{dt}+\frac{r_p^2U}{\nu L}\hat{\mathbf{w}}^{(\mathbf{1})}\cdot\nabla\mathbf{w}^{(0)}+\frac{r_pW^{(0)}}{\nu}\mathbf{w}^{(0)}\cdot\nabla\hat{\mathbf{w}}^{(\mathbf{1})}\\ &+\frac{r_pW^{(1)}}{\nu}\hat{\mathbf{w}}^{(\mathbf{1})}\cdot\nabla\hat{\mathbf{w}}^{(\mathbf{1})}=-\frac{r_pP^{(1)}}{\nu\rho W^{(1)}}\nabla\hat{p}^{(1)}+\nabla^2\hat{\mathbf{w}}^{(\mathbf{1})}\\ &\nabla\cdot\mathbf{w}^{(1)}=0\end{aligned} \tag{1.53}$$

We now require $\frac{r_pW^{(0)}}{\nu} \ll 1$ - and, as a consequence, $\frac{r_pW^{(1)}}{\nu}$ -, which means that the *Reynolds number* of the relative velocity with respect to the radius of the particle is very small. We also require that $\frac{r_p^2U}{\nu L} \ll 1$. Thus, Eqs. (1.51) simplify as follows:

$$\begin{aligned}\frac{d\mathbf{w}^{(1)}}{dt} &= -\frac{1}{\rho}\nabla p^{(1)}+\nu\nabla^2\mathbf{w}^{(1)}\\ \nabla\cdot\mathbf{w}^{(1)} &= 0\end{aligned} \tag{1.54}$$

that is, the advective terms are ruled out. This is preparatory for neglecting advective terms in Eq.(1.49), which allows us to substitute:

$$m_f\frac{D\mathbf{u}}{Dt}m_f=\frac{\partial\mathbf{u}}{\partial t}+m_f\mathbf{u}\cdot\nabla\mathbf{u}\Longrightarrow m_f\frac{d\mathbf{u}}{dt}=m_f\frac{\partial\mathbf{u}}{\partial t}+m_f\mathbf{V}\cdot\nabla\mathbf{u}$$

Indeed, their difference $m_f \mathbf{w} \cdot \nabla \mathbf{u}$ is of order $\sim O(W^{(0)} r_p^3 \rho_f U/L)$. The Stokes viscous friction term in Eq. (1.49), which is the one proportional to the relative velocity of the particle with respect to the flow, is instead of order $\sim O(r_p \nu \rho W^{(0)})$. Their ration thus is $\sim O(\frac{r_p^2 U}{\nu L})$, which was supposed to be $\ll 1$ in Maxey-Riley hypothesis. This two kinds of derivative in the terms proportional to the flow mass can be interchanged freely, since their difference is not appreciable due to the presence of the viscous Stokes term. Numerical simulations in Gollub oscillating cell flows at high frequency have shown that the two derivative are indistinguishable until $\frac{r_p^2 U}{\nu L}$ is of order $\sim 10^{-3}$, which therefore defines a range of validity of the Maxey-Riley model. Maxey-Riley equation assumes now the following aspect:

$$m_{\mathrm{p}} \frac{\mathrm{d}\mathbf{V}}{\mathrm{d}t} = 6\pi r_{\mathrm{p}} \mu [\mathbf{u}(\boldsymbol{\mathcal{X}}(t), t) - \mathbf{V}(t) + \frac{1}{6} r_{\mathrm{p}}^2 \nabla^2 \mathbf{u}|_{\boldsymbol{\mathcal{X}}(t)}] + m_{\mathrm{f}} \frac{\mathrm{d}\mathbf{u}}{\mathrm{d}t}\bigg|_{\boldsymbol{\mathcal{X}}(t)} + (m_{\mathrm{p}} - m_{\mathrm{f}})\mathbf{g} +$$
$$+ \frac{1}{2} m_{\mathrm{f}} \left(\frac{\mathrm{d}}{\mathrm{d}t} \left[\mathbf{u} + \frac{1}{10} r_{\mathrm{p}}^2 (\nabla^2 \mathbf{u}) \right) \bigg|_{\boldsymbol{\mathcal{X}}(t)} - \frac{\mathrm{d}\mathbf{V}}{\mathrm{d}t}\bigg|_{\boldsymbol{\mathcal{X}}(t)} \right] +$$
$$+ 6 r_{\mathrm{p}}^2 \rho_{\mathrm{f}} \sqrt{\pi \nu} \int_0^t \frac{1}{\sqrt{t-\tau}} \frac{\mathrm{d}}{\mathrm{d}\tau} [\mathbf{u}(\boldsymbol{\mathcal{X}}(t), t) - \mathbf{V}(t) + \frac{1}{6} r_{\mathrm{p}}^2 \nabla^2 \mathbf{u}|_{\boldsymbol{\mathcal{X}}(t)}] \, \mathrm{d}\tau \ , \quad (1.55)$$

Similarly, the Faxen corrections $\propto r_p^2 \nabla^2 \mathbf{u}$ are in ratio of $O(r_p^2/L^2)$ with respect to the velocity $\mathbf{u}$ and thus can be always neglected in the square brackets of Eq. (1.55) by virtue of the limit of very small particles.

Henceforth we will suppose gravity is not present, even though it does not complicate the diffusion problem that much in general . By introducting the parameter $\beta = \frac{3\rho_f}{2\rho_p + \rho_f}$ and the *Stokes time* $\tau = r_p^2/(3\nu\beta)$ (the previous condition $\frac{r_p^2 U}{\nu L} \ll 1$ becomes $\tau\beta U/L \ll 1$), we can rearrange Eq. (1.55) in the following form (without gravity):

$$\begin{aligned} \frac{\mathrm{d}\boldsymbol{V}(t)}{\mathrm{d}t} &= -\frac{\boldsymbol{V}(t) - \boldsymbol{u}(\boldsymbol{\mathcal{X}}(t), t)}{\tau} + \beta \frac{d\boldsymbol{u}(\boldsymbol{\mathcal{X}}(t), t)}{dt} \\ &+ \sqrt{\frac{27}{\pi} \frac{3\beta}{(3-\beta)^2 \tau}} \int_0^t \frac{\mathrm{d}t'}{\sqrt{t-t'}} \frac{\mathrm{d}}{\mathrm{d}t'} [\boldsymbol{u}(\boldsymbol{\mathcal{X}}(t'), t') - \boldsymbol{V}(t')] \end{aligned} \quad (1.56)$$

The last term, *Basset term*, is always negligible for *heavy particles* (i.e. $\beta \to 0$, such as metal particles in air for which it is of order 10^4). Very often, Basset term is neglected in any case, due to the difficulty of evaluating it computationally, owing to the history dependence. Besides, its correctness has been questioned by more efficient model for not-too-small Reynolds numbers with respect to the particle radius [8]. However, in point-like particles microscopical molecular collisions might become important, and then

a Wiener noise contribution ought to be added to the forces. This is what we are going to do in the next chapters.

It is worth to point out that original Maxey-Riley equation – i. e. Eq. (1.49) with the original term $\frac{1}{2}m_{\mathrm{f}}\left[\left.\frac{\mathrm{d}\mathbf{u}}{\mathrm{d}t}\right|_{\boldsymbol{\mathcal{X}}(t)} - \frac{\mathrm{d}\mathbf{V}}{\mathrm{d}t}\right]$ instead of Auton's term $\frac{1}{2}m_{\mathrm{f}}\left[\left.\frac{\mathrm{D}\mathbf{u}}{\mathrm{D}t}\right|_{\boldsymbol{\mathcal{X}}(t)} - \frac{\mathrm{d}\mathbf{V}}{\mathrm{d}t}\right]$ – had been derived by splitting the force in the undisturbed flow contribution plus that from the disturbance. Namely:

$$m_p\frac{d\mathbf{V}}{dt} = (m_p - m_f)\mathbf{g} + \left.\frac{D\mathbf{u}}{Dt}\right|_{\boldsymbol{\mathcal{X}}(t)} + \mathbf{F}^{(1)}$$

where $F^{(1)}$ is obtained by applying a reciprocity theorem on the disturbance for Stokes flows and expressions for particles in a time-dependent flow where a spatial distribution of forces is assigned [9]. The Laplace transform of $F^{(1)}$ Maxey and Riley arrived at is:

$$\hat{F}_i^{(1)}(s) = -\hat{A}_i[6\pi r_p\mu(1+\lambda r_p)+\frac{1}{2}m_f s]-r_p^2[(\hat{C}_{1jj}+2\hat{C}_{jj1})\pi\mu r_p(1+\lambda r_p)+\frac{1}{20}s\hat{C}_{1jj}]$$

where

$$\lambda^2 = \rho_f s/\mu, \qquad A_i(t) = V_i(t) - u_i(\mathcal{X}(t),t), \qquad C_{ijk} = -\frac{\partial^2 u_i}{\partial x_j \partial x_k}$$

Then, by means of Laplace antitransform, we obtain Maxey-Riley equation *provided that* $\mathbf{u}(\boldsymbol{\mathcal{X}}(0),0)-\mathbf{V}(0) = 0$. The latter represents then a condition of validity for Maxey-Riley equation. However, when one neglects Basset term and studies diffusion problems, numerical evidences show that asymptotic diffusion statistics on a large amount of particles is independent of the initial velocity, and this initial condition can be ignored. Sometimes analitical proofs, such as the one will see in Chapter 3, allow to see the independence of the initial velocity of particles too.

1.C Taylor formula and Central Limit Theorem

We consider the process:

$$\boldsymbol{x}(t) = \int_0^t \boldsymbol{v}(s)ds \tag{1.57}$$

where the field has a Lagrangian second-order stationary statistics and a given probability density function. This means that:

$$\langle\boldsymbol{x}(t)\rangle = \langle\int_0^t \boldsymbol{v}(s)ds\rangle = \langle\int_{t'}^{t+t'} \boldsymbol{v}(s)ds\rangle = \langle\boldsymbol{v}\rangle t$$

As to the variance,

$$\sigma(t) \equiv \langle \int_0^t ds \int_0^t ds' \boldsymbol{v}(s) \otimes \boldsymbol{v}(s') \rangle = \int_0^t ds \int_0^t C(|s-s'|) ds' = \int_0^t ds \int_{-s}^{t-s} C(|s'|) ds'$$

Its long-time asymptotics is:

$$\sigma(t) \sim_{t\to\infty} \int_0^t ds \int_{-s}^t C(|s'|) ds' = \int_0^t C(|s'|) ds' \int_0^t ds + \int_{-t}^0 C(|s'|) ds' \int_{-s'}^t ds$$

$$= \int_0^t ds C(|s|)(2t - s)$$

after a variable change $s \to -s$ in the last passage. If we evaluate:

$$\lim_{t\to\infty} \frac{d}{dt}\sigma = 2 \int_0^\infty C(s) ds \equiv 2D^{(ef)} \equiv 2\langle v^2 \rangle T_c$$

provided that $tC(t) \to 0$ as $t \to \infty$, where T_c is the *integrated correlation time (tensor)* and $\langle v^2 \rangle$ is the root-mean-square velocity. The displacement variance then:

$$\sigma \sim_{t\to\infty} 2D^{(ef)} t$$

having indicated with $D^{(ef)}$ the *eddy (or effective) diffusivity*. As $t \to \infty$, if the correlation function decays sufficiently fast as we supposed, the Central Limit Theorem applies to the position process $\boldsymbol{x}(t)$. In that case indeed, after a time $t \sim T_c$, the random variables:

$$\int_0^{T_c} \boldsymbol{v}(t) dt, \qquad \dots, \qquad \int_{nT_c}^{(n+1)T_c} \boldsymbol{v}(t) dt, \qquad \dots \tag{1.58}$$

can be considered independent, and they will have the same probability density function owing to the second order stationarity, with the mean value:

$$\int_0^{T_c} \langle \boldsymbol{v}(t) \rangle dt = \dots = \int_{nT_c}^{(n+1)T_c} \langle \boldsymbol{v}(t) \rangle = \dots = \langle \boldsymbol{v} \rangle T_c$$

thanks to the stationarity of the average of the velocity. Besides, its variance tensor will be:

$$\int_0^{T_c} dt \int_0^{T_c} dt' \langle \boldsymbol{v}(t) \otimes \boldsymbol{v}(t') \rangle = \dots = \int_{nT_c}^{(n+1)T_c} dt \int_{nT_c}^{(n+1)T_c} dt' \langle \boldsymbol{v}(t) \otimes \boldsymbol{v}(t') \rangle = \dots$$

where we have exploited the substitutions $t + nT_c \to t$, $t' + nT_c \to t'$and the stationarity of the correlation tensor $\langle \boldsymbol{v}(t) \otimes \boldsymbol{v}(t') \rangle = C(|t - t'|)$. It follows that the Central Limit theorem applies to the random variables (1.58), and after a large number of n steps, the process can be considered as a sum over independent Gaussian processes. This is exactly the same as having a white

noise – the distributional derivative of Wiener process, which is δ-correlated in time – whose single time step would play the role of $n \gg 1$ time steps as long as T_c of the process in Eq. (1.57). In particular, if we heuristically define a *large scale* $T = m\Delta t = mnT_c$, with $n \gg 1$, the system (1.57) is equivalent to a white noise in the sense that:

$$\boldsymbol{x}(T) = \int_0^T \boldsymbol{v}(s)ds \to_{n\to\infty} \sqrt{2D^{(ef)}} \int_0^T \boldsymbol{\eta}(s)ds = \sqrt{2D^{(ef)}} \int_0^T d\boldsymbol{\omega}(s)$$

This heuristically justifies the use of multiple scale analysis for chaotic and stochastic systems we also will perform in the next chapters.

However, if the correlation function does not satisfy $tC(t) \to 0$, or if the process is not stationary, previous arguments fail and anomalous diffusion can arise. The latter is nomore a Gaussian process, the Central Limit Theorem not being applicable any longer and σ not being anymore defined .

Chapter 2

Explicit closure for eddy-diffusivity fields and effective large-scale advection in turbulent transport

2.1 Introduction

Turbulent transport of passive particles and heat is a problem of paramount importance in a variety of situations ranging from environmental sciences and engineering to biophysics. Heat-transfer problems in heat exchangers, gas turbines, and nuclear reactors, pollution dispersal in urban atmospheres and spore dispersal are a few examples.
It is also important as a playground where analytical methods borrowed from the realm of statistical mechanics can be successfully exploited in relation to many long-standing issues related, e.g., to closure problems [43], intermittency [38, 44, 45, 46] and strong anomalous diffusion [16, 19].

In many relevant situations one is not interested to study the dispersion phenomenon in detail but, rather, to focus the attention on a sub-set of active degrees of freedom. In fully developed turbulence, for a Prandtl number of order one, their number diverges as $Pe^{9/4}$ when the Péclet number, Pe, goes to infinity. The situation is similar to the well-known $Re^{9/4}$ divergence of the number of active degrees of freedom by increasing the Reynolds number, Re, in hydrodynamic turbulence [58]. Because of the fact that the Péclet number is often very large (e.g., in the atmosphere it is of the order of 10^6 or even larger) the need to focus the attention on the sole large-scale features of the dispersion phenomenon has, *de facto*, a practical motivation related to the prohibitive cost of direct numerical simulations. A similar situation also happens for the large-scale Navier–Stokes dynamics and it is intimately related to the old concept of eddy-viscosity [39, 40].

The focus on the sole large-scale scalar transport must be accompanied by a proper statistical description of the interactions between scalar field and velocity in the range of (small) scales not explicitly resolved. These dynamical interactions, appearing in the form of beat interactions originated by the advective term in the advection-diffusion equation [14, 15], are the physical mechanism at the origin of the well-know eddy-diffusivity concept [57, 58]. The crucial point is that the eddy-diffusivity idea is intimately related to the concept of scale separation between advecting velocity and scalar field. As a matter of fact, this latter property is however absent in many circumstances where an inertial range of scales continuously extends from the largest to the smallest scales. This fact poses the natural question on whether an eddy-diffusivity description may still work with acceptable errors for the large-scale scalar dynamics even in the absence of scale separation. Answering this question is one of the concerns of the present chapter.

The requirement of scale-separation was relaxed by [15, 17, 50] where the advecting velocity was assumed in the form $\boldsymbol{v}(\boldsymbol{x},t) = \boldsymbol{U}(\boldsymbol{x},t) + \boldsymbol{u}(\boldsymbol{x},t)$, with $\boldsymbol{U}$ being the velocity large-scale component and $\boldsymbol{u}$ are small-scale turbulent fluctuations. Under this hypothesis, the scalar dynamics was investigated on the scales of variations of $\boldsymbol{U}$ (but still much larger than those of $\boldsymbol{u}$). In the absence of scale separation between $\boldsymbol{U}$ and $\boldsymbol{u}$, the identification of large scales and small scales is clearly arbitrary. On the contrary, the situation becomes clear when the two velocity components, thought in Fourier space, are separated by a spectral gap. In that ideal case, exact results have been obtained for the large-scale transport by [15] (on scales comparable to those which characterize $\boldsymbol{U}$) on the basis of a perturbative multiple-scale expansion [48, 53, 47]. [17] and [50] have considered approximate, explicit, expressions for the renormalized transport coefficients (actually tensor fields, the so-called eddy-diffusivity tensor) under different limits: $\boldsymbol{U} \gg \boldsymbol{u}$ by [17] and $\boldsymbol{U} \ll \boldsymbol{u}$ by [50].

Our main purpose here is to consider again the general formulation from [15] with the main aim of quantifying the expected deterioration of the eddy-diffusivity description in the absence of spectral gap separating the two components $\boldsymbol{U}$ and $\boldsymbol{u}$. The idea is to mimic small-scale turbulent fluctuations via random, statistically isotropic, homogeneous, stationary and scaling invariant fields such that the space/time-dependent eddy-diffusivity field can be obtained analytically. Scaling invariance is the reminiscence of the well-known scaling-law behavior of multipoint statistical observables in turbulence [58]. With such an expression for the eddy-diffusivity field we will address the question related to the quantification of the deterioration of the eddy-diffusivity description by reducing to zero the spectral gap separating $\boldsymbol{U}$ and $\boldsymbol{u}$. Also, we will quantify the importance of the nontrivial correction to the large-scale advection component identified by [15] and never analyzed before. Finally, we will compare the accuracy of our closure against other simple options.

The chapter is organized as follows. In Sec. 2.2 we recall known results on the large-scale transport obtained by means of multiple-scale expansions. These results are the basis on which the present chapter is founded. In Sec. 2.4 a simple model for the small-scale advection is presented through which the eddy-diffusivity field and the large-scale effective advection can be computed analytically. These explicit expressions are presented in Sec. 2.5. Section 2.6 is devoted to the verification of the accuracy of our expressions for the eddy-diffusivity field and the large-scale effective advection by varying the extension of the spectral gap of the carrier flow. Comparison of the performance of our strategy against other strategies are also presented. Concluding remarks are presented in Sec. 2.7.

2.2 Known results for the eddy-diffusivity field

In this section we formulate the large-scale problem of a passive scalar field and report known results obtained by [15] exploiting the multiple-scale expansion. These results are the foundation of the present chapter. Let us start our analysis from the equation ruling the evolution of a passive scalar field, $\theta(\boldsymbol{x},t)$, in an incompressible velocity field $\boldsymbol{v}$:

$$\partial_t\theta(\boldsymbol{x},t)+\boldsymbol{v}\cdot\boldsymbol{\partial}\theta(\boldsymbol{x},t)=D_0\partial^2\theta(\boldsymbol{x},t)\ , \tag{2.1}$$

where D_0 is the molecular diffusivity.
The corresponding Lagrangian point of view is:

$$\frac{d\boldsymbol{x}}{dt}=\boldsymbol{v}(\boldsymbol{x}(t),t)+\sqrt{2D_0}\,\boldsymbol{\eta}(t) \tag{2.2}$$

where $\boldsymbol{x}(t)$ is the particle position at time t and $\boldsymbol{\eta}$ is a Gaussian white noise.

Let us now recast the velocity field as a superposition of its large-scale component, denoted by $\boldsymbol{U}$, and its small-scale counterpart, $\boldsymbol{u}$. This latter mimics small-scale turbulent fluctuations. The two components are assumed to be well-separated in scale, i.e., if one Fourier-transforms both components and looks at the corresponding energy spectra, the two sets of associated wavenumbers do not overlap (see Fig. 2.1 for a sketch). The scale separation is controlled by the dimensionless parameter $\epsilon = q_L/q_l$. Large gaps thus correspond to small ϵ. A vanishing extension of the gap corresponds to $\epsilon = 1$. Our claim is that the scale separation in the velocity domain is also the scale separation one needs in the scalar dynamics for an eddy-diffusivity field to emerge. This claim was actually the main result of [15]: by formal multiple-scale expansion, it has been shown that when the scalar dynamics reaches temporal/spatial scales of the order of those of $\boldsymbol{U}$, an effective transport equation arises with a tensor eddy diffusivity. Note that we have introduced the concept of scale separation both in term of spatial scales and in term of temporal scales. This turns out to be possible in view

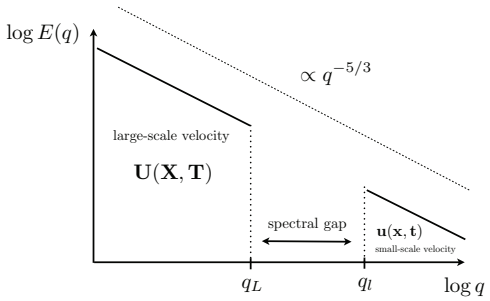

Figure 2.1: Schematic representation of energy containing eddies in the presence of spectral gap separating the large-scale velocity component from the small-scale component. A Kolmogorov $q^{-5/3}$ spectral behavior is assumed for the sake of example. Capital letters for spatial coordinates are used following the multiple-scale expansion jargon where they denote large scales.

of the fact that turbulence decay-times are indeed related to spatial scales via sweeping effects [67].

In the multiple-scale expansion spirit, the large-scale character of $\boldsymbol{U}$ is encoded in its dependence on a new set of 'slow' variables $\boldsymbol{X}$ and T. These latter are related to the usual set of 'fast' variables by $\boldsymbol{X} = \epsilon\boldsymbol{x}$ and $T = \epsilon^2 t$ [14] with the prescription to be treated as independent. The main aim is to determine the large-scale dynamics of θ on spatial/temporal scales comparable to those of $\boldsymbol{U}$. We will denote by Θ this coarser scalar field and, following [17], we define its dynamics as 'pre-asymptotic' to distinguish it from the asymptotic transport which corresponds to the large-scale dynamics of θ on spatial/temporal scales much larger than those of $\boldsymbol{U}$. This latter regime is diffusive and fully controlled by an eddy-diffusivity tensor [14].

For the pre-asymptotic case, the main focus of the present chapter, naive arguments would suggest a simple (wrong) conclusion: $\boldsymbol{U}$ gives the advection contribution in the large-scale equation for θ while (eddy) diffusion emerges from small-scale interactions between θ and $\boldsymbol{u}$. A detailed analysis [15] actually shows that such a conclusion is doubly wrong : the large-scale velocity, $\boldsymbol{U}$, is indeed not responsible for the sole large-scale advection, but it also enters into the renormalized diffusivity; the interaction between small scales gives rise not only to the expected eddy-diffusivity transport but also to an additional large-scale advection contribution.

2.3 Multiple-scale analysis

The starting point of our analysis is the equation ruling the evolution of a passive scalar field, $\theta(\boldsymbol{x},t)$, in an incompressible velocity field $\boldsymbol{v}$:

$$\partial_t\theta(\boldsymbol{x},t)+\boldsymbol{v}\cdot\boldsymbol{\partial}\theta(\boldsymbol{x},t)=D_0\partial^2\theta(\boldsymbol{x},t) \quad . \tag{2.3}$$

In many situations of interest (e.g., in geophysics), $\boldsymbol{v}$ is active in a continuous of scales from the largest to the smallest where, soon or later, viscous effects will dissipate all fluctuations. Frequently, in real applications, one is interested to study the scalar dynamics on large scales where the advecting velocity is however still relevant (i.e., on such wave-numbers the velocity is appreciably non-zero). Following Refs. [15, 17], the simplest way to treat a similar situation is to decompose $\boldsymbol{v}$ as the sum of $\boldsymbol{u}(\boldsymbol{x},t)$ and $\boldsymbol{U}(\boldsymbol{x},t)$. The former is assumed to vary on what we call "small scales" (i.e. wave-numbers of $O(q_l)$) while the latter evolves on "large scales" having wave-numbers of $O(q_L)$, the same at which we aim at investigating the scalar dynamics, and $\epsilon=q_L/q_l$.

Naive arguments would suggest a simple (wrong) conclusion: $\boldsymbol{U}(\boldsymbol{x},t)$ gives the advection contribution in the large-scale equation for θ while the renormalized diffusion coefficient emerges from small-scale interactions between θ and $\boldsymbol{u}$. A detailed analysis actually shows that such conclusion is wrong: the large-scale velocity, $\boldsymbol{U}(\boldsymbol{x},t)$, is not responsible for the sole large scale advection, but it also enters in the renormalized diffusivity.

An heuristic argument in favor of such a mechanism is provided in Ref. [17].

Let us now recall the formal analysis presented in [15, 17] and decompose $\boldsymbol{v}$ as $\boldsymbol{v}(\boldsymbol{x},t)\equiv\boldsymbol{U}(\boldsymbol{x},t)+\boldsymbol{u}(\boldsymbol{x},t)$ where $\boldsymbol{U}(\boldsymbol{x},t)$ and $\boldsymbol{u}(\boldsymbol{x},t)$ are assumed to be periodic in boxes of sides $O(\epsilon^{-1})$ and $O(1)$ (remember that $\epsilon=q_L/q_l$), respectively. The technique we are going to describe can be extended with some modifications to handle the case of a random, homogeneous and stationary velocity field. We will exploit this fact when we will extend our results to deal with turbulent velocity fields.

Our focus is on the large-scale dynamics of the field $\theta(\boldsymbol{x},t)$ on spatial scales of $O(\epsilon^{-1})$.

In the spirit of multiple-scale analysis, we introduce a set of *slow variables* $\boldsymbol{X}=\epsilon\boldsymbol{x}$, $T=\epsilon^2t$ and $\tau=\epsilon t$ in addition to the *fast variables* $(\boldsymbol{x},t)$. The scaling of the times T and τ are suggested by physical reasons: we are searching for diffusive behavior on large time scales of $O(\epsilon^{-2})$ taking into account the effects played by the advection contribution occurring on time scales of $O(\epsilon^{-1})$.

The prescription of the technique is to treat the variables as independent. It then follows that

$$\partial_i\mapsto\partial_i+\epsilon\nabla_i\,;\qquad \partial_t\mapsto\partial_t+\epsilon\partial_\tau+\epsilon^2\partial_T, \tag{2.4}$$

$$\boldsymbol{u}\mapsto\boldsymbol{u}(\boldsymbol{x},t)\,;\qquad \boldsymbol{U}\mapsto\boldsymbol{U}(\boldsymbol{X},T) \tag{2.5}$$

where ∂ and ∇ denote the derivatives with respect to fast and slow space variables, respectively. The solution is sought as a perturbative serie

$$\theta(\boldsymbol{x},t;\boldsymbol{X},T;\tau)=\theta^{(0)}+\epsilon\theta^{(1)}+\epsilon^2\theta^{(2)}+\ldots, \tag{2.6}$$

where the functions $\theta^{(n)}$ depend, *a priori*, on both fast and slow variables. By inserting (2.6) and (2.4) into (2.1) and equating terms having equal powers in ϵ, we obtain a hierarchy of equations in which both fast and slow variables appear. The solutions of interest to us are those having the same periodicities as the velocity field, $\boldsymbol{u}(\boldsymbol{x},t)$.

By averaging such equations over the small-scale periodicity (here denoted by $\langle\cdot\rangle$), a set of equations involving the sole large-scale fields (i.e. depending on $\boldsymbol{X}$, T and τ) are easily obtained. Obviously, such equations must be solved recursively, because of the fact that solutions of a given order appear as coefficients in the equations at the higher orders. Let us show in detail this point.

It is not difficult to verify that the equations at order ϵ and ϵ^2 read [15, 17]:

$$O(\epsilon): \quad \begin{array}{l}\partial_t\theta^{(1)}+(\boldsymbol{v}\cdot\boldsymbol{\partial})\,\theta^{(1)}-D_0\,\partial^2\theta^{(1)}=\\ -(\boldsymbol{v}\cdot\boldsymbol{\nabla})\theta^{(0)}-\partial_\tau\theta^{(0)}\end{array} \tag{2.7}$$

$$O(\epsilon^2): \quad \begin{array}{l}\partial_t\theta^{(2)}+(\boldsymbol{v}\cdot\boldsymbol{\partial})\,\theta^{(2)}-D_0\,\partial^2\theta^{(2)}=\\ -\partial_T\theta^{(0)}-(\boldsymbol{v}\cdot\boldsymbol{\nabla})\theta^{(1)}+D_0\nabla^2\theta^{(0)}\\ +2D_0(\boldsymbol{\partial}\cdot\boldsymbol{\nabla})\theta^{(1)}-\partial_\tau\theta^{(1)}\quad .\end{array} \tag{2.8}$$

The linearity of (2.7) permits to search for a solution in the form

$$\begin{array}{rcl}\theta^{(1)}(\boldsymbol{x},t;\boldsymbol{X},T;\tau) &=& \langle\theta^{(1)}\rangle(\boldsymbol{X},T;\tau)\\ &+& \boldsymbol{\chi}(\boldsymbol{x},t;\boldsymbol{X},T)\cdot\boldsymbol{\nabla}\theta^{(0)}(\boldsymbol{X},T;\tau)\quad ,\end{array} \tag{2.9}$$

where $\theta^{(0)}$ depends on the sole large-scale variables as in Ref. [14]. Plugging (2.9) into the solvability condition for (2.8), one obtains the equation

$$\partial_T\theta^{(0)}+(\boldsymbol{U}\cdot\boldsymbol{\nabla})\langle\theta^{(1)}\rangle+\partial_\tau\langle\theta^{(1)}\rangle=\nabla_i\left(D_{ij}\nabla_j\theta^{(0)}\right) \tag{2.10}$$

where

$$D_{ij}(\boldsymbol{X},T)=\delta_{ij}D_0-\langle u_i\chi_j\rangle \tag{2.11}$$

is a second-order tensorial field and $\boldsymbol{\chi}(\boldsymbol{x},t;\boldsymbol{X},T)$ has a vanishing average over the periodicities and satisfies the following equation:

$$\partial_t\chi_j+[(\boldsymbol{u}+\boldsymbol{U})\cdot\boldsymbol{\partial}]\,\chi_j-D_0\,\partial^2\chi_j=-u_j\quad . \tag{2.12}$$

Note that, when $\boldsymbol{U}$ is not a pure mean flow but depends on $\boldsymbol{X}$ and T, the equation (2.12) must be solved for each value of $\boldsymbol{X}$ (and eventually T).

From Eq. (2.10) and from the solvability condition of Eq. (2.7),

$$\partial_\tau \langle \theta^{(0)} \rangle + (\boldsymbol{U} \cdot \boldsymbol{\nabla}) \langle \theta^{(0)} \rangle = 0, \tag{2.13}$$

one obtains the equation for the large-scale field Θ defined as: $\Theta \equiv \langle \theta^{(0)} \rangle + \epsilon \langle \theta^{(1)} \rangle$:

$$\partial_t \Theta + (\boldsymbol{U} \cdot \boldsymbol{\partial}) \Theta = \partial_i \left(D_{ij} \partial_j \Theta \right) \tag{2.14}$$

where the usual variables $\boldsymbol{x}, t$ are used.

The important point to note is that D_{ij} is in general neither symmetric nor positive defined. On the contrary, it is easy to show [15], that $D^E_{ij} \equiv (D_{ij} + D_{ji})/2$ is (obviously) symmetric and positive defined. Its expression can immediately be obtained from (2.12) in term of the sole auxiliary field :

$$D^E_{ij} = D_0 \left[\delta_{ij} + \langle (\partial_p \chi_i)(\partial_p \chi_j) \rangle \right] \ . \tag{2.15}$$

In terms of D^E_{ij} and $D^A_{ij} \equiv (D_{ij} - D_{ji})/2$, the pre-asymptotic equation (2.14) takes the form

$$\partial_t \Theta + \boldsymbol{\partial} \cdot (\boldsymbol{U}^E \Theta) = \partial_i \partial_j \left(D^E_{ij} \Theta \right). \tag{2.16}$$

where

$$U^E_i(\boldsymbol{x}, t) \equiv \left[U_i(\boldsymbol{x}, t) + \partial_j D^E_{ij}(\boldsymbol{x}, t) + \partial_j D^A_{ij}(\boldsymbol{x}, t) \right] \tag{2.17}$$

is an effective compressible advecting velocity [53]. Advection by compressible velocities have been investigated, e.g., in Refs. [41] and [49].

In plain terms, the pre-asymptotic regime is fully described by the following equations:

$$\partial_t \Theta + \boldsymbol{U} \cdot \boldsymbol{\partial} \Theta = \partial_i \left(D_{ij} \partial_j \Theta \right) \tag{2.18}$$

or, in the equivalent form,

$$\partial_t \Theta(\boldsymbol{x}, t) + \boldsymbol{\partial} \cdot \left(\boldsymbol{U}^E \Theta \right) = \partial_i \partial_j \left(D^E_{ij} \Theta \right) \tag{2.19}$$

where Θ denotes the scalar field varying on pre-asymptotic scales and

$$U^E_i \equiv U_i + \partial_j D_{ij} \tag{2.20}$$

$$D^E_{ij} \equiv \frac{D_{ij} + D_{ji}}{2} \ . \tag{2.21}$$

The eddy-diffusivity, $D_{ij}(\boldsymbol{x}, t)$, is a tensor field in general neither symmetric nor positive definite. Its symmetric part (which is also positive definite) contributes to the diffusion process while both the symmetric and the anti-symmetric parts enter, in general, into the effective advection velocity $\boldsymbol{U}^E$ which turns out to be compressible [49, 41]. The eddy-diffusivity, often associated to the sole small-scale activity, here explicitly depends on the large-scale advection $\boldsymbol{U}$. This fact causes the space/time dependence in the eddy-diffusivity.

The Eulerian view for the large-scale dynamics given by (2.19) is equivalent to the Lagrangian description:

$$\frac{d\boldsymbol{x}(t)}{dt} = \boldsymbol{U}^E(\boldsymbol{x}(t),t) + \boldsymbol{\sigma}(\boldsymbol{x}(t),t)\boldsymbol{\eta}(t)\,, \tag{2.22}$$

where $\boldsymbol{\sigma}$ is the unique positive-definite solution of the matrix equation $D^E_{ij}(\boldsymbol{x},t) = \frac{1}{2}\left(\sigma_{ip}(\boldsymbol{x},t)\sigma_{jp}(\boldsymbol{x},t)\right)$. No explicit expression for $D_{ij}(\boldsymbol{x},t)$ is available in general. A perturbative strategy has been carried out by [17] to obtain an approximate explicit expression for $D_{ij}(\boldsymbol{x},t)$ in the limit of strong large-scale advection. The opposite limit has been analyzed by [50].

The complexity of the problem is hidden inside the auxiliary equation through which $D^E_{ij}(\boldsymbol{x},t)$ can be determined. The equation for the auxiliary field, χ, reads:

$$\partial_t\chi_j + \big(\boldsymbol{u}+\boldsymbol{U}(\boldsymbol{X},T)\big)\cdot\boldsymbol{\partial}\chi_j - D_0\,\partial^2\chi_j = -u_j \ , \tag{2.23}$$

from which the expression for the eddy-diffusivity tensor follows:

$$D_{ij}(\boldsymbol{X},T) = \delta_{ij}D_0 - \langle u_i\chi_j\rangle \ . \tag{2.24}$$

In Eqs. (2.23)–(2.24), brackets denote averages on the small-scale statistics. An explicit, parametric, dependence on slow variables does appear in the eddy-diffusivity which becomes a large-scale varying field. To obtain the eddy-diffusivity tensor field, Eq. (2.23) must be solved for each value of the slow variables thus making the problem highly complex and costly.

2.4 A simple model for the small-scale velocity fluctuations

As we have already emphasized in the last section, the exact results from the multiple-scale expansion leading to the expression for the eddy-diffusivity tensor field (2.24) are intrinsically formal. To obtain the eddy-diffusivity one has indeed to know the small-scale velocity. Moreover, the space/time dependence of the eddy-diffusivity tensor implies that one has to numerically solve the auxiliary differential problem for all space and time collocation points. This is clearly a daunting task especially in relation to applications, e.g. related to the study of pollutant dispersion in the atmospheric environment.

To overcome these problems, our idea here is to build a stochastic model for small-scale velocity fluctuations mimicking relevant features of small-scale turbulence which, at the same time, allows one to obtain an explicit expression for the eddy-diffusivity tensor field. The statistical properties we require for our small-scale velocity field are: isotropy, stationarity, homogeneity and scale-invariance of two-point statistics. This latter property is equivalent to

imposing a power-law behavior for the kinetic energy spectrum, e.g., à la Kolmogorov.
There are of course infinitely many possibilities to generate a stochastic field with the required statistical properties. Conversely, the requirement of having an explicit expression for the eddy-diffusivity tensor field leads to the exploitation of a specific class of velocity fields: the so-called parallel flows. Indeed, for parallel flows, in the auxiliary problem (2.23) the advective term disappears and explicit solutions can be obtained. In way of example, this class of flows was exploited by [64] to investigate interference phenomena in scalar transport.

Focusing henceforth on two dimensions, the stream function of our small-scale velocity field is sought as a superposition of N independent randomly oriented parallel flows (here referred to as spatial modes) as:

$$\Psi(\boldsymbol{x}, t; \boldsymbol{x}(0)) = \sum_{i=1}^{N} \frac{A_i(\boldsymbol{x}(0), t)}{q_i} \sin[q_i \mathbf{n}(\boldsymbol{x}(0)) \cdot \boldsymbol{x} + \theta_i(\boldsymbol{x}(0))] \tag{2.25}$$

where $\boldsymbol{x}$ is the spatial coordinate, $\boldsymbol{x}(0)$ is meant to stress that we choose independent random processes for each space location (in the following $\boldsymbol{x}(0)$ will be the initial conditions of Lagrangian particles through which we will investigate the transport problem; each $\boldsymbol{x}(0)$ will correspond to a given realization of the random process), $A_i(\boldsymbol{x}(0), t)$ and q_i are the velocity amplitude and wavenumber modulus associated to the spatial mode i. Finally, $\mathbf{n}(\boldsymbol{x}(0))$ is the direction angle associated to the initial condition $\boldsymbol{x}(0)$ and $\theta_i(\boldsymbol{x}(0))$ is the phase of the i-th mode. Direction angles and phases are random variables kept constant along each realization and uniformly distributed in $[0, 2\pi)$.

Following [35], where relative dispersion properties were analyzed via multiscale kinematic velocity field, we distribute spatial modes according to a given density factor (here $\sqrt{2}$): $q_{i+1} = \sqrt{2} q_i$. Wavelengths follow from the usual definition $\lambda_i = 2\pi/q_i$. It has been shown in the previous chapter [65] that such a distribution guarantees a good description of the continuous limit $q_{i+1} - q_i \to 0$.

To ensure a nontrivial temporal decay of two-point velocity statistics, velocity amplitudes can be generated via the Ornstein-–Uhlenbeck process

$$\frac{dA_i}{dt} = -\frac{A_i}{\tau_i} + \sqrt{\frac{2B_i}{\tau_i}} \eta_i \tag{2.26}$$

where $\boldsymbol{\eta}$ is a zero-mean Gaussian white noise process with $\langle \eta_i(t) \eta_j(t') \rangle = \delta_{ij} \delta(t - t')$.

It is easy to verify from (2.26) that the following properties hold:

$$\begin{aligned} \langle A_i(\boldsymbol{x}(0), t) \rangle &= 0 \\ \langle A_i^2(\boldsymbol{x}(0), t) \rangle &= B_i \\ \langle A_i(\boldsymbol{x}(0), t) A_i(\boldsymbol{x}(0), t') \rangle &= B_i e^{-\frac{|t - t'|}{\tau_i}} \quad , \end{aligned} \tag{2.27}$$

showing that the above process is thus stationary. From the numerical evidences reported by [67], decorrelation times τ_i can be related to the large-scale sweeping via the simple relation $\tau_i = \alpha/(\mathcal{U}_{rms} q_i)$ where α is a free parameter (set equal to unity in the present study), and $\mathcal{U}_{rms}$ is the root mean square velocity.

From the stream-function (2.25) the expression for the velocity field becomes a superposition of independent normal modes $\boldsymbol{u} = \sum_{i=1}^{N} \boldsymbol{u}_i$. Namely,

$$\begin{aligned} u_1 &= \sum_{i=1}^{N} A_i(\boldsymbol{x}(0), t) \sin[\phi(\boldsymbol{x}(0))] \\ &\times \cos\{q_i \cos[\phi(\boldsymbol{x}(0))] x + q_i \sin[\phi(\boldsymbol{x}(0))] y + \theta_i(\boldsymbol{x}(0))\} \\ u_2 &= -\sum_{i=1}^{N} A_i(\boldsymbol{x}(0), t) \cos[\phi(\boldsymbol{x}(0))] \\ &\times \cos\{q_i \cos[\phi(\boldsymbol{x}(0))] x + q_i \sin[\phi(\boldsymbol{x}(0))] y + \theta_i(\boldsymbol{x}(0))\} \end{aligned} \tag{2.28}$$

where $\phi(\boldsymbol{x}(0))$ is the angle between the x-direction and the wavenumber direction. This latter is the same for each mode, i, and only changes for different realizations. Note that because of the fact that the velocity field is generated along each particle path, there is thus for each value of the wavenumber modulus q_i just one mode direction. However, because of the fact that each particle experiences independent random processes (in particular, different random angles, ϕ), the fact that we follow many particles to study the dispersion phenomenon actually implies that many directions for each value of q_i are actually present, as in real turbulence.
Let us now show that our flow field is indeed homogeneous, isotropic and stationary. To do that, let us expand the velocity correlation function and exploit independence of random processes associated to different modes:

$$\begin{aligned} &\langle \boldsymbol{u}(\boldsymbol{x}, t) \cdot \boldsymbol{u}(\boldsymbol{x}', t') \rangle = \sum_{i=1}^{N} \langle A_i(\boldsymbol{x}(0), t) A_i(\boldsymbol{x}(0), t') \rangle \times \\ &\langle \cos[q_i \mathbf{n}(\boldsymbol{x}(0)) \cdot \boldsymbol{x} + \theta_i(\boldsymbol{x}(0))] \cos[q_i \mathbf{n}(\boldsymbol{x}(0)) \cdot \boldsymbol{x}' + \theta_i(\boldsymbol{x}(0))] \rangle \,. \end{aligned} \tag{2.29}$$

By means of well-known trigonometric identities, the above expression can be recast in the form:

$$\begin{aligned} &\langle \boldsymbol{u}(\boldsymbol{x}, t) \cdot \boldsymbol{u}(\boldsymbol{x}', t') \rangle = \sum_{i=1}^{N} \frac{1}{2} \langle A_i(\boldsymbol{x}(0), t) A_i(\boldsymbol{x}(0), t') \rangle \times \big\{ \\ &\langle \cos[q_i \mathbf{n}(\boldsymbol{x}(0)) \cdot (\boldsymbol{x} + \boldsymbol{x}') + 2\theta_i(\boldsymbol{x}(0))] \rangle + \langle \cos[q_i \mathbf{n}(\boldsymbol{x}(0)) \cdot (\boldsymbol{x} - \boldsymbol{x}')] \rangle \big\} \,. \end{aligned} \tag{2.30}$$

The phase average can be computed explicitly because phases are uniformly distributed:

$$\langle \cos[q_i \mathbf{n}(\boldsymbol{x}(0)) \cdot (\boldsymbol{x} + \boldsymbol{x}') + 2\theta_i(\boldsymbol{x}(0))] \rangle = \\ = \frac{1}{2\pi} \int_0^{2\pi} d\theta_i \cos[q_i \mathbf{n}(\boldsymbol{x}(0)) \cdot (\boldsymbol{x} + \boldsymbol{x}') + 2\theta_i] = 0 \ . \tag{2.31}$$

Taking into account Eq. (2.27), we arrive to the final result:

$$\langle \boldsymbol{u}(\boldsymbol{x}, t) \cdot \boldsymbol{u}(\boldsymbol{x}', t') \rangle = \sum_{i=1}^{N} \frac{B_i}{2} e^{-\frac{|t-t'|}{\tau_i}} \langle \cos[q_i \mathbf{n}(\boldsymbol{x}(0)) \cdot (\boldsymbol{x} - \boldsymbol{x}')] \rangle \ , \tag{2.32}$$

from which the stationarity and homogeneity clearly follow. Finally, the flow in Eq. (2.28) is also isotropic, due to our choice to consider randomly oriented uniformly distributed wavenumbers.

It now remains to choose B_i in a way to obtain the desired kinetic energy spectrum. To do that, we recall the well-known definition of isotropic kinetic energy spectrum:

$$E_{kin} \equiv \frac{1}{2} \langle |\boldsymbol{u}(\boldsymbol{x}, t)|^2 \rangle = \int_0^{\infty} dq \, E(q) \sim \sum_{i=1}^{N} E(q_i) \delta q_i \tag{2.33}$$

where $\delta q_i = q_{i+1} - q_i$ and the left-hand-side of this relationship easily follows from Eq. (2.28):

$$\frac{1}{2} \langle |\boldsymbol{u}(\boldsymbol{x}, t)|^2 \rangle = \sum_{i=1}^{N} \frac{\langle A_i^2 \rangle}{4} = \sum_{i=1}^{N} \frac{B_i}{4} \ . \tag{2.34}$$

By simple identification one ends up with:

$$E(q_i) \delta q_i = \frac{1}{4} B_i \qquad E_{kin} = \frac{1}{4} \sum_{i=1}^{N} B_i \ . \tag{2.35}$$

In the specific case of a two-dimensional velocity field obeying, in way of example, the equivalent of the Kolmogorov 1941 theory, $E(q) = C\varepsilon^{2/3} q^{-5/3}$ (valid for two-dimensional turbulence in the inverse energy cascade [42]), where C is the Kolmogorov constant and ε denotes the energy dissipation rate, one has $B_i = 4C\varepsilon^{2/3} q_i^{-5/3} \delta q_i$. Different relationships can be trivially obtained starting from different assumptions for the spectrum.

Assuming, as in Fig. 2.1, that small-scale turbulence is active for $q > q_l$, one can simply express $C\varepsilon^{2/3}$ in terms of the turbulent kinetic energy $E_{kin}^{>} \equiv \int_{q_l}^{\infty} E(q) \, dq$:

$$C\epsilon^{2/3} = \frac{2}{3} E_{kin}^{>} q_l^{2/3} \ . \tag{2.36}$$

Note that $E_{kin}^{>}$ is easily accessible in many CFD models (both RANS and LES) which use a closed equation for $E_{kin}^{>}$ to construct their closure models.

2.4.1 The model for the large-scale advection

To complete the definition of our flow model, the large-scale component, $\boldsymbol{U}$, has to be defined. This latter is obtained in terms of the same model for the small-scale fluctuations except for the fact that we erased the dependence on $\boldsymbol{x}(0)$ in A_i, ϕ_i and θ_i. This choice allows us to maintain an explicit dependence on large-scale space coordinates in the eddy-diffusivity tensor field. In plain words, we generate only one realization for each large-scale mode i of the processes $A_i(t)$, ϕ_i (here dependent on the i-th mode unlike what happens for the small-scale velocity component) and θ_i (here set to zero), which will be the same for every particle. The flow $\boldsymbol{U}$ is therefore:

$$\begin{aligned} U_1 &= U_1^0 + \sum_{i=1}^{M} A_i(t)\sin(\phi_i)\cos[q_i\cos(\phi_i)x + q_i\sin(\phi_i)y] \\ U_2 &= U_2^0 - \sum_{i=1}^{M} A_i(t)\cos(\phi_i)\cos[q_i\cos(\phi_i)x + q_i\sin(\phi_i)y] \end{aligned} \tag{2.37}$$

where M is the number of active wavenumbers q_i with $q_i < q_L$ and $\boldsymbol{U}_0$ is the flow mean component. Note that the randomness of the direction angle ϕ_i guarantees that $\boldsymbol{U} - \boldsymbol{U}^0$ is zero-mean valued, since the flow is a $2\pi-$periodic function with respect to the angles, and

$$\begin{aligned} &\int_0^{\pi} d\phi_i \sin(\phi_i)\cos[q_i\cos(\phi_i)x + q_i\sin(\phi_i)y] + \\ + &\int_{\pi}^{2\pi} d\phi_i \sin(\phi_i)\cos[q_i\cos(\phi_i)x + q_i\sin(\phi_i)y] = 0 \ , \end{aligned} \tag{2.38}$$

$$\begin{aligned} &\int_0^{\pi} d\phi_i \cos(\phi_i)\cos[q_i\cos(\phi_i)x + q_i\sin(\phi_i)y] + \\ + &\int_{\pi}^{2\pi} d\phi_i \cos(\phi_i)\cos[q_i\cos(\phi_i)x + q_i\sin(\phi_i)y] = 0 \ , \end{aligned} \tag{2.39}$$

having done the substitution $\phi \to \phi - \pi$ in the two integrals from π to 2π.

To conclude this section, let us make a comment on $\mathcal{U}_{rms}$. The total kinetic energy is obtained by averaging on both the small and large scales. We will keep the bracket notation for the small scale ensemble mean value, whereas we will use an overline to indicate the large scale mean value, which we can obtain by means of a space-time average (ergodicity hypothesis), recalling that the amplitude processes are realizations of Eq. (2.26) and

then they fulfill Eqs.(2.27). The result is easily as follows:

$$E_{kin} = \frac{1}{2}\overline{\langle(\boldsymbol{u}+\boldsymbol{U})\cdot(\boldsymbol{u}+\boldsymbol{U})\rangle} = \tag{2.40}$$
$$= \frac{1}{2}\sum_{i,j=1}^{N}\langle \boldsymbol{u}_i\cdot\boldsymbol{u}_j\rangle + \frac{1}{2}\sum_{i,j=1}^{M}\overline{\boldsymbol{U}_i\cdot\boldsymbol{U}_j} + \frac{1}{2}|\boldsymbol{U}^0|^2 = E^{>}_{kin} + E^{<}_{kin}$$

which follows from the fact that amplitudes of different modes are uncorrelated and where we have defined

$$E^{<}_{kin} = \frac{|\boldsymbol{U}^0|^2}{2} + \sum_{i=1}^{M}\frac{B_i}{4} \ . \tag{2.41}$$

It then follows that the velocity root-mean square reads

$$\mathcal{U}_{rms} \equiv \sqrt{2E_{kin}} = \sqrt{2(E^{<}_{kin} + E^{>}_{kin})} \ . \tag{2.42}$$

The fact that $\boldsymbol{U}^0$ explicitly enters in $\mathcal{U}_{rms}$, thus acting as a sweeping effect in the same ways as large eddies do, is a consequence of our choice not to assume Galilean invariance. This latter symmetry is indeed often broken in the presence of realistic boundary conditions, e.g. those encountered in environmental problems.

2.5 Explicit expression for the eddy-diffusivity field

To obtain the eddy-diffusivity field associated to the flow field defined in Sec. 2.4, one can proceed along two different ways. One is based on the Eulerian view and follows from the application of (2.24). The second possibility is to start from the definition of eddy-diffusivity in Lagrangian terms and proceed with the calculation in this framework. We decided to follows the second option and we provide here some details of the calculation which, at the very end, will lead to an explicit expression for both the eddy-diffusivity tensor and the effective large-scale advection defined in (2.20).

The starting point is the well-known definition of eddy-diffusivity in Lagrangian terms:

$$D_{\alpha\beta}(\boldsymbol{U}) = \lim_{t\to\infty}\frac{1}{2}\frac{d}{dt}\langle(x_\alpha(t) - \langle x_\alpha(t)\rangle)(x_\beta(t) - \langle x_\beta(t)\rangle)\rangle \tag{2.43}$$

where brackets denotes averages with respect to the random small-scale velocity statistics and $x_\alpha(t)$ defines a particle trajectory ruled by the Langevin equation

$$\frac{d\boldsymbol{x}(t)}{dt} = \boldsymbol{U}(\boldsymbol{X}(T),T) + \boldsymbol{u}(\boldsymbol{x}(t),t) \ . \tag{2.44}$$

From now on we neglect the molecular diffusivity as customary when studying transport in turbulent (chaotic) environment and adopt the convection that Greek indexes are used for vector components while Latin indexes select different normal modes. As already said, capital letters for spatial coordinates originate from the multiple-scale jargon and are meant to stress that $\boldsymbol{U}(\boldsymbol{X},T)$ evolve on scales much larger than those of $\boldsymbol{u}$. The space/time dependence in $\boldsymbol{U}(\boldsymbol{X},T)$ will thus be considered as parametric. Physically, this amounts to saying that in the transport process, particles see a constant large-scale advection for the entire duration of the renormalization stage associated to the small-scale dynamics.

Because of the fact that the spatial modes involved in (2.28) are mutually uncorrelated and statistically homogeneous, we can proceed by analyzing the transport process for each single mode and then adding all contributions. This interesting result is reported in Appendix 2.A.

The starting point is to rotate coordinates in a way to have the wavenumber aligned with the x-axis. This is easily done in terms of suitable rotation matrices $R_{\alpha\beta}(\phi(\boldsymbol{x}(0)))$, $x'_\alpha = R_{\alpha\beta}(\phi(\boldsymbol{x}(0)))x_\beta$ with an angle such that in the new coordinate system $\mathbf{n}' = \mathbf{R}\mathbf{n} = (1,0)$. Recalling that for a matrix belonging to the rotation group in two dimensions, SO(2,$\mathbb{R}$), one has $R_{11} = R_{22}$ and $R_{12} = -R_{21}$, the expression for the velocity field in the rotated system is easily obtained:

$$\begin{aligned} u'_{i\,1}(x',y',t) &= 0 \\ u'_{i\,2}(x',y',t) &= -A_i(\boldsymbol{x}'(0),t)\cos[q_i x' + \theta_i(\boldsymbol{x}(0))] \ . \end{aligned} \tag{2.45}$$

For each normal mode $\boldsymbol{u}'_i$, in its new reference frame, the equation of motion turns out to be (omitting for the sake of brevity dependence on large-scale variables in $\boldsymbol{U}'$):

$$\frac{dx'_i}{dt} = \boldsymbol{u}'_i(\boldsymbol{x}'_i(t),t) + \boldsymbol{U}' \tag{2.46}$$

where $\boldsymbol{U}' = \boldsymbol{R}\boldsymbol{U}$. Thus the solution for the i-th mode is:

$$\begin{aligned} x'_i &= x'(0) + U'_1 t \\ y'_i &= y'(0) + U'_2 t - \int_0^t dt' A_i(\boldsymbol{x}'(0),t')\cos[q_i(x'(0) + U'_1 t') + \theta_i(\boldsymbol{x}(0))] \end{aligned} \tag{2.47}$$

Straightforwardly, only $D_{i\,22} \equiv \langle (y'_i(t) - \langle y'_i(t)\rangle)^2\rangle$ is non zero in this new coordinate system. From Eq. (2.27), it follows that:

$$\langle y'_i\rangle = y'(0) + U'_2 t \quad . \tag{2.48}$$

Exploiting well-known trigonometric identities, the expression for $D_{i\,22}$ reads:

$$D_{i\,22} = \frac{1}{4}\frac{d}{dt}\int_0^t dt' \int_0^t dt'' \langle A_i(t')A_i(t'')\rangle \langle \cos[q_i U_1'(t'-t'')] + \\ + \cos[q_i(2x'(0) + U_1'(t'+t'')) + 2\theta_i]\rangle \tag{2.49}$$

where we have exploited the fact that A_i and θ_i are independent random processes together with the properties given by (2.27).
The phase average inside the above integral can be computed explicitly because phases are uniformly distributed:

$$\langle \cos[q_i(2x'(0) + U_1'(t'+t'')) + 2\theta_i]\rangle = \\ = \frac{1}{2\pi}\int_0^{2\pi} d\theta_i \cos[q_i(2x'(0) + U_1'(t'+t'')) + 2\theta_i] = 0 \ , \tag{2.50}$$

from which, after simple manipulations and exploiting again (2.27), expression (2.50) becomes:

$$D'_{i\,22} = \lim_{t\to\infty}\int_0^t dt' B_i \frac{e^{-\frac{|t'-t|}{\tau_i}}}{2}\cos[q_i U_1'(t'-t)] = \frac{B_i}{2}\frac{\tau_i}{\tau_i^2 q_i^2 {U_1'}^2 + 1} \tag{2.51}$$

The effect of the large-scale velocity at the denominator always causes a reduction of the eddy diffusivity.
The last step is to go back to the original coordinate system for each normal mode remembering that $\mathbf{n}' = (1,0)$ and thus $U_1 = \mathbf{n}'\cdot\mathbf{U}' = \mathbf{n}\cdot\mathbf{U}$. We also have to sum all contributions coming from different modes i (see again Appendix 2.A) and average over the angular directions:

$$\begin{aligned} D_{11} &= \sum_{i=1}^N \langle D'_{i\,22} R_{21}^2\rangle = \sum_{i=1}^N \frac{B_i}{2}\langle \frac{\tau_i \sin^2[\phi]}{\tau_i^2 q_i^2 (\mathbf{n}(\phi)\cdot\boldsymbol{U})^2 + 1}\rangle \\ D_{12} &= \sum_{i=1}^N \langle D'_{i\,22} R_{21} R_{11}\rangle = -\sum_{i=1}^N \frac{B_i}{2}\langle \frac{\tau_i \sin[\phi]\cos[\phi]}{\tau_i^2 q_i^2 (\mathbf{n}(\phi)\cdot\boldsymbol{U})^2 + 1}\rangle \\ D_{22} &= \sum_{i=1}^N \langle D'_{i\,22} R_{22}^2\rangle = \sum_{i=1}^N \frac{B_i}{2}\langle \frac{\tau_i \cos^2[\phi]}{\tau_i^2 q_i^2 (\mathbf{n}(\phi)\cdot\boldsymbol{U})^2 + 1}\rangle \, . \end{aligned} \tag{2.52}$$

It is worth recalling that $D_{12} = D_{21}$ since $R_{22} = R_{11}$. Eventually, the

angular averages give rise to the following three integrals:

$$\begin{array}{l} \displaystyle\int_0^{2\pi} \frac{\sin^2\phi d\phi}{\tau_i^2 q_i^2 (U_1\cos\phi + U_2\sin\phi)^2 + 1} \\ \displaystyle -\int_0^{2\pi} \frac{\sin\phi\cos\phi d\phi_i}{\tau_i^2 q_i^2 (U_1\cos\phi + U_2\sin\phi)^2 + 1} \\ \displaystyle\int_0^{2\pi} \frac{\cos^2\phi d\phi}{\tau_i^2 q_i^2 (U_1\cos\phi + U_2\sin\phi)^2 + 1} \quad . \end{array} \tag{2.53}$$

The three integrals involved in the above expressions can be evaluated exactly. This is the very last step to obtain the explicit expression of the eddy diffusivity field. The final result reads:

$$\begin{aligned} D_{11} &= \frac{\mathcal{U}_{rms}^2}{\alpha^2}\left[\frac{\alpha^2}{\mathcal{U}_{rms}^2}U_1^2(U_2^2+U_1^2) + (U_2^2-U_1^2)\sqrt{\frac{\alpha^2}{\mathcal{U}_{rms}^2}(U_1^2+U_2^2)+1} + U_1^2 - U_2^2\right]\times \\ &\quad \left[\sqrt{\frac{\alpha^2}{\mathcal{U}_{rms}^2}(U_1^2+U_2^2)+1}(U_1^2+U_2^2)^2\right]^{-1}\sum_{i=1}^{N}\frac{B_i}{2}\tau_i \end{aligned} \tag{2.54}$$

$$\begin{aligned} D_{22} &= \frac{\mathcal{U}_{rms}^2}{\alpha^2}\left[\frac{\alpha^2}{\mathcal{U}_{rms}^2}U_2^2(U_2^2+U_1^2) + (U_1^2-U_2^2)\sqrt{\frac{\alpha^2}{\mathcal{U}_{rms}^2}(U_1^2+U_2^2)+1} + U_2^2 - U_1^2\right]\times \\ &\quad \left[\sqrt{\frac{\alpha^2}{\mathcal{U}_{rms}^2}(U_1^2+U_2^2)+1}(U_1^2+U_2^2)^2\right]^{-1}\sum_{i=1}^{N}\frac{B_i}{2}\tau_i \end{aligned} \tag{2.55}$$

$$\begin{aligned} D_{12} &= \frac{\mathcal{U}_{rms}^2}{\alpha^2}U_2U_1\Big[\frac{\alpha^2}{\mathcal{U}_{rms}^2}(U_2^2+U_1^2) - 2\sqrt{\frac{\alpha^2}{\mathcal{U}_{rms}^2}(U_1^2+U_2^2)+1} + 2\Big]\times \\ &\quad \Big[\sqrt{\frac{\alpha^2}{\mathcal{U}_{rms}^2}(U_1^2+U_2^2)+1}(U_1^2+U_2^2)^2\Big]^{-1}\sum_{i=1}^{N}\frac{B_i}{2}\tau_i\,. \end{aligned} \tag{2.56}$$

In tensorial form, the above expressions can be written as:

$$D_{\beta\gamma} = \frac{\frac{\mathcal{U}_{rms}^2}{\alpha^2}\left[\frac{\alpha^2}{\mathcal{U}_{rms}^2}|\mathbf{U}|^2U_\beta U_\gamma + (|\mathbf{U}|^2\,\delta_{\beta\gamma} - 2U_\beta U_\gamma)\left(\sqrt{\frac{\alpha^2}{\mathcal{U}_{rms}^2}|\mathbf{U}|^2+1}-1\right)\right]}{\sqrt{\frac{\alpha^2}{\mathcal{U}_{rms}^2}|\mathbf{U}|^2+1}\,|\mathbf{U}|^4}\sum_{i=1}^{N}\frac{B_i}{2}\tau_i \tag{2.57}$$

where it is now evident how the effect of the large-scale velocity acts to renormalize the bare correlation time. Note that in the limit $\boldsymbol{U} \to 0$ one obtains the 'bare' diffusivity whose entries are $D_{11} = D_{22} = \sum_{i=1}^{N} \frac{B_i \tau_i}{4}$ and $D_{12} = 0$.

To conclude this section it is worth remarking that expressions similar to (2.57) can also be derived in three dimensions. Their final form, toghether with a sketch of the derivation, is reported in Appendix 2.C).

2.5.1 The effective advecting velocity

To determine the effective advection field (2.20) one has to take the divergence of $D_{\alpha\beta}$ from the explicit expressions (2.54-2.56). This can be easily done via chain rule for derivatives, once returned to the original variables $\boldsymbol{x}, t$.
Recalling that $D_{\alpha\beta} = \sum_{p=1}^{N} D_{p\,\alpha\beta}$, one arrives at:

$$\frac{\partial D_{\alpha\beta}}{\partial x_\beta} = \sum_{p=1}^{N} \frac{\partial D_{p\,\alpha\beta}}{\partial U_\gamma} \frac{\partial U_\gamma}{\partial x_\beta} \ . \tag{2.58}$$

The resulting expressions for $\frac{\partial D_{p\,\alpha\beta}}{\partial U_\gamma}$ are reported in Appendix 2.B together with the velocity gradient tensor.

2.6 Numerical study

The main aim of this section is to verify the reliability of our expressions for the eddy-diffusivity and effective advection by varying the extension of the spectral gap depicted in Fig. 2.1. The limiting case will be a situation where the spectral gap reduces to zero, as in many situations of interest. As a further objective, in the absence of spectral gap, we will perform a comparison between our model performances and other possible simpler choices to describe the effect of the unresolved small-scale motion.

For these purposes we perform kinematic simulations mimicking homogeneous, isotropic and stationary turbulence in two dimensions accompanied by Lagrangian simulations. Kinematic simulations are a widely used tool to investigate turbulent dispersion both from the point of view of relative dispersion and absolute dispersion. Interested readers can refer, in way of example, to [51] and [52], and references therein .

Once fully resolved flow fields are available, it is easy to isolate their large-scale components $\boldsymbol{U}$ (i.e. active for $q < q_L$) and small-scale components $\boldsymbol{u}$ (i.e. active for $q > q_l$). The extension of the spectral gap will be a free parameter. In the following we will set $\varepsilon = 1$ and $q_l = 2\pi$ which fix the dimensionless form of our model.
The total field $\boldsymbol{U} + \boldsymbol{u}$ we obtain in this way will be the background in which

a puff of $\mathcal{N}$ seeded particles will evolve according to the Langevin equation (2.2).
The evolution given by (2.2) in terms of the fully resolved velocity field is what we can define as our "exact" evolution. One the other hand, retaining the sole large-scale flow component $\boldsymbol{U}$, we can easily calculate the eddy-diffusivity field and the effective advection. Through these fields the evolution equation of the same initial puff of seeded particles can be determined via Eq. (2.22) and properly compared with the "exact" puff evolution.

For testing purposes, let us start by considering the simpler situation where the velocity field is of the form $\boldsymbol{U} + \boldsymbol{u}$ with $\boldsymbol{U}$ constant in space and time and $\boldsymbol{u}$ built in terms of N=5 modes in Eq. (2.28) for $q > q_l$. For $i = 1, \cdots, 5$ we assume $B_i = 4C\varepsilon^{2/3} q_i^{-5/3}$, with $C = 1.4$ (remember that $\varepsilon = 1$ and $q_l = 2\pi$). $\boldsymbol{U}$ is $(20, 3)$ and $\mathcal{U}_{rms} \sim 20.3$. This means that the maximum and minimum decay times of the small-scale modes are $\tau_{max} \sim 0.008$ and $\tau_{min} \sim 0.002$, respectively. Because of the fact that no large-scale velocity component is present here (we only have the mean field component), a pure diffusive regime is expected for times sufficiently larger than $\tau_{max} \sim 0.008$. The expression for the eddy-diffusivity tensor follow from Eqs. (2.54)-(2.56) from which we have: $\langle (x_\alpha - \langle x_\alpha \rangle)(x_\beta - \langle x_\beta \rangle) \rangle = 2D_{\alpha\beta}t$, with $D_{11} = 0.0051$, $D_{22} = 0.0037$, $D_{12} = 0.00022$. The numerical results obtained from the integration of the Langevin equation with the fully resolved velocity field are shown in Fig. 2.2. Averages are performed by following 9×10^4 particles and their initial position are uniformly spread on a unit square. The resulting time behavior of $\langle (x_\alpha - \langle x_\alpha \rangle)(x_\beta - \langle x_\beta \rangle) \rangle$ from the numerical integration of the Langevin equation is fitted with the function $at + b$ for $t > \tau_{max}$. The best fit curves agree with our model predictions with relative errors of $\sim 2\%$ (for D_{11}), 1% (for D_{22}) and 8% (for D_{12}).

2.6.1 Observables to measure model reliability

Let us now pass to analyze the general situation in the presence of a large-scale velocity component. A possible way to assess the performances of our eddy-diffusivity and effective advection model for the evolution of a puff of initially seeded particles is to compare (against the "exact" evolution) different absolute dispersion observables associated to the puff as a function of time. Here we focus on different moments of particle displacements from their initial positions in the frame of reference moving with the mean flow $\boldsymbol{U}^0$. In formulae, we will compute

$$M_p(t) = \langle |\boldsymbol{x} - \boldsymbol{x}(0) - \boldsymbol{U}^0 t|^p \rangle \tag{2.59}$$

for different p. Another observable we will consider is the probability density function, P, of $\Delta(t) \equiv |\boldsymbol{x} - \boldsymbol{x}(0) - \boldsymbol{U}^0 t|$ at different times. This latter quantity encodes both large and small fluctuations of particle displacements thus giving a complete description of the absolute dispersion phenomenon.

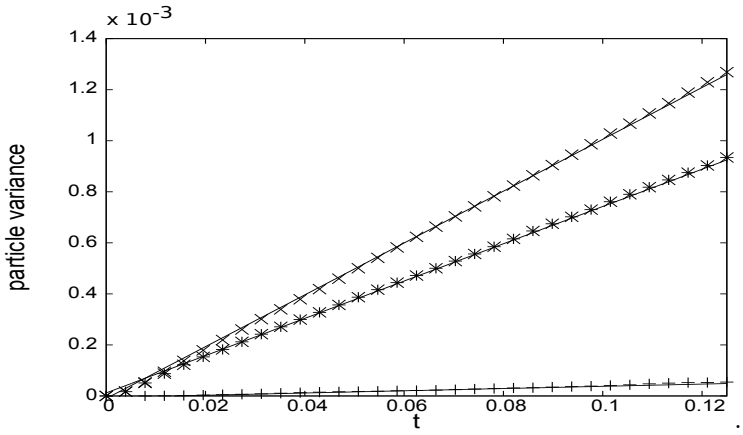

Figure 2.2: Particle variance $\zeta_{\alpha\beta} = \langle (x_\alpha - \langle x_\alpha \rangle)(x_\beta - \langle x_\beta \rangle) \rangle$ vs time in a small-scale flow plus a constant component. Continuous lines represent the theoretical slopes; symbols represent the numerical results for ζ_{11} ($\times$), ζ_{12} ($+$), and ζ_{22} ($*$).

2.6.2 Results and discussions

Let us start to investigate the reliability of our closure model based on the eddy-diffusivity tensor field (2.54)–(2.56) and effective advection (2.58) by varying the extension of the spectral gap depicted in Fig. 2.1. In Fig. 2.3 we report the moment $M_2(t)$ defined by (2.59) for the "exact" evolution (continuous line) and for our closure model (dotted line) for $\epsilon = q_L/q_l = 1$ (lower panel), corresponding to the absence of spectral gap, and $\epsilon = 0.125$, upper panel. The small-scale field has $N = 14$ modes, while the large-scale component has one active mode (i.e. $M = 1$). The mean field component is $\boldsymbol{U}^0 = (4, 0)$.
As one can see from Fig. 2.3, the two descriptions are almost indistinguishable already for $\epsilon = 0.125$. For $\epsilon = 1$ our closure works reasonably well and captures the relevant feature of the exact curve.

Note that at the final observation time the mean particle displacement is of order one and thus comparable to $2\pi/q_L = 1$ (case corresponding to $\epsilon = 1$) and smaller than $2\pi/q_L = 8$ (case corresponding to $\epsilon = 0.125$). This tells us that we are observing the dispersion phenomenon in the pre-asymptotic regime. In terms of typical times, the largest small-scale velocity correlation time $\tau_{max} \sim 0.035$ is four times smaller than the observation time $t = 0.125$ which also justifies a description based on the eddy-diffusivity.

To quantitatively estimate the discrepancy between the two descriptions we have computed the relative errors for different values of ϵ. Errors have been defined in terms of the L^2-norm $||f||^2_{L^2} \equiv \int dt |f(t)|^2$ from which the

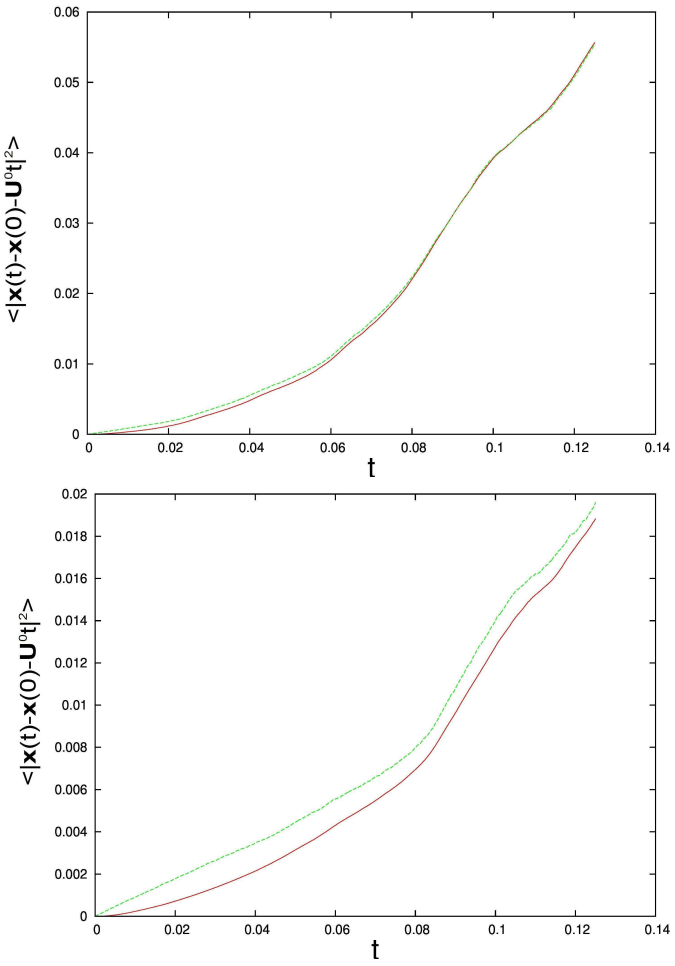

Figure 2.3: M_2 vs time, following the exact evolution (continuous red line) and our description with eddy diffusivity plus effective velocity (dotted green line). In the upper panel, $\epsilon = 0.125$, and $\mathcal{U}_{rms} = 4.8$. In the lower panel, $\epsilon = 1$ and $\mathcal{U}_{rms} = 4.5$.

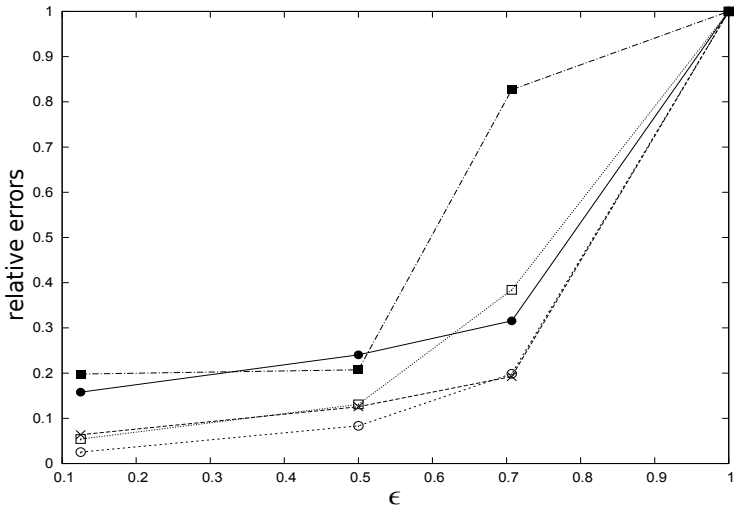

Figure 2.4: L^2-relative errors $D_p(\epsilon)/D_p(1)$ (see text) for different orders of the moment p as a function of the gap extension ϵ. Full circles refer to $p = 1/2$, $\times$ to $p = 1$, empty circles to $p = 2$, empty squares to $p = 3$, and full squares to $p = 4$. $\mathcal{U}_{rms} = 4.5$. The normalizing factors $D_p(1)$ are: $D_{1/2}(1) = 0.34$, $D_1(1) = 0.12$, $D_2(1) = 0.019$, $D_3(1) = 0.0035$, $D_4(1) = 0.00072$.

relative error follows from the definition of relative functional distance:

$$D_p(\epsilon) \equiv \frac{||M_p(\epsilon) - M_p^E(\epsilon)||_{L^2}^2}{||M_p(\epsilon)||_{L^2}||M_p^E(\epsilon)||_{L^2}}. \tag{2.60}$$

In this expression $M_p^E(\epsilon)$ refers to the exact evolution while $M_p(\epsilon)$ corresponds to our closure.

The results are summarized in Fig. 2.4 where $D_p(\epsilon)/D_p(1)$ is shown for different values of ϵ. As expected, the smallest errors are for $p = 2$ corresponding to the errors calculated on second-order moments. It is interesting to remark that also $p \neq 2$ provide satisfactory results. This is probably related to the quasi-Gaussian character of the dispersion process on pre-asymptotic scales.

Having shown that our closure model works even in the absence of scale separation within the pre-asymptotic stage of the dispersion phenomenon, we are now ready to investigate how our closure compares with alternative strategies. We decided to choose as reference closures the following cases. Case A: our closure; Case B: evolution with the sole large-scale velocity (i.e. no closure at all); Case C: our closure without the effective (compressible) large-scale advection; Case D: a naive closure based on the naive idea that the eddy diffusivity only depends on the small-scale advection. Accordingly, in this latter case the eddy diffusivity is obtained by setting to zero the large-scale velocity component (including the mean field component). All cases

have $\mathcal{U}_{rms} \sim 4.5$.
The results are reported in Figs. 2.5 and 2.6. In Fig. 2.5 we show the behavior of the moments $M_2(t)$ (upper panel) and $M_4(t)$ (lower panel) as a function of time for the "exact" evolution (continuous line), which we indicate with the letter E, and for cases A, B, C and D, with $\epsilon = 1$. In Fig. 2.6, $P(\Delta(t))$ is shown for $t = 0.0325$ (corresponding to $t \sim \tau_{max}$) and $t = 0.125$ (corresponding to $t \sim 4\tau_{max}$) for the cases A,C,D and the exact evolution. As one can see from these figures, our closure works significantly better than the other strategies. This is true also with respect to the simpler closure where the effective large-scale advection is neglected even if in this case the differences are quite small.

The discrepancies seen in the left panel of Fig. 2.6 are due to the small observation time (of the order of τ_{max}). This implies that the particle dynamics is still self-correlated and, as a result, the renormalization process giving rise to the eddy-diffusivity is still in progress. Anyway, also in this case our closure works better then the other strategies. Also note that the accuracy of our closure becomes significantly better as the observation time becomes sufficiently larger than τ_{max} (lower panel of Fig. 2.6). This is expected as a result of the increased time-scale separation between the small-scale velocity and the particle dynamics ensuring the development of the renormalization process.

2.7 Conclusions

The key requirement shared by all closure strategies is the presence of scale separation. As a matter of fact, in real situations this requirement is not always fulfilled and a natural question arises on the level of accuracy of a description based on the eddy-diffusivity concept forced to work even in the absence of scale separation. Moreover, a long-standing accepted idea in the realm of large-scale transport is that small-scale features of a carrier flow gives rise to the concept of eddy-diffusivity while the large-scale velocity component only acts as a large-scale advection. In this chapter both issues have been analyzed on the basis of known results in the field of large-scale transport obtained via multiple-scale expansions. From these results it clearly emerges that the eddy-diffusivity has an explicit dependence also on the large-scale advection and, conversely, small scales affect the large-scale advection via an effective compressible velocity field.
Theoretical results are thus somehow contrasting the general belief, a fact that led us to quantitatively address these important issues.
To do that, our idea has been to define a stochastic velocity ensemble mimicking relevant features of small-scale turbulence which, at the same time, allowed us to obtain an explicit expression both for the eddy-diffusivity tensor field and for the effective large-scale advection. Once the explicit expressions

for both quantities have been obtained, we have quantified i) the deterioration of the eddy-diffusivity description by reducing the scale-separation in the carrier flow; ii) the importance of the contribution of small-scales to the large-scale advection emerging as a new compressible velocity components, and, iii) we have also compared the accuracy of our closure against other simple (apparently reasonable) possible strategies. In relation to i) we quantitatively measured the quality of the performance of our closure by a direct comparison against the results obtained from the exact evolution equation. This comparison has been carried out for different extensions of the spectral gap, including the situation corresponding to the absence of scale separation. Although a deterioration of the closure performance is clearly detectable by reducing the scale separation, relevant features of the large-scale transport are still captured by our closure. As far as ii) is concerned, we have shown that, in all analyzed cases, the contribution to the large-scale advection coming from small-scale velocity fluctuations is negligible. Although small, its contribution is however in the direction of the exact solution. This finding is thus in agreement with the common belief which considers the large-scale velocity component as the sole contribution to the large-scale advection. Finally, in relation to iii) we can state that our closure performs better than other reasonable alternative strategies. In particular, the approach that assumes an eddy-diffusivity only dependent on small-scale velocity fluctuations works considerably worse than our closure. This clearly points to the conclusion that the large-scale velocity component has a role to determine the eddy-diffusivity. Unlike the previous conclusion, this evidence is against the common belief that sees the eddy-diffusivity as a product of small-scale fluctuations. Also, the simplest description in terms of a tracer equation without any kind of eddy diffusivity (a model often considered to study surface dispersion in the ocean and in the atmosphere) turns out to be the worst option.

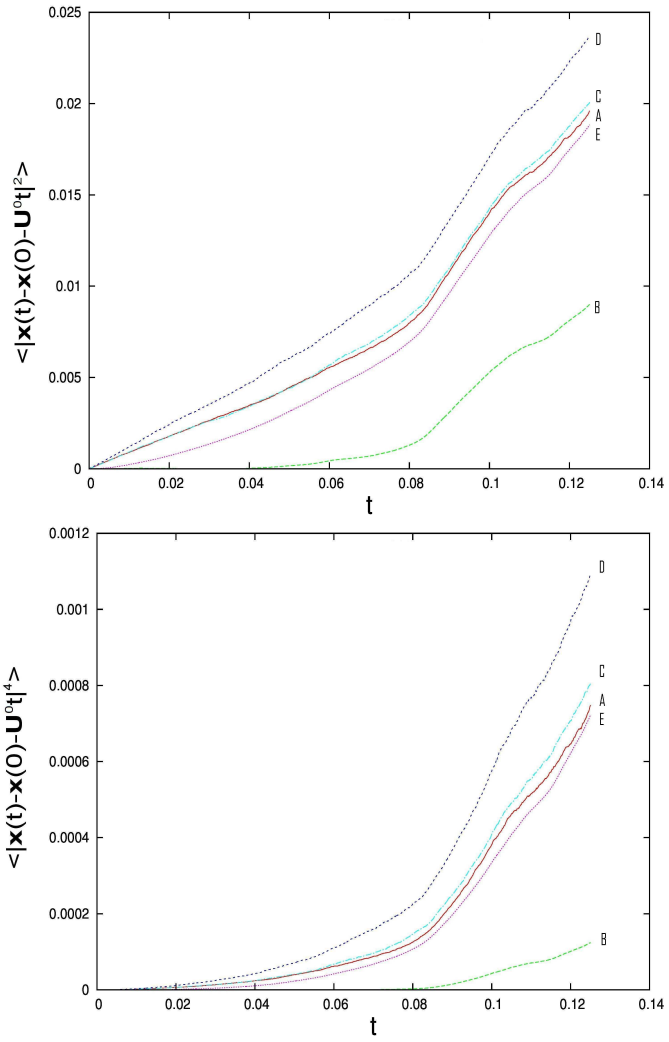

Figure 2.5: M_2 (upper panel) and M_4 (lower panel) vs time for $\epsilon = 1$ and $\mathcal{U}_{rms} = 4.5$. The continuous line depicts the exact evolution, and it is indicated by the letter E; case A is our closure; case B is the evolution with large-scale flow only; case C represent our closure without the effective compressible velocity contribution; "naive" description is finally indicated by letter D.

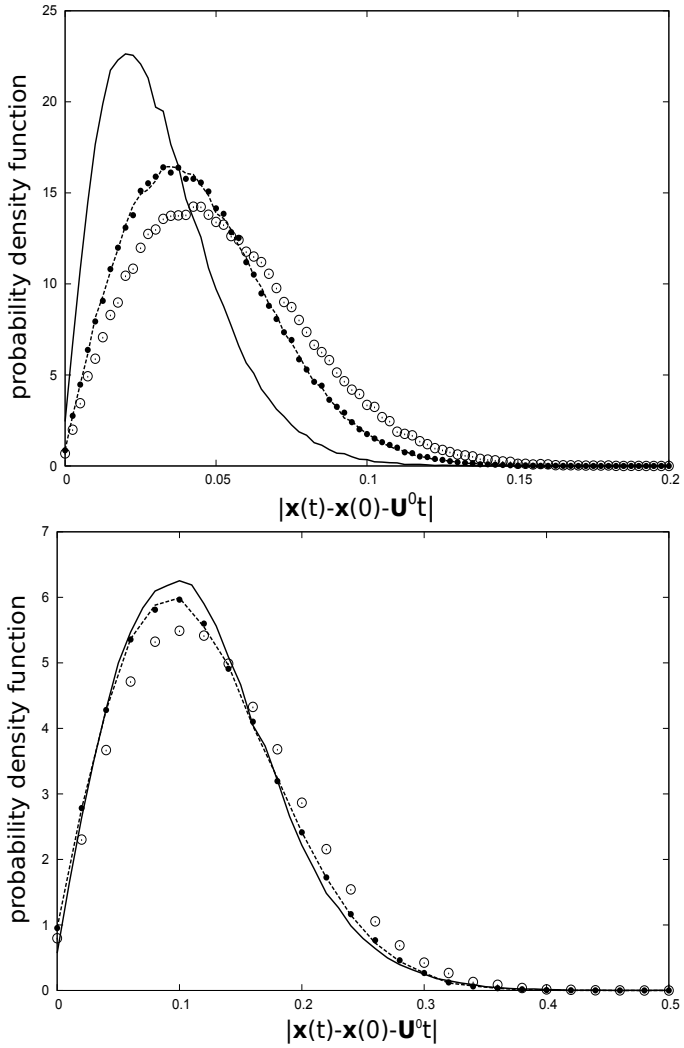

Figure 2.6: Probability density functions of $\Delta(t)$ for $\epsilon = 1$ and $\mathcal{U}_{rms} = 4.5$. In the upper panel $t = 0.0325$, in the lower panel $t = 0.125$. The continuous line depicts the exact evolution; the dashed line is the case A; full circles the case C; empty circles indicate case D.

Appendix

2.A A superposition principle for the eddy-diffusivities

In this Appendix we show the existence of a superposition principle which holds for the eddy-diffusivity field with advection by statistically homogeneous parallel flows. For the sake of simplicity our focus will be restricted to two-dimensional cases. A simple generalization allows one to extend our results to three dimensions.
Let us start from the definition (2.43) of eddy-diffusivity in Lagrangian terms. From this equation the well-known Taylor expression easily follows (the molecular diffusivity is assumed to be negligible in this work):

$$\boldsymbol{D} = \lim_{t\to\infty} \langle \int_0^t dt' \boldsymbol{u}(\boldsymbol{x}(t),t) \otimes \boldsymbol{u}(\boldsymbol{x}(t'),t') \rangle \quad . \tag{2.61}$$

In Fourier space, the incompressible velocity field reads $\mathbf{u}(\boldsymbol{x},t) = \int \mathbf{dq} \frac{A(\mathbf{q},t)\mathbf{q}^\perp}{q} e^{i\mathbf{q}\cdot\boldsymbol{x}}$ which, plugged into (2.61), gives

$$\boldsymbol{D} = \lim_{t\to\infty} \int_0^t dt' \int d\mathbf{q} \int d\mathbf{q}' \frac{\mathbf{q}^\perp \otimes \mathbf{q}'^\perp}{q^2} \langle A(\mathbf{q},t) A(\mathbf{q}',t') e^{i(\mathbf{q}\cdot\boldsymbol{x}(t) + \mathbf{q}'\cdot\boldsymbol{x}(t'))} \rangle \quad . \tag{2.62}$$

where $\boldsymbol{x}(t)$ is solution of the (multiple-scale) system

$$\frac{d\boldsymbol{x}_i}{dt} = \int d\mathbf{q} \frac{A(\mathbf{q},t)\mathbf{q}^\perp}{q} e^{i\mathbf{q}\cdot\boldsymbol{x}(t)} + \mathbf{U}(\mathbf{X},T) \quad . \tag{2.63}$$

The main problem for the analytical calculation of D is that the solution of (2.63) has to be used in (2.62). This is in general a daunting task.
To overcome the problem, let us suppose $\boldsymbol{u}$ to be a parallel flow pointing along a constant direction $\mathbf{q}^\perp/q = \mathbf{n}^\perp$. If one assumes it is built in terms of a finite superposition of Fourier harmonics, the (discrete) Fourier decomposition becomes:

$$\boldsymbol{u}(\boldsymbol{x},t) = \sum_i A(q_i,t)\mathbf{n}^\perp e^{iq_i\mathbf{n}\cdot\boldsymbol{x}} \quad . \tag{2.64}$$

Note that it corresponds to the kinematic models we introduced in Sec. 2.4, after absorbing the phases $e^{i\theta_i}$ in the amplitudes, which are now complex

numbers.
By multiplying Eq. (2.63) by $\mathbf{n}$ the following important result is obtained:

$$\mathbf{n} \cdot \boldsymbol{x}(t) = \mathbf{n} \cdot \mathbf{U}(\mathbf{X}, T)t \quad .$$

It allows one to replace in Eq. (2.62) the term depending on the trajectory $\mathbf{x}(t)$ with a more innocent contribution not depending on the particle trajectory:

$$\boldsymbol{D} = \lim_{t\to\infty} \left(\mathbf{n}^\perp \otimes \mathbf{n}^\perp\right) \int_0^t dt' \sum_{i,j} \langle A(q_i,t)A(q_j,t')\rangle e^{i(q_i \mathbf{n}\cdot\mathbf{U}t + q_j \mathbf{n}\cdot\mathbf{U}t')} \quad . \quad (2.65)$$

Let us now show that to arrive to the superposition principle it is enough to assume an homogeous statistics for the velocity field. In Fourier space, homogeneity is equivalent to the well-known condition

$$\langle \hat{\boldsymbol{u}}(\mathbf{q}_i,t) \otimes \hat{\boldsymbol{u}}(\mathbf{q}_j,t')\rangle \propto \delta(\mathbf{q}_i + \mathbf{q}_j)$$

that simply says, toghether with the relation $\hat{\boldsymbol{u}}(-\mathbf{q}_i,t) = \hat{\boldsymbol{u}}^*(\mathbf{q}_i,t)$, independence of Fourier modes. Since $\hat{\boldsymbol{u}}(\mathbf{q}_i,t) \propto A(q_i,t)\mathbf{n}^\perp$, we have in the discrete case that $\langle A(q_i,t)A(q_j,t')\rangle = \langle A(q_i,t)A^*(q_i,t')\rangle \delta_{q_i,-q_j}$, and (2.65) becomes:

$$\boldsymbol{D} = \lim_{t\to\infty} \left(\mathbf{n}^\perp \otimes \mathbf{n}^\perp\right) \int_0^t dt' \sum_i \langle A(q_i,t)A^*(q_i,t')\rangle e^{iq_i \mathbf{n}\cdot\mathbf{U}(t-t')} = \sum_i \boldsymbol{D}_i$$

where $\boldsymbol{D}_i$ is the eddy-diffusivity associated to the i-th mode:

$$\begin{aligned} \boldsymbol{D}_i &= \lim_{t\to\infty} \left(\mathbf{n}^\perp \otimes \mathbf{n}^\perp\right) \int_0^t dt' \langle A(q_i,t)A^*(q_i,t')\rangle e^{iq_i \mathbf{n}\cdot\mathbf{U}(t-t')} \\ &\equiv \lim_{t\to\infty} \int_o^t dt' \langle \boldsymbol{u}_i(\boldsymbol{x}_i(t),t) \otimes \boldsymbol{u}_i^*(\boldsymbol{x}_i(t'),t')\rangle \end{aligned}$$

and to compute trajectories only the i-th mode is involved:

$$\frac{d\boldsymbol{x}_i}{dt} = \boldsymbol{u}_i(\boldsymbol{x}_i(t),t) + \mathbf{U}(\mathbf{X},T) = A(q_i,t)\mathbf{n}^\perp e^{iq_i \mathbf{n}\cdot\boldsymbol{x}_i(t)} + \mathbf{U}(\mathbf{X},T)$$

where we have identified $\boldsymbol{u}_i$ with $A(q_i,t)\mathbf{n}^\perp e^{i\mathbf{q}_i\cdot\boldsymbol{x}}$.

2.B Explicit expression for the effective advection

To determine the effective advection we need to evaluate

$$\frac{\partial D_{\alpha\beta}}{\partial x_\beta} = \sum_{p=1}^{N} \frac{\partial D_{p\,\alpha\beta}}{\partial U_\gamma} \frac{\partial U_\gamma}{\partial x_\beta} \quad . \quad (2.66)$$

To obtain the divergence of the eddy-diffusivity field we again consider the following three integrals, which are related to the eddy diffusivity itself through Eqs. (2.53):

$$\int_0^{2\pi} \frac{\sin^2\phi d\phi}{\tau_i^2 q_i^2 (U_1\cos\phi + U_2\sin\phi)^2 + 1}$$

$$-\int_0^{2\pi} \frac{\sin\phi\cos\phi d\phi}{\tau_i^2 q_i^2 (U_1\cos\phi + U_2\sin\phi)^2 + 1}$$

$$\int_0^{2\pi} \frac{\cos^2\phi d\phi}{\tau_i^2 q_i^2 (U_1\cos\phi + U_2\sin\phi)^2 + 1} \quad .$$

Our first remark is that, if in the third integral we perform the transformation $\phi \to \pi/2 - \phi$, then we obtain:

$$\int_{-\frac{3\pi}{2}}^{\frac{\pi}{2}} \frac{\sin^2\phi d\phi}{\tau_i^2 q_i^2 (U_2\cos\phi + U_1\sin\phi)^2 + 1} \, .$$

The value of the latter does not change if we evaluate it between 0 an 2π. This because the integrating function has a period of 2π. Thus we obtain an integral similar to the first one after commuting $U_1 \leftrightarrows U_2$. This means that $D_{11}(U_1, U_2) = D_{22}(U_2, U_1)$ and we only have to compute two integrals. By means of a similar argument, by exploiting the fact that $\sin\phi\cos\phi = 1/2\sin 2\phi$ and $\sin(\pi - 2\phi) = \sin 2\phi$, one can also easily prove that $D_{12}(U_1, U_2) = D_{12}(U_2, U_1)$. We are going to use these properties to evaluate the eddy diffusivity divergence below.

By direct computation, after lengthy algebra one obtains:

$$\begin{aligned}
&\frac{\partial D_{p\,11}}{\partial U_1} = -\Big[U_1^6\tau_p^4 q_p^4 + 3\tau_p^2 q_p^2 U_1^4 - 3U_1^2 U_2^4 \tau_p^4 q_p^4 + \\
&-6\tau_p^2 q_p^2 U_2^2 U_1^2 + 2U_1^2 + \\
&+(4U_1^2\tau_p^2 q_p^2 U_2^2 - 2U_1^2 - 2U_1^4\tau_p^2 q_p^2)\sqrt{\tau_p^2 q_p^2 (U_1^2 + U_2^2) + 1} + \\
&-9U_2^4\tau_p^2 q_p^2 - 6U_2^2 - 2U_2^6\tau_p^4 q_p^4 + \\
&+6(U_2^2 + U_2^4\tau_p^2 q_p^2)\sqrt{\tau_p^2 q_p^2 (U_1^2 + U_2^2) + 1)}\Big] U_1 B_p^2 \times \\
&\Big[2(U_1^2 + U_2^2)^3 q_p^2 \tau_p \Big(\tau_p^2 q_p^2 (U_1^2 + U_2^2) + 1\Big)^{3/2}\Big]^{-1} \quad ,
\end{aligned} \tag{2.67}$$

$$\frac{\partial D_{p\,11}}{\partial U_2} = -\Big[3U_1^2(U_1^4+U_2^4)\tau_p^4 q_p^4 + 6U_1^4\tau_p^4 U_2^2 q_p^4 + \\ +9\tau_p^2 q_p^2 U_1^4 + 6\tau_p^2 q_p^2 U_2^2 U_1^2 + 6U_1^2 + \\ -4U_1^2\tau_p^2 q_p^2 U_2^2\sqrt{\tau_p^2 q_p^2(U_1^2+U_2^2)+1} + \\ +\sqrt{\tau_p^2 q_p^2(U_1^2+U_2^2)+1}(2U_2^4\tau_p^2 q_p^2 - 6U_1^2 - 6U_1^4\tau_p^2 q_p^2) + \\ -3U_2^4\tau_p^2 q_p^2 - 2U_2^2 + 2U_2^2\sqrt{\tau_p^2 q_p^2(U_1^2+U_2^2)+1}\,\Big]U_2 B_p^2 \times \\ \Big[2(U_1^2+U_2^2)^3 q_p^2\tau_p\Big(\tau_p^2 q_p^2(U_1^2+U_2^2)+1\Big)^{3/2}\Big]^{-1}\,, \tag{2.68}$$

Since in the three integrals (2.53) the integrating functions and their derivatives with respect to the velocity are limited, one can interchange integration and differentiation to compute $\frac{\partial D_{\alpha\beta}}{\partial U_\gamma}$, and it is easy to see that:

$$\frac{\partial D_{12}}{\partial U_2} = -\frac{\partial D_{11}}{\partial U_1}$$

Also notice that, for the symmetry properties of the eddy-diffusivity tensor with respect to U_1 and U_2, other derivatives of the eddy-diffusivity with respect to the velocity can be easily obtained from the above expressions, by simply substituting:

$$\begin{aligned}\frac{\partial D_{p\,12}}{\partial U_1} &= \frac{\partial D_{p\,12}}{\partial U_2}\Big|_{\substack{U_1\to U_2\\ U_2\to U_1}}\,,\\ \frac{\partial D_{p\,22}}{\partial U_1} &= \frac{\partial D_{p\,11}}{\partial U_2}\Big|_{\substack{U_1\to U_2\\ U_2\to U_1}}\,,\\ \frac{\partial D_{p\,22}}{\partial U_2} &= \frac{\partial D_{p\,11}}{\partial U_1}\Big|_{\substack{U_1\to U_2\\ U_2\to U_1}}\,.\end{aligned} \tag{2.69}$$

As a consequence, one has:

$$\frac{\partial D_{p\,12}}{\partial U_1} = \Big[U_2^6\tau_p^4 q_p^4 + 3\tau_p^2 q_p^2 U_2^4 - 3U_2^2 U_1^4\tau_p^4 q_p^4 + \\ -6\tau_p^2 q_p^2 U_1^2 U_2^2 + 2U_2^2 + \\ +(4U_2^2\tau_p^2 q_p^2 U_1^2 - 2U_2^2 - 2U_2^4\tau_p^2 q_p^2)\sqrt{\tau_p^2 q_p^2(U_1^2+U_2^2)+1} + \\ -9U_1^4\tau_p^2 q_p^2 - 6U_1^2 - 2U_1^6\tau_p^4 q_p^4 + \\ +6(U_1^2 + U_1^4\tau_p^2 q_p^2)\sqrt{\tau_p^2 q_p^2(U_1^2+U_2^2)+1)}\Big]U_2 B_p^2 \times \\ \Big[2(U_1^2+U_2^2)^3 q_p^2\tau_p\Big(\tau_p^2 q_p^2(U_1^2+U_2^2)+1\Big)^{3/2}\Big]^{-1}\,, \tag{2.70}$$

$$\frac{\partial D_{p\,12}}{\partial U_2} = \Big[U_1^6\tau_p^4 q_p^4 + 3\tau_p^2 q_p^2 U_1^4 - 3U_1^2 U_2^4 \tau_p^4 q_p^4 + \\ -6\tau_p^2 q_p^2 U_2^2 U_1^2 + 2U_1^2 + \\ +(4U_1^2\tau_p^2 q_p^2 U_2^2 - 2U_1^2 - 2U_1^4\tau_p^2 q_p^2)\sqrt{\tau_p^2 q_p^2(U_1^2+U_2^2)+1} + \\ -9U_2^4\tau_p^2 q_p^2 - 6U_2^2 - 2U_2^6\tau_p^4 q_p^4 + \\ +6(U_2^2 + U_2^4\tau_p^2 q_p^2)\sqrt{\tau_p^2 q_p^2(U_1^2+U_2^2)+1)}\Big] U_1 B_p^2 \times \\ \Big[2(U_1^2+U_2^2)^3 q_p^2\tau_p\Big(\tau_p^2 q_p^2(U_1^2+U_2^2)+1\Big)^{3/2}\Big]^{-1} \;, \tag{2.71}$$

$$\frac{\partial D_{p\,22}}{\partial U_1} = -\Big[3U_2^2(U_2^4+U_1^4)\tau_p^4 q_p^4 + 6U_2^4\tau_p^4 U_1^2 q_p^4 + \\ +9\tau_p^2 q_p^2 U_2^4 + 6\tau_p^2 q_p^2 U_1^2 U_2^2 + 6U_2^2 + \\ -4U_2^2\tau_p^2 q_p^2 U_1^2\sqrt{\tau_p^2 q_p^2(U_1^2+U_2^2)+1} + \\ +\sqrt{\tau_p^2 q_p^2(U_1^2+U_2^2)+1}(2U_1^4\tau_p^2 q_p^2 - 6U_2^2 - 6U_2^4\tau_p^2 q_p^2) + \\ -3U_1^4\tau_p^2 q_p^2 - 2U_1^2 + 2U_1^2\sqrt{\tau_p^2 q_p^2(U_1^2+U_2^2)+1}\,\Big] U_1 B_p^2 \times \\ \Big[2(U_1^2+U_2^2)^3 q_p^2\tau_p\Big(\tau_p^2 q_p^2(U_1^2+U_2^2)+1\Big)^{3/2}\Big]^{-1} \;, \tag{2.72}$$

$$\frac{\partial D_{p\,22}}{\partial U_2} = -\Big[U_2^6\tau_p^4 q_p^4 + 3\tau_p^2 q_p^2 U_2^4 - 3U_2^2 U_1^4 \tau_p^4 q_p^4 + \\ -6\tau_p^2 q_p^2 U_1^2 U_2^2 + 2U_2^2 + \\ +(4U_2^2\tau_p^2 q_p^2 U_1^2 - 2U_2^2 - 2U_2^4\tau_p^2 q_p^2)\sqrt{\tau_p^2 q_p^2(U_1^2+U_2^2)+1} + \\ -9U_1^4\tau_p^2 q_p^2 - 6U_1^2 - 2U_1^6\tau_p^4 q_p^4 + \\ +6(U_1^2 + U_1^4\tau_p^2 q_p^2)\sqrt{\tau_p^2 q_p^2(U_1^2+U_2^2)+1)}\Big] U_2 B_p^2 \times \\ \Big[2(U_1^2+U_2^2)^3 q_p^2\tau_p\Big(\tau_p^2 q_p^2(U_1^2+U_2^2)+1\Big)^{3/2}\Big]^{-1} \;. \tag{2.73}$$

In a similar way, from the definition of our large-scale velocity (2.37)

herein used, the velocity gradient tensor reads:

$$\begin{aligned}
\frac{\partial U_1}{\partial x} &= -\sum_{i=1}^{M} A_i(t) q_i \sin(\phi_i)\cos(\phi_i)\sin[q_i(\cos(\phi_i)x+\sin(\phi_i)y)] \\
\frac{\partial U_1}{\partial y} &= -\sum_{i=1}^{M} A_i(t) q_i \sin^2(\phi_i)\sin[q_i(\cos(\phi_i)x+\sin(\phi_i)y)] \\
\frac{\partial U_2}{\partial x} &= \sum_{i=1}^{M} A_i(t) q_i \cos^2(\phi_i)\cos[q_i(\sin(\phi_i)x+\sin(\phi_i)y)] \\
\frac{\partial U_2}{\partial y} &= \sum_{i=1}^{M} A_i(t) q_i \sin(\phi_i)\cos(\phi_i)\cos[q_i(\sin(\phi_i)x+\sin(\phi_i)y)] \quad .(2.74)
\end{aligned}$$

2.C Explicit expressions for the eddy-diffusivity field in three dimensions

In this Appendix we generalize to three-dimensions the results of Sec. 2.5. The main technical difference with respect to Sec. 2.5 is that a single Fourier harmonic of a parallel flow needs three angles to be identified, instead of one as in two dimensions. This makes the problem more cumbersome from the geometrical point of view. Indeed, it is still true that the wavenumber in each Fourier harmonic is perpendicular to the velocity, but now it can lie in any direction on the plane orthogonal to that. This fact is related to the three coordinates we need to parametrize the group connected to the invariance under three-dimensional rotations (the so-called $SO(3,\mathbb{R})$ group).
In order to have isotropy, we have therefore to rotate the generical vector, or tensor, for each element of the group (i.e., along any possible direction) and finally integrate with respect to the Haar measure on the group itself, to have an average over any rotation.
The simplest way to generalize to three dimensions the statistically isotropic small-scale flow we described in Sec. 3 is to generate a flow for each initial condition $\boldsymbol{x}(0)$ having also the wavenumber direction $\mathbf{n}$ fixed. This flow is univocally identified by three angles as described above, and there always exists an orientation of the coordinate system such that our flow takes the form $(0, u'(z'), 0)$. Its $i-$th harmonic turns out to be depending again just on the wavenumber modulus q_i:

$$\begin{aligned}
u_1'(x',y',z',t) &= 0 \\
u_2'(x',y',z',t) &= \sum_{i=1}^{N} A_i(\boldsymbol{x}'(0),t)\cos[q_i z' + \theta_i(\boldsymbol{x}(0))] \\
u_3'(x',y',z',t) &= 0 \quad .
\end{aligned}$$

In order to obtain an isotropic statistics, we need to associate three random angles to each particle initial condition and take the average over their evolution.
There are several possible choices to fix a coordinate system on the group with its associated expression of the Haar measure. We decided to proceed in the following way, remembering that in $SO(3,\mathbb{R})$ rotations are not commutative and thus the order of their action has to be defined. In our case, before performing the two rotations to align the wavenumber $\mathbf{n}$ along the z-axis , which is similar to what we did in two dimensions, we do a preliminar coordinate rotation around $\mathbf{n}$ itself so that the velocity will eventually lie on the $y-$axis.
Once we know that $\mathbf{n}' = (0,0,1) = \mathbf{R}\mathbf{n}$, to get back to the old system the following relationship has to be taken into account:

$$\begin{pmatrix}0\\0\\1\end{pmatrix} = \begin{pmatrix}\cos\theta & 0 & -\sin\theta\\ 0 & 1 & 0\\ \sin\theta & 0 & \cos\theta\end{pmatrix}\begin{pmatrix}\cos\phi & \sin\phi & 0\\ -\sin\phi & \cos\phi & 0\\ 0 & 0 & 1\end{pmatrix}\begin{pmatrix}\sin\theta\cos\phi\\ \sin\theta\sin\phi\\ \cos\theta\end{pmatrix} \tag{2.75}$$

where the unit vector $\mathbf{n}$ is identified by the two spherical angles θ and ϕ. The preliminar rotation we need is the one around the unit vector $\mathbf{n}$, which can be expressed as [59]:

$$\mathbf{R}(\psi,\mathbf{n}) = \boldsymbol{I} + \boldsymbol{N}\sin\psi + \boldsymbol{N}^2(1-\cos\psi)$$

where ψ is the rotation angle, $\boldsymbol{I}$ is the identity and $N_{\alpha\beta} = -\eta_{\alpha\beta\gamma}n_\gamma$, $\eta_{\alpha\beta\gamma}$ being the Levi-Civita symbol. Notice that this rotation has effect solely on the velocity unit vector, since it maps $\mathbf{n} = (\sin\theta\cos\phi, \sin\theta\sin\phi, \cos\theta)$ in itself. The most general rotation can then be expressed as $\boldsymbol{R}(\theta)\,\boldsymbol{R}(\phi)\,\boldsymbol{R}(\psi,\mathbf{n})$. The eddy-diffusivity tensor will transform as:

$$\begin{aligned}\boldsymbol{D} &= \frac{1}{2\pi^2}\int_0^{2\pi}\sin^2\frac{\psi}{2}d\frac{\psi}{2}\int_0^{\pi}\sin\theta d\theta\int_0^{2\pi}d\phi\\ &\times \left[\boldsymbol{R}(\theta)\,\boldsymbol{R}(\phi)\,\boldsymbol{R}(\psi,\mathbf{n})\right]^{-1}\boldsymbol{D}'\boldsymbol{R}(\theta)\,\boldsymbol{R}(\phi)\,\boldsymbol{R}(\psi,\mathbf{n})\end{aligned} \tag{2.76}$$

after averaging over the angles by integrating over the Haar measure in the so-called parametrization $(\psi,\mathbf{n})$ [59]. Here $\boldsymbol{D}'$ is:

$$D'_{\alpha\beta} = \sum_{i=1}^{N}\begin{pmatrix}0 & 0 & 0\\ 0 & \frac{B_i}{2}\frac{\tau_i}{(\boldsymbol{U}\cdot\mathbf{n}(\phi,\theta))^2 q_i^2\tau_i^2+1} & 0\\ 0 & 0 & 0\end{pmatrix} \tag{2.77}$$

Since the integrating function does never depend on ψ, the integral over this angle is easily doable, but to compute the integral over ϕ and eventually θ, we need to rotate the coordinates further to have $\boldsymbol{U}$ along the $z-$axis, so

that $\mathbf{n}\cdot\boldsymbol{U} = |\boldsymbol{U}|\cos\theta$. This can be done by means of the rotation:

$$R_{\alpha\beta}(\boldsymbol{U}) = \begin{pmatrix} \frac{U_3}{\sqrt{U_1^2+U_2^2+U_3^2}} & 0 & -\frac{\sqrt{U_1^2+U^2}}{\sqrt{U_1^2+U_2^2+U_3^2}} \\ 0 & 1 & 0 \\ \frac{\sqrt{U_1^2+U^2}}{\sqrt{U_1^2+U_2^2+U_3^2}} & 0 & \frac{U_3}{\sqrt{U_1^2+U_2^2+U_3^2}} \end{pmatrix} \begin{pmatrix} \frac{U_1}{\sqrt{U_1^2+U_2^2}} & \frac{U_2}{\sqrt{U_1^2+U_2^2}} & 0 \\ -\frac{U_2}{\sqrt{U_1^2+U_2^2}} & \frac{U_1}{\sqrt{U_1^2+U_2^2}} & 0 \\ 0 & 0 & 1 \end{pmatrix} \tag{2.78}$$

Now the eddy-diffusivity tensor turns out to be:

$$\begin{aligned} D_{\alpha\beta} &= \frac{1}{2\pi^2}\sum_{i=1}^{N}\int_0^{2\pi}\sin^2\frac{\psi}{2}d\frac{\psi}{2}\int_0^{\pi}\sin\theta d\theta\int_0^{2\pi}d\phi \\ &\times \quad R(\boldsymbol{U})^{-1}_{\alpha\gamma}[R(\theta)\,R(\phi)\,R(\psi,\mathbf{n})]^{-1}_{\gamma 2} \\ &\times \quad \frac{B_i}{2}\frac{\tau_i}{(|\boldsymbol{U}|\cos\theta)^2 q_i^2\tau_i^2+1} \\ &\times \quad [R(\theta)\,R(\phi)\,R(\psi,\mathbf{n})]_{2\delta}R(\boldsymbol{U})_{\delta\beta} \end{aligned} \tag{2.79}$$

and the three integrals can be finally computed sequentially. The result is too cumbersome to write here entry by entry; however, its tensorial form reads:

$$\begin{aligned} D_{\alpha\beta} = \Bigg[\frac{\alpha}{\mathcal{U}_{rms}}|\mathbf{U}|\left(|\mathbf{U}|^2\delta_{\alpha\beta}-3U_\alpha U_\beta\right)+\Bigg((3+\frac{\alpha^2}{\mathcal{U}_{rms}^2}|\mathbf{U}|^2)U_\alpha U_\beta-|\mathbf{U}|^2\delta_{\alpha\beta} \\ +\frac{\alpha^2}{\mathcal{U}_{rms}^2}|\mathbf{U}|^4\delta_{\alpha\beta}\Bigg)\arctan\left(\frac{\alpha}{\mathcal{U}_{rms}}|\mathbf{U}|\right)\Bigg]\left[4\frac{\alpha^3}{\mathcal{U}_{rms}^3}|\mathbf{U}|^5\right]^{-1}\sum_{i=1}^{N}\frac{B_i}{2}\tau_i \end{aligned} \tag{2.80}$$

It is noteworthy that, as $\mathbf{U}\to 0$, we recover the isotropic expression $D_{\alpha\beta} = \delta_{\alpha\beta}\sum_{i=1}^{N}\frac{B_i}{6}\tau_i$

Chapter 3

The role of inertia on large-scale particle transport

3.1 Introduction

Understanding the role of particle inertia on the late-time dispersion process is a problem of paramount importance in a variety of situations, mainly related to geophysics and atmospheric sciences. Airborne particulate matter in the atmosphere has indeed a well-recognized role for the Earth's climate system because of its effect on global radiative budget by scattering and absorbing long-wave and short-wave radiation [54]. For the sake of example, one of the most intriguing issue in this context is related to the evidence of anomalous large fluctuations in the residence times of mineral dust observed in different experiments carried out in the atmosphere [60].

Those observations naturally lead to the idea that settling and dispersion of inertial particles, both contributing to the residence time of particles in the atmosphere, crucially depend on the peculiar properties of the carrier flow encountered in the specific experiment. For the gravitational settling, this question was addressed in Ref. [29]. It turned out that the value of the Stokes number alone, St, directly related to the particle size, is not sufficient to argue if the sedimentation is faster or slower with respect to what happens in still fluid. With minor variations of the carrier flow, for a given St, it has been shown that either an increase or a reduction of the falling velocity are possible thus affecting in a different way the particle residence time in the fluid.

Our aim here is to shed some light on how dispersion of inertial particles does depend on relevant properties of the turbulent carrier flow. Our focus will be on the late-time evolution of the particle dynamics, a regime fully described in terms of eddy-diffusivities [57, 58, 26]. Our main question can be thus rephrased in terms of the behavior of the eddy diffusivity by varying some relevant features of the carrier flow (e.g. the form of its auto-correlation

function), for a given inertia of the particle.
This analysis for generic carrier flows is a task of formidable difficulty and forces to the exploitation of numerical approaces which, however, make it difficult to isolate simple machanisms on large-scale transport induced by inertia. To overcome the problem, we decided to focus on simple flow field where the problem can be entirely grasped via analytic (or perturbative) techniques. As we will see, quasi-parallel flows are natural candidates to allow one the analytical treatment of large-scale transport.

3.2 Eddy diffusivity for parallel flows

To start our analysis let us considered the well-known model [63, 31] for transport of heavy particles in a given carrier flow $\boldsymbol{u}(\mathcal{X}(t),t)$:

$$\begin{aligned} \mathrm{d}\boldsymbol{\mathcal{X}}(t) &= \boldsymbol{v}(t)\,\mathrm{d}t \\ \mathrm{d}\boldsymbol{v}(t) &= -\left(\frac{\boldsymbol{v}(t)-\boldsymbol{u}(\boldsymbol{\mathcal{X}}(t),t)}{\tau}\right)\mathrm{d}t + \frac{\sqrt{2\,D_0}}{\tau}\,\mathrm{d}\boldsymbol{\omega}(t) \end{aligned} \tag{3.1}$$

with $\mathrm{d}\boldsymbol{\omega}$ being a white-noise process coupled by a constant molecular diffusivity D_0 [32], $\boldsymbol{v}(t)$ is the particle velocity, $\mathcal{X}$ is its trajectory and τ denotes the Stokes time.
Focusing on a d-dimensional space (here d=2 or 3), let us assume for the carrier flow a parallel flow with the sole non-zero component $u_1(x_2,\ldots,x_d,t)$. The latter is a stationary and homogenoeus random field such that:

$$\begin{gathered} \langle u_1(x_2,\ldots,x_d,t)\rangle = 0, \\ \langle u_1(x_2,\ldots,x_d,t)u_1(0,\ldots,0,0)\rangle = \mathsf{B}(x_2,\ldots,x_d,|t|), \end{gathered} \tag{3.2}$$

and $\boldsymbol{\omega}(t)$ is the Wiener process, with the following well-known properties:

$$\begin{gathered} \boldsymbol{\omega}_0 = 0 \quad a.s. \\ s_1 \le s_2 \le t_1 \le t_2 \Longrightarrow \langle \Delta\boldsymbol{\omega}(s_2-s_1)\otimes\Delta\boldsymbol{\omega}(t_2-t_1)\rangle = 0 \\ s_1 \le s_2 \Longrightarrow \omega_n(s_2)-\omega_n(s_1) \sim G_n(0,s_2-s_1) \end{gathered} \tag{3.3}$$

Here, $G_n(0,s_2-s_1)$ is the zero-mean Gaussian process of the n-th component with variance s_2-s_1, and $\Delta\boldsymbol{\omega}(s_2-s_1)$ is the time increment $\boldsymbol{\omega}(s_2)-\boldsymbol{\omega}(s_1)$. The expressions $\boldsymbol{v}(t)$ and $\boldsymbol{\mathcal{X}}(t)$ easily follow from Eqs. (3.1). It is sufficient to define a new field $\boldsymbol{v}'(t)=e^{t/\tau}\boldsymbol{v}(t)$ and proceed by direct integration. The final result is:

$$v_n(t) = e^{-\frac{t-t_o}{\tau}}\,v_n(t_0) + \frac{\sqrt{2\,D_0}}{\tau}\int_{t_o}^{t}\mathrm{d}\omega_n(s)\,e^{-\frac{t-s}{\tau}} \tag{3.4}$$

$$\begin{aligned}\mathcal{X}_n(t) &= \mathcal{X}_n(t_0) + \tau(1-e^{-\frac{t-t_o}{\tau}})v_n(t_0) \\ &+ \sqrt{2\,D_0}\int_{t_o}^{t} \mathrm{d}\omega_n(s)\,(1-e^{-\frac{t-s}{\tau}})\end{aligned} \tag{3.5}$$

for $n \neq 1$, and

$$\begin{aligned}v_1(t) = e^{-\frac{t-t_o}{\tau}}\,v_1(t_0) + \frac{\sqrt{2\,D_0}}{\tau}\int_{t_o}^{t}\mathrm{d}\omega_1(s)\,e^{-\frac{t-s}{\tau}} \\ +\frac{1}{\tau}\int_{t_o}^{t}\mathrm{d}s\,u_1(\mathcal{X}_2(s),\ldots,\mathcal{X}_d(s),s)\,e^{-\frac{t-s}{\tau}}\end{aligned} \tag{3.6}$$

$$\begin{aligned}\mathcal{X}_1(t) &= \mathcal{X}_1(t_0) + \tau v_1(t_0)(1-e^{-\frac{t-t_o}{\tau}}) \\ &+ \sqrt{2\,D_0}\int_{t_o}^{t}\mathrm{d}\omega_1(s)\,(1-e^{-\frac{t-s}{\tau}}) \\ &+ \int_{t_o}^{t}\mathrm{d}s\,u_1(\mathcal{X}_2(s),\ldots,\mathcal{X}_d(s),s)\,(1-e^{-\frac{t-s}{\tau}})\end{aligned} \tag{3.7}$$

for n=1. Here the integral with respect to $\mathrm{d}\boldsymbol{\omega}(s)$ are meant in Ito's sense. The eddy diffusivity can be now obtained in terms of $\boldsymbol{v}(t)$ and $\boldsymbol{\mathcal{X}}(t)$:

$$\mathrm{D}^{\mathrm{ef}} = \lim_{t\uparrow\infty}\frac{1}{d}\langle \boldsymbol{v}(t)\cdot\boldsymbol{\mathcal{X}}(t)\rangle \tag{3.8}$$

The explicit calculation gives:

$$\begin{aligned}&\lim_{t\uparrow\infty}\frac{1}{d}\langle v_n(t)\mathcal{X}_n(t)\rangle = \\ &= \lim_{t\uparrow\infty}\frac{1}{d}\frac{2\,D_0}{\tau}\int_{t_o}^{t}\int_{t_o}^{t}\langle \mathrm{d}\omega_n(s)\mathrm{d}\omega_n(s')\rangle\,(1-e^{-\frac{t-s}{\tau}})e^{-\frac{t-s'}{\tau}} = \\ &= \lim_{t\uparrow\infty}\frac{1}{d}\frac{2\,D_0}{\tau}\int_{t_o}^{t} ds\,(1-e^{-\frac{t-s}{\tau}})e^{-\frac{t-s}{\tau}} = \frac{D_0}{d}\end{aligned} \tag{3.9}$$

for $n \neq 1$, and:

$$\begin{aligned}&\lim_{t\uparrow\infty}\frac{1}{d}\langle \mathcal{X}_1(t)v_1(t)\rangle = \frac{D_0}{d} + \lim_{t\uparrow\infty}\frac{1}{d\tau}\int_{t_o}^{t}\mathrm{d}s\int_{t_o}^{t}\mathrm{d}s' \\ &\times\langle u_1(\mathcal{X}_2(s),\ldots,\mathcal{X}_d(s),s)u_1(\mathcal{X}_2(s'),\ldots,\mathcal{X}_d(s'),s')\rangle \\ &\times e^{-\frac{t-s}{\tau}}(1-e^{-\frac{t-s'}{\tau}})\end{aligned} \tag{3.10}$$

for $n = 1$. Note that, to obtain Eqs. (3.9-3.10) we have neglected the decaying terms proportional to $e^{-(t-t_0)/\tau}$. This has been possible because of

the limit $t \to \infty$ contained in the definition of $D^{\rm ef}$. We also have exploited the independence between $\boldsymbol{\omega}(t)$ and $\boldsymbol{u}(\boldsymbol{\mathcal{X}}(t),t)$.

The following quantity:

$$\begin{aligned}
&\langle u_1(\mathcal{X}_2(s),\ldots,\mathcal{X}_d(s),s)u_1(\mathcal{X}_2(s'),\ldots,\mathcal{X}_d(s'),s')\rangle \\
&= \int \frac{\mathrm{d}^{d-1}\boldsymbol{k}}{(2\,\pi)^{d-1}}\check{\mathsf{B}}(k_2,\ldots,k_d,|s-s'|) \\
&\times \left\langle e^{\imath[k_2(\mathcal{X}_2(s)-\mathcal{X}_2(s'))+\cdots+k_d(\mathcal{X}_d(s)-\mathcal{X}_d(s'))]}\right\rangle ,
\end{aligned} \tag{3.11}$$

where $\boldsymbol{\mathcal{X}}(t)$ is given by Eq. (3.5), must be plugged into Eq. (3.10) to obtain:

$$\begin{aligned}
&\lim_{t\uparrow\infty}\frac{1}{d}\langle\mathcal{X}_1(t)v_1(t)\rangle = \frac{D_0}{d} + \lim_{t\uparrow\infty}\frac{1}{d\tau}\int_{t_o}^{t}\mathrm{d}s\int_{t_o}^{t}\mathrm{d}s'\int\frac{\mathrm{d}^{d-1}\boldsymbol{k}}{(2\,\pi)^{d-1}} \\
&\times \left\langle e^{\imath[k_2(\mathcal{X}_2(s)-\mathcal{X}_2(s'))+\cdots+k_d(\mathcal{X}_d(s)-\mathcal{X}_d(s'))]}\right\rangle e^{-\frac{t-s}{\tau}}(1-e^{-\frac{t-s'}{\tau}}) \\
&\times \check{\mathsf{B}}(k_2,\ldots,k_d,|s-s'|)
\end{aligned} \tag{3.12}$$

The mean value in the previous formula can be computed via path integral over the infinitesimal increments of the Wiener process ($n \geq 2$). We start by inserting Eq. (3.5) in the exponential argument:

$$\begin{aligned}
&\left\langle e^{\imath k_n(\mathcal{X}_n(s)-\mathcal{X}_n(s'))}\right\rangle = e^{\imath k_n v_n(t_0)(e^{-\frac{s'-t_o}{\tau}}-e^{-\frac{s-t_o}{\tau}})} \\
&\times\left\langle e^{\imath\sqrt{2\,D_0}\int_{t_o}^{\infty}\mathrm{d}\omega_n(r)\,[H(s-r)(1-e^{-\frac{s-r}{\tau}})-H(s'-r)(1-e^{-\frac{s'-r}{\tau}})]}\right\rangle
\end{aligned} \tag{3.13}$$

To evaluate the mean value, we have to integrate over the Wiener measure along the paths. By discretizing the pahts in the Ito sense, and partitioning time so that $r_0 = t_0$:

$$\begin{aligned}
&\left\langle e^{\imath k_n(\mathcal{X}_n(s)-\mathcal{X}_n(s'))}\right\rangle = e^{\imath k_n v_n(t_0)(e^{-\frac{s'-t_o}{\tau}}-e^{-\frac{s-t_o}{\tau}})} \\
&\times \lim_{\Delta\omega_n(r_m)\to 0}\int\prod_{m=0}^{\infty}\mathrm{d}\Delta\omega_n(r_m)\left[\frac{e^{-\frac{(\Delta\omega_n(r_m))^2}{2\Delta r_m}}}{\sqrt{2\pi\Delta r_m}}\right. \\
&\left.\times e^{\imath k_n\sqrt{2\,D_0}\Delta\omega_n(r_m)\,[H(s-r_m)(1-e^{-\frac{s-r_m}{\tau}})-H(s'-r_m)(1-e^{-\frac{s'-r_m}{\tau}})]}\right] \\
&= e^{\imath k_n v_n(t_0)(e^{-\frac{s'-t_o}{\tau}}-e^{-\frac{s-t_o}{\tau}})} \\
&\times e^{-|k_n|^2 D_0\int_{t_0}^{\infty}\mathrm{d}r\,[H(s-r)(1-e^{-\frac{s-r}{\tau}})-H(s'-r)(1-e^{-\frac{s'-r}{\tau}})]^2}
\end{aligned} \tag{3.14}$$

where $\Delta\omega_n(r_m) \equiv \omega_n(r_{m+1}) - \omega_m(r_m)$. Upon taking into accout that:

$$
\begin{aligned}
&\int_{t_0}^{\infty} \mathrm{d}r\,[H(s-r)(1-e^{-\frac{s-r}{\tau}}) - H(s'-r)(1-e^{-\frac{s'-r}{\tau}})]^2 = \\
&= \int_{t_0}^{s} \mathrm{d}r(1-e^{-\frac{s-r}{\tau}})^2 + \int_{t_0}^{s'} \mathrm{d}r(1-e^{-\frac{s'-r}{\tau}})^2 \\
&-2\int_{t_0}^{\min(s,s')} \mathrm{d}r(1-e^{-\frac{s-r}{\tau}})(1-e^{-\frac{s'-r}{\tau}}) = \\
&= \left[s - t_0 - 2\tau(1-e^{-\frac{s-t_0}{\tau}}) + \frac{\tau}{2}(1-e^{-\frac{2s-2t_0}{\tau}})\right] \\
&+ \left[s' - t_0 - 2\tau(1-e^{-\frac{s'-t_0}{\tau}}) + \frac{\tau}{2}(1-e^{-\frac{2s'-2t_0}{\tau}})\right] \\
&- \left[2\left(\min(s,s') - t_0\right) - 2\tau\left(1 + e^{-\frac{|s-s'|}{\tau}}\right.\right. \\
&\left.\left. -e^{-\frac{s-t_0}{\tau}} - e^{-\frac{s'-t_0}{\tau}}\right) + \tau\left(e^{-\frac{|s-s'|}{\tau}} - e^{-\frac{s-t_0}{\tau}-\frac{s'-t_0}{\tau}}\right)\right] = \\
&= \tau\Big[\frac{|s-s'|}{\tau} - 1 - \frac{e^{-\frac{2s-2t_0}{\tau}} + e^{-\frac{2s'-2t_0}{\tau}}}{2} \\
&+e^{-\frac{|s-s'|}{\tau}} + e^{-\frac{s-t_0}{\tau}-\frac{s'-t_0}{\tau}}\Big]
\end{aligned}
\tag{3.15}
$$

from Eq. (3.12) we easily arrive at:

$$
\begin{aligned}
&\mathrm{D}^{\mathrm{ef}} = D_0 + \lim_{t_3\uparrow\infty} \frac{1}{\tau\, d} \int \frac{\mathrm{d}^{d-1}\boldsymbol{k}}{(2\,\pi)^{d-1}} \int_{[t_0,t_3]^2} \mathrm{d}t_1\mathrm{d}t_2 \\
&\times e^{\imath\,\boldsymbol{k}\cdot\boldsymbol{v}(t_0)\tau\,(e^{-\frac{t_{20}}{\tau}} - e^{-\frac{t_{10}}{\tau}})} \\
&\times e^{-D_0\|\boldsymbol{k}\|^2\left[|t_{12}| + \tau\left(1 - e^{-\frac{|t_{12}|}{\tau}} + e^{-\frac{t_{10}+t_{20}}{\tau}} - \frac{e^{-\frac{2t_{10}}{\tau}} + e^{-\frac{2t_{20}}{\tau}}}{2}\right)\right]} \\
&\times e^{-\frac{t_{31}}{\tau}}\ \check{\mathsf{B}}(k_2,\ldots,k_d,|t_{12}|)\,(1-e^{-\frac{t_{32}}{\tau}})
\end{aligned}
\tag{3.16}
$$

where we have introduced the new symbol $t_{ab} = t_a - t_b$. This is the same result as the first perturbation order for Gaussian flows which we present in Appendix 3.6.

Proposition 3.2.1. Eddy diffusivity in Eq. (3.16) does actually not depend on t_0.

Proof. To evaluate the needed asymptotic limit in Eq. (3.16), we first perform the substition $t_1 - t_0 \to t_1$, $t_2 - t_0 \to t_2$, and $t_3 - t_0 = T$, which means $t_3 \to \infty \Longrightarrow T \to \infty$, since t_0 is finite (or, if t_0 is equivalent to $-\infty$, then T

will tend to infinity as well):

$$\begin{aligned}
\mathrm{D}^{\mathrm{ef}} &= D_0 + \lim_{T\uparrow\infty} \frac{1}{d} \int \frac{\mathrm{d}^{d-1}\boldsymbol{k}}{(2\,\pi)^{d-1}} \int_{[0,T]^2} \mathrm{d}t_1 \mathrm{d}t_2\, e^{\imath\,\boldsymbol{k}\cdot\boldsymbol{v}(t_0)\tau\,(e^{-\frac{t_2}{\tau}}-e^{-\frac{t_1}{\tau}})} \\
&\times e^{-D_0\|\boldsymbol{k}\|^2\left[|t_{12}|+\tau\left(1-e^{-\frac{|t_{12}|}{\tau}}+e^{-\frac{t_1+t_2}{\tau}}-\frac{e^{-\frac{2t_1}{\tau}}+e^{-\frac{2t_2}{\tau}}}{2}\right)\right]} \\
&\times \frac{e^{-\frac{T-t_1}{\tau}}}{\tau}\ \check{\mathsf{B}}(k_2,\ldots,k_d,|t_{12}|)\,(1-e^{-\frac{T-t_2}{\tau}})
\end{aligned}$$

The latter, in which the dependence on t_0 is disappeared owing to the limit, is equivalent to Eq. (3.16). □

Having stated this independence on the initial condition, which physically means that the diffusion process losts its memory, we can freely choose $t_0 = -\infty$. After a further substition $T-t_1 \to t_1,\ T-t_2 \to t_2$, the eddy-diffusivity takes the following, simpler form:

$$\begin{aligned}
\mathrm{D}^{\mathrm{ef}} &= D_0 + \frac{1}{\tau\,d} \int \frac{\mathrm{d}^{d-1}\boldsymbol{k}}{(2\,\pi)^{d-1}} \int_0^\infty \mathrm{d}t_1 \int_0^\infty \mathrm{d}t_2 \\
&\times \quad e^{-D_0\|\boldsymbol{k}\|^2\left[|t_{12}|-\tau\left(1-e^{-\frac{|t_{12}|}{\tau}}\right)\right]} \\
&\times \quad e^{-\frac{t_1}{\tau}}\ \check{\mathsf{B}}(k_2,\ldots,k_d,|t_{12}|)\,(1-e^{-\frac{t_2}{\tau}}) \quad . \qquad (3.17)
\end{aligned}$$

Proposition 3.2.2. Let it $f(t)$ be a bounded and integrable function vanishing at $t \to \infty$. Thus:

$$\lim_{T\uparrow\infty} \frac{1}{\tau} \int_0^T \mathrm{d}t_1 \int_0^T \mathrm{d}t_2\, e^{-\frac{t_1}{\tau}}\ f(|t_{12}|)\,(1-e^{-\frac{t_2}{\tau}}) = \int_0^\infty \mathrm{d}t f(t)$$

Proof. The starting point is:

$$\lim_{T\uparrow\infty} \frac{1}{\tau} \int_0^T \mathrm{d}t_1 \int_0^T \mathrm{d}t_2\, e^{-\frac{t_1}{\tau}}\ f(|t_{12}|)\,(1-e^{-\frac{t_2}{\tau}}) \quad . \qquad (3.18)$$

Let us perform the substition $t_1 - t_2 \to \overline{t}$, $t_1 \to t_1$. Thus

$$= \lim_{T\uparrow\infty} \frac{1}{\tau} \int_0^T \mathrm{d}t_1 \int_{t_1-T}^{t_1} \mathrm{d}\overline{t} f(|\overline{t}|)\,(e^{-\frac{t_1}{\tau}} - e^{-\frac{2t_1-\overline{t}}{\tau}}) \quad . \qquad (3.19)$$

Looking at Fig. 3.1, we switch the order of integration, performing it with

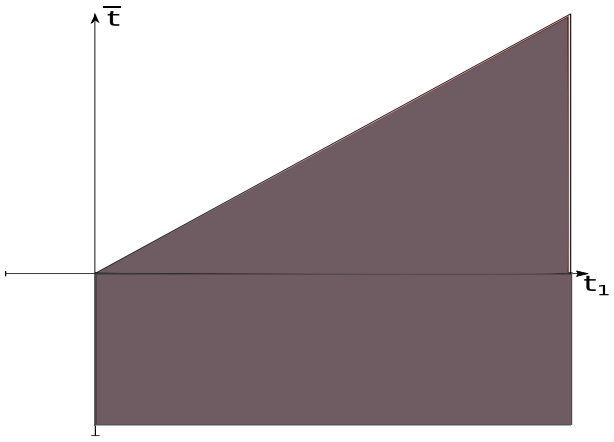

Figure 3.1: Integral domain in the new variables $\overline{t}$ and t_1.

respect to t_1 first:

$$\begin{aligned}
&= \frac{1}{\tau}\int_{-\infty}^{0} \mathrm{d}\overline{t} \int_{0}^{+\infty} \mathrm{d}t_1 f(|\overline{t}|)\,(e^{-\frac{t_1}{\tau}} - e^{-\frac{2t_1-\overline{t}}{\tau}}) \\
&+ \lim_{T\uparrow\infty} \frac{1}{\tau}\int_{0}^{T} \mathrm{d}\overline{t} \int_{\overline{t}}^{T} \mathrm{d}t_1 f(|\overline{t}|)\,(e^{-\frac{t_1}{\tau}} - e^{-\frac{2t_1-\overline{t}}{\tau}}) \\
&= \int_{-\infty}^{0} \mathrm{d}\overline{t} f(|\overline{t}|)\,\left(1 - \frac{e^{\frac{\overline{t}}{\tau}}}{2}\right) + \lim_{T\uparrow\infty}\int_{0}^{T} \mathrm{d}\overline{t} f(|\overline{t}|) \\
&\times \left(-e^{-\frac{T}{\tau}} + e^{-\frac{\overline{t}}{\tau}} + \frac{e^{-\frac{2T-\overline{t}}{\tau}} - e^{-\frac{\overline{t}}{\tau}}}{2}\right) \\
&= \lim_{T\uparrow\infty}\int_{0}^{T} \mathrm{d}\overline{t} f(|\overline{t}|)\left(1 - e^{-\frac{T}{\tau}} + \frac{e^{-\frac{2T-\overline{t}}{\tau}}}{2}\right)
\end{aligned} \tag{3.20}$$

The second addend $e^{-\frac{T}{\tau}}\int_0^T \mathrm{d}\overline{t} f(|\overline{t}|)$ tends to 0 as $T \uparrow \infty$ since the integral is bounded. As to the third one:

$$\begin{aligned}
0 &\leq \left|\int_0^T \mathrm{d}\overline{t} f(|\overline{t}|)\frac{e^{-\frac{2T-\overline{t}}{\tau}}}{2}\right| \leq \int_0^T \mathrm{d}\overline{t}\left|f(|\overline{t}|)\frac{e^{-\frac{2T-\overline{t}}{\tau}}}{2}\right| \\
&\leq \sup_t |f(t)|\,\tau\,\frac{e^{-\frac{T}{\tau}} - e^{-\frac{2T}{\tau}}}{2} \to_{T\uparrow\infty} 0
\end{aligned} \tag{3.21}$$

As a result, we have shown that Eq. (3.18) equals the first and only non-zero addend.

□

We can apply this result to the time-correlation function in spatial Fourier space $\check{\mathsf{B}}(k_2,\dots,k_d,|t|)$, which is integrable and bounded. When $D_0 \neq 0$, the role of $f(t)$ would be played by $\exp[-D_0\|\boldsymbol{k}\|^2(t-\tau\,(1-e^{-\frac{t}{\tau}}))]\,\check{\mathsf{B}}(k_2,\dots,k_d,|t|)$, and we see that D_0 could even regularize a bad behaviour of the pure flow time correlation function on long times. If we now apply Prop. (3.2.2) to Eq. (3.17), we arrive at the final expression:

$$\begin{aligned}\mathrm{D}^{\mathrm{ef}} &= D_0 + \frac{1}{d}\int \frac{\mathrm{d}^{d-1}\boldsymbol{k}}{(2\,\pi)^{d-1}}\int_0^\infty \mathrm{d}t \\ \times &\quad e^{-D_0\|\boldsymbol{k}\|^2\left[t-\tau\left(1-e^{-\frac{t}{\tau}}\right)\right]}\check{\mathsf{B}}(k_2,\dots,k_d,t) \quad . \end{aligned} \tag{3.22}$$

It is interesting to note that such an expression coincides with the one for tracer particles with coloured noise [70]. Notice that the presence of the molecular diffusivity can even regularize bad ultra-violet behaviors of the correlation function. This means it could give a finite eddy diffusivity also when the diffusion for particles in the pure flow without Brownian noise is anomalous. Certainly, no anomalous diffusion can origin from the presence of τ. This gives a ful theoretical explanation to the numerical observations accomplished in Chapter 1.

3.3 Generalization to general density ratio β

Let us now move to the general inertial case for $0 < \beta \leq 3$. In this more complicate situation, we can leverage the generalized Taylor formula achieved in [65] and the previous relations for heavy particles. The equation of motion are now:

$$\begin{aligned}\mathrm{d}\boldsymbol{\mathcal{X}}(t) &= (\boldsymbol{\mathcal{V}}(t) + \beta\boldsymbol{u}(\boldsymbol{\mathcal{X}}(t),t)\,\mathrm{d}t \\ \mathrm{d}\boldsymbol{\mathcal{V}}(t) &= -\left(\frac{\boldsymbol{\mathcal{V}}(t)-(1-\beta)\boldsymbol{u}(\boldsymbol{\mathcal{X}}(t),t)}{\tau}\right)\mathrm{d}t + \frac{\sqrt{2\,D_0}}{\tau}\,\mathrm{d}\boldsymbol{\omega}(t)\end{aligned} \tag{3.23}$$

where now $\boldsymbol{\mathcal{V}}(t)$ has no longer the immediate physical meaning of particle velocity, but it is rather the more general and so-called *covelocity*.

The flow being parallel, nothing changes in comparison to the component along $n \neq 1$, and Eqs. (3.5), (3.9), (3.11), (3.10), (3.13), and (3.15) still hold true. In the x direction, instead, the position process is:

$$\begin{aligned}&\mathcal{X}_1(t) = \mathcal{X}_1(t_0) + \tau\mathcal{V}_1(t_0)(1-e^{-\frac{t-t_o}{\tau}}) \\ &+(1-\beta)\int_{t_o}^t \mathrm{d}s\, u_1(\mathcal{X}_2(s),\dots,\mathcal{X}_d(s),s)\,(1-e^{-\frac{t-s}{\tau}}) \\ &+\beta\int_{t_o}^t \mathrm{d}s\, u_1(\mathcal{X}_2(s),\dots,\mathcal{X}_d(s),s) \\ &+\sqrt{2\,D_0}\int_{t_o}^t \mathrm{d}\omega_1(s)\,(1-e^{-\frac{t-s}{\tau}})\end{aligned} \tag{3.24}$$

and the *velocity* is:

$$
\begin{aligned}
&\dot{\mathcal{X}}_1(t) = \mathcal{V}_1(t_0) e^{-\frac{t-t_o}{\tau}} \\
&+\frac{1-\beta}{\tau}\int_{t_o}^{t} \mathrm{d}s\, u_1(\mathcal{X}_2(s),\ldots,\mathcal{X}_d(s),s)\, e^{-\frac{t-s}{\tau}} \\
&+\beta\, u_1(\mathcal{X}_{2t},\ldots,\mathcal{X}_{dt},t) + \frac{\sqrt{2\,D_0}}{\tau}\int_{t_o}^{t} \mathrm{d}\omega_1(s)\, e^{-\frac{t-s}{\tau}}
\end{aligned}
\tag{3.25}
$$

This means that the entire eddy diffusivity now reads:

$$
\begin{aligned}
\mathrm{D}^{\mathrm{ef}} \quad &= \lim_{t\uparrow\infty}\frac{1}{d}\langle \dot{\boldsymbol{\mathcal{X}}}(t)\cdot\boldsymbol{\mathcal{X}}(t)\rangle = D_0 \\
+ \quad & \frac{(1-\beta)^2}{\tau\, d}\int \frac{\mathrm{d}^{d-1}\boldsymbol{k}}{(2\,\pi)^{d-1}}\int_0^\infty \mathrm{d}t_1\int_0^\infty \mathrm{d}t_2 \\
\times \quad & e^{-D_0\|\boldsymbol{k}\|^2\left[|t_{12}|+\tau\left(1-e^{-\frac{|t_{12}|}{\tau}}\right)\right]} \\
\times \quad & e^{-\frac{t_1}{\tau}}\ \check{\mathsf{B}}(k_2,\ldots,k_d,|t_{12}|)\,(1-e^{-\frac{t_2}{\tau}}) \\
+ \quad & \frac{\beta(1-\beta)}{\tau\, d}\int \frac{\mathrm{d}^{d-1}\boldsymbol{k}}{(2\,\pi)^{d-1}}\int_0^\infty \mathrm{d}t_1\int_0^\infty \mathrm{d}t_2 \\
\times \quad & e^{-D_0\|\boldsymbol{k}\|^2\left[|t_{12}|+\tau\left(1-e^{-\frac{|t_{12}|}{\tau}}\right)\right]} \\
\times \quad & e^{-\frac{t_1}{\tau}}\ \check{\mathsf{B}}(k_2,\ldots,k_d,|t_{12}|) \\
+ \quad & \frac{\beta(1-\beta)}{d}\int \frac{\mathrm{d}^{d-1}\boldsymbol{k}}{(2\,\pi)^{d-1}}\int_0^\infty \mathrm{d}t_1 \\
\times \quad & e^{-D_0\|\boldsymbol{k}\|^2\left[t_1+\tau\left(1-e^{-\frac{t_1}{\tau}}\right)\right]} \\
\times \quad & (1-e^{-\frac{t_1}{\tau}})\ \check{\mathsf{B}}(k_2,\ldots,k_d,t_1) \\
+ \quad & \frac{\beta^2}{d}\int \frac{\mathrm{d}^{d-1}\boldsymbol{k}}{(2\,\pi)^{d-1}}\int_0^\infty \mathrm{d}t_1 \\
\times \quad & e^{-D_0\|\boldsymbol{k}\|^2\left[t_1+\tau\left(1-e^{-\frac{t_1}{\tau}}\right)\right]}\check{\mathsf{B}}(k_2,\ldots,k_d,t_1)
\end{aligned}
\tag{3.26}
$$

where we have again integrated over the Wiener measure for the molecular diffusion and chosen the initial condition at $-\infty$ by virtue of the independence of it.

By applying Prop. (3.2.2), we can recast Eq. (3.26) after some algebra:

$$
\begin{aligned}
\mathrm{D}^{\mathrm{ef}} \quad &= D_0 + \frac{1-\beta+\beta^2}{d} \int \frac{\mathrm{d}^{d-1}\boldsymbol{k}}{(2\,\pi)^{d-1}} \int_0^\infty \mathrm{d}t_1 \\
\times \quad & e^{-D_0\|\boldsymbol{k}\|^2\left[t_1+\tau\left(1-e^{-\frac{t_1}{\tau}}\right)\right]} \check{\mathsf{B}}(k_2,\ldots,k_d,t_1) \\
+ \quad & \frac{\beta(1-\beta)}{\tau\, d} \int \frac{\mathrm{d}^{d-1}\boldsymbol{k}}{(2\,\pi)^{d-1}} \int_0^\infty \mathrm{d}t_1 \int_0^\infty \mathrm{d}t_2 \\
\times \quad & e^{-D_0\|\boldsymbol{k}\|^2\left[|t_{12}|+\tau\left(1-e^{-\frac{|t_{12}|}{\tau}}\right)\right]} e^{-\frac{t_1}{\tau}}\ \check{\mathsf{B}}(k_2,\ldots,k_d,|t_{12}|) \\
- \quad & \frac{\beta(1-\beta)}{d} \int \frac{\mathrm{d}^{d-1}\boldsymbol{k}}{(2\,\pi)^{d-1}} \int_0^\infty \mathrm{d}t_1 \\
\times \quad & e^{-D_0\|\boldsymbol{k}\|^2\left[t_1+\tau\left(1-e^{-\frac{t_1}{\tau}}\right)\right]} e^{-\frac{t_1}{\tau}}\ \check{\mathsf{B}}(k_2,\ldots,k_d,t_1)
\end{aligned}
\tag{3.27}
$$

Let us consider the second addend. We can again perform the substition $t_1 - t_2 \to \overline{t}$, $t_1 \to t_1$, similarly to what was done for Eq. (3.18). Thus:

$$
\begin{aligned}
&\lim_{T\uparrow\infty} \frac{1}{\tau} \int_0^T \mathrm{d}t_1 \int_0^T \mathrm{d}t_2\, e^{-\frac{t_1}{\tau}} \\
&\times e^{-D_0\|\boldsymbol{k}\|^2\left[|t_{12}|+\tau\left(1-e^{-\frac{|t_{12}|}{\tau}}\right)\right]}\ \check{\mathsf{B}}(k_2,\ldots,k_d,|t_{12}|) \\
&= \lim_{T\uparrow\infty} \frac{1}{\tau} \int_0^T \mathrm{d}t_1 \int_{t_1-T}^{t_1} \mathrm{d}\overline{t}\, e^{-\frac{t_1}{\tau}} \\
&\times e^{-D_0\|\boldsymbol{k}\|^2\left[|\overline{t}|+\tau\left(1-e^{-\frac{|\overline{t}|}{\tau}}\right)\right]}\ \check{\mathsf{B}}(k_2,\ldots,k_d,|\overline{t}|)
\end{aligned}
\tag{3.28}
$$

Looking at Fig. 3.1, we switch the order of integration, performing it with

respect to t_1 first:

$$
\begin{aligned}
&= \frac{1}{\tau}\int_{-\infty}^{0} \mathrm{d}\overline{t}\int_{0}^{+\infty} \mathrm{d}t_1\, e^{-\frac{t_1}{\tau}} \\
&\times \quad e^{-D_0\|\boldsymbol{k}\|^2\left[|\overline{t}|+\tau\left(1-e^{-\frac{|\overline{t}|}{\tau}}\right)\right]}\,\check{\mathsf{B}}(k_2,\ldots,k_d,|\overline{t}|) \\
&+ \lim_{T\uparrow\infty}\frac{1}{\tau}\int_{0}^{T} \mathrm{d}\overline{t}\int_{\overline{t}}^{T} \mathrm{d}t_1\, e^{-\frac{t_1}{\tau}} \\
&\times \quad e^{-D_0\|\boldsymbol{k}\|^2\left[|\overline{t}|+\tau\left(1-e^{-\frac{|\overline{t}|}{\tau}}\right)\right]}\,\check{\mathsf{B}}(k_2,\ldots,k_d,|\overline{t}|) \\
&= \int_{0}^{\infty} \mathrm{d}\overline{t}\, e^{-D_0\|\boldsymbol{k}\|^2\left[\overline{t}+\tau\left(1-e^{-\frac{\overline{t}}{\tau}}\right)\right]}\,\check{\mathsf{B}}(k_2,\ldots,k_d,\overline{t}) \\
&+ \int_{0}^{\infty} \mathrm{d}\overline{t}\, e^{-\frac{\overline{t}}{\tau}} e^{-D_0\|\boldsymbol{k}\|^2\left[\overline{t}+\tau\left(1-e^{-\frac{\overline{t}}{\tau}}\right)\right]}\,\check{\mathsf{B}}(k_2,\ldots,k_d,\overline{t}) \\
&- \lim_{T\uparrow\infty} e^{-\frac{T}{\tau}}\int_{0}^{T} \mathrm{d}\overline{t}\, e^{-D_0\|\boldsymbol{k}\|^2\left[\overline{t}+\tau\left(1-e^{-\frac{\overline{t}}{\tau}}\right)\right]}\,\check{\mathsf{B}}(k_2,\ldots,k_d,\overline{t})
\end{aligned}
\tag{3.29}
$$

If the integral in the last line is bounded, then that term vanishes as $T\to\infty$:

$$
\begin{aligned}
&\lim_{T\uparrow\infty}\frac{1}{\tau}\int_{0}^{T} \mathrm{d}t_1\int_{0}^{T} \mathrm{d}t_2\, e^{-\frac{t_1}{\tau}} \\
&\quad\times e^{-D_0\|\boldsymbol{k}\|^2\left[|t_{12}|+\tau\left(1-e^{-\frac{|t_{12}|}{\tau}}\right)\right]}\,\check{\mathsf{B}}(k_2,\ldots,k_d,|t_{12}|) \\
&= \int_{0}^{\infty} \mathrm{d}\overline{t}\, e^{-D_0\|\boldsymbol{k}\|^2\left[\overline{t}+\tau\left(1-e^{-\frac{\overline{t}}{\tau}}\right)\right]}\,\check{\mathsf{B}}(k_2,\ldots,k_d,\overline{t}) \\
&+ \int_{0}^{\infty} \mathrm{d}\overline{t}\, e^{-\frac{\overline{t}}{\tau}} e^{-D_0\|\boldsymbol{k}\|^2\left[\overline{t}+\tau\left(1-e^{-\frac{\overline{t}}{\tau}}\right)\right]}\,\check{\mathsf{B}}(k_2,\ldots,k_d,\overline{t})
\end{aligned}
\tag{3.30}
$$

By plugging Eq. (3.30) into Eq. (3.27), many terms cancel out and we arrive at:

$$
\begin{aligned}
\mathrm{D}^{\mathrm{ef}} &= D_0 + \frac{1}{d}\int\frac{\mathrm{d}^{d-1}\boldsymbol{k}}{(2\,\pi)^{d-1}}\int_{0}^{\infty}\mathrm{d}t_1 \\
&\times \quad e^{-D_0\|\boldsymbol{k}\|^2\left[t_1+\tau\left(1-e^{-\frac{t_1}{\tau}}\right)\right]}\check{\mathsf{B}}(k_2,\ldots,k_d,t_1)
\end{aligned}
\tag{3.31}
$$

which is the same as the heavy particle case $\beta = 0$.

3.4 Analysis and results

To play more easily with Eq. (3.22), let us first consider the limit od small D_0. This would make the resulting integrals easier to manage and carry out. A first order expression carried out on Eq. (3.22) gives:

$$\begin{aligned} \mathrm{D}^{\mathrm{ef}} &= D_0 + \frac{1}{d}\int \frac{\mathrm{d}^{d-1}\boldsymbol{k}}{(2\,\pi)^{d-1}} \int_0^\infty \mathrm{d}t\, \mathrm{tr}\,\check{\mathsf{B}}(\boldsymbol{k},t) \\ &\times \quad \left(1 - D_0\|\boldsymbol{k}\|^2 \left(t - \tau\, \left(1 - e^{-\frac{t}{\tau}}\right)\right)\right) + \dots \end{aligned} \tag{3.32}$$

or, in physical space:

$$\begin{aligned} &\mathrm{D}^{\mathrm{ef}} = D_0 + \frac{1}{d}\int_0^\infty \mathrm{d}t \langle \boldsymbol{u}(\boldsymbol{x},t)\cdot\boldsymbol{u}(\boldsymbol{x},0)\rangle - \frac{D_0}{d} \\ &\times \int_0^\infty \mathrm{d}t \left[t - \tau\, \left(1 - e^{-\frac{t}{\tau}}\right)\right] \langle [\partial_\alpha u_\beta(\boldsymbol{x},t)][\partial_\alpha u_\beta(\boldsymbol{x},0)]\rangle \\ &+ \dots \end{aligned} \tag{3.33}$$

For $\tau \to 0$, the limit of vanishing intertia easily follows:

$$\begin{aligned} &\mathrm{D}^{\mathrm{ef}} \longrightarrow_{\tau\to 0} D_0 + \frac{1}{d}\int_0^\infty \mathrm{d}t\, \langle \boldsymbol{u}(\boldsymbol{x},0)\cdot\boldsymbol{u}(\boldsymbol{x},t)\rangle \\ &-\frac{D_0}{d}\int_0^\infty \mathrm{d}t\, t\, \langle [\partial_\alpha u_\beta(\boldsymbol{x},0)][\partial_\alpha u_\beta(\boldsymbol{x},t)]\rangle \\ &+ \dots \end{aligned} \tag{3.34}$$

which correspond to the result reported in [64].

Returning to the heavy particle case, in order to further simplify the expression for the eddy diffusivity, let us focus on a 2D carrier flow with a single wave-number $\boldsymbol{k}_0$. The correlation function we consider is [66]:

$$\begin{aligned} \mathrm{tr}\,\check{\mathsf{B}}(\boldsymbol{k},|t|) &= (2\pi)^{d-1} E(\boldsymbol{k}_0) e^{-\frac{|t|}{T_c}} \cos(\Omega t) \\ &\times [\delta(\boldsymbol{k}-\boldsymbol{k}_0) + \delta(\boldsymbol{k}+\boldsymbol{k}_0)] \end{aligned} \tag{3.35}$$

$E(\boldsymbol{k}_0)$ being the turbulent kinetic energy associated to the wave-number. In principle, the decay time T_c would depend on $\boldsymbol{k}$ itself, typically like $1/\|\boldsymbol{k}\|$ or $1/\|\boldsymbol{k}\|^2$ [67, 68, 69]. However, since we are considering a single wave-number flow, we can consider it as a constant. We can now nondimensionalize our system by setting $\boldsymbol{k}_0 = T_c = 1$ and dimensionless, as to have the Stokes

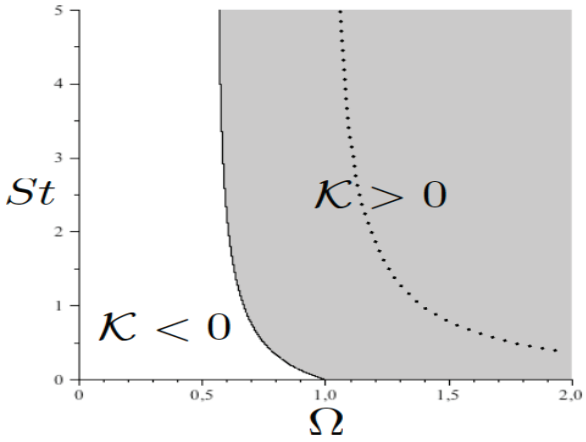

Figure 3.2: The sign of $\mathcal{K}$ in the $St - \Omega$ plane. Gray corresponds to $\mathcal{K} > 0$; white to $\mathcal{K} < 0$. The dotted line separates the region on its left, corresponding to transport enhancement due to inertia, from that on its right relative to transport reduction.

number $St = \tau$. By plugging Eq. (3.35) into Eq. (3.32), one obtains :

$$\mathrm{D}^{\mathrm{ef}} = D_0 + E(\boldsymbol{k}_0)\left[\frac{1}{d}\frac{2}{1+\Omega^2} + \frac{D_0}{d}\mathcal{K}(\mathrm{St},\Omega)\right] \tag{3.36}$$

$$\mathcal{K} = -\left[\frac{4}{(1+\Omega^2)^2} - \frac{2(1+\mathrm{St})}{1+\Omega^2} - \frac{2\mathrm{St}^2(1+\mathrm{St})^2}{(1+\mathrm{St}(2+\mathrm{St}+\mathrm{St}\Omega^2))^2}\right.$$
$$\left. + \frac{\mathrm{St}^2(4+3\mathrm{St})}{1+\mathrm{St}(2+\mathrm{St}+\mathrm{St}\Omega^2)} - \frac{\mathrm{St}^2(2+\mathrm{St})}{4+\mathrm{St}(4+\mathrm{St}+\mathrm{St}\Omega^2)}\right]$$

The above expression is uniform in St. Indeed, it is a continuous function of St$\in [0, +\infty)$, and it tends to 0 as St$\to +\infty$ $\forall\Omega$, then it is limited for any St. This means that the perturbation expansion at first order in D_0 can be used for any value of St. However, note that, since $\max|\mathcal{K}| \leq 1$, we have a constraint on D_0 in order to have a uniform perturbation expansion, which is $D_0 \ll \frac{2}{(1+\Omega^2)}$.

The term $\mathcal{K}$ can be either positive or negative, depending on the importance of negative correlated regions in the correlation function (3.35). This fact can be detected from Fig. 3.2 where the regions inside which $\mathcal{K}$ is positive (gray region) and negative (white region) are shown in the plane $St-\Omega$. It is worth recalling that, for the tracer case, the condition for having $\mathcal{K} > 0$ is simply $\Omega > 1$. The presence of inertia thus causes a change of the sign of $\mathcal{K}$ from negative to positive in a subset of the $St - \Omega$ plane. In this region inertia thus plays to increase transport with respect to the tracer case. The region where transport is enhanced with respect to the tracer case actually extends up to the dotted line. To observe a reduction of transport, the Stokes

time has thus to be sufficiently large. Larger and larger values are required for increasing Ω.

The behavior of $\mathcal{K}$ as a function of St is reported in Fig. 3.3 for different values of Ω. For sufficiently small Ω, $\mathcal{K}$ is negative and inertia increases

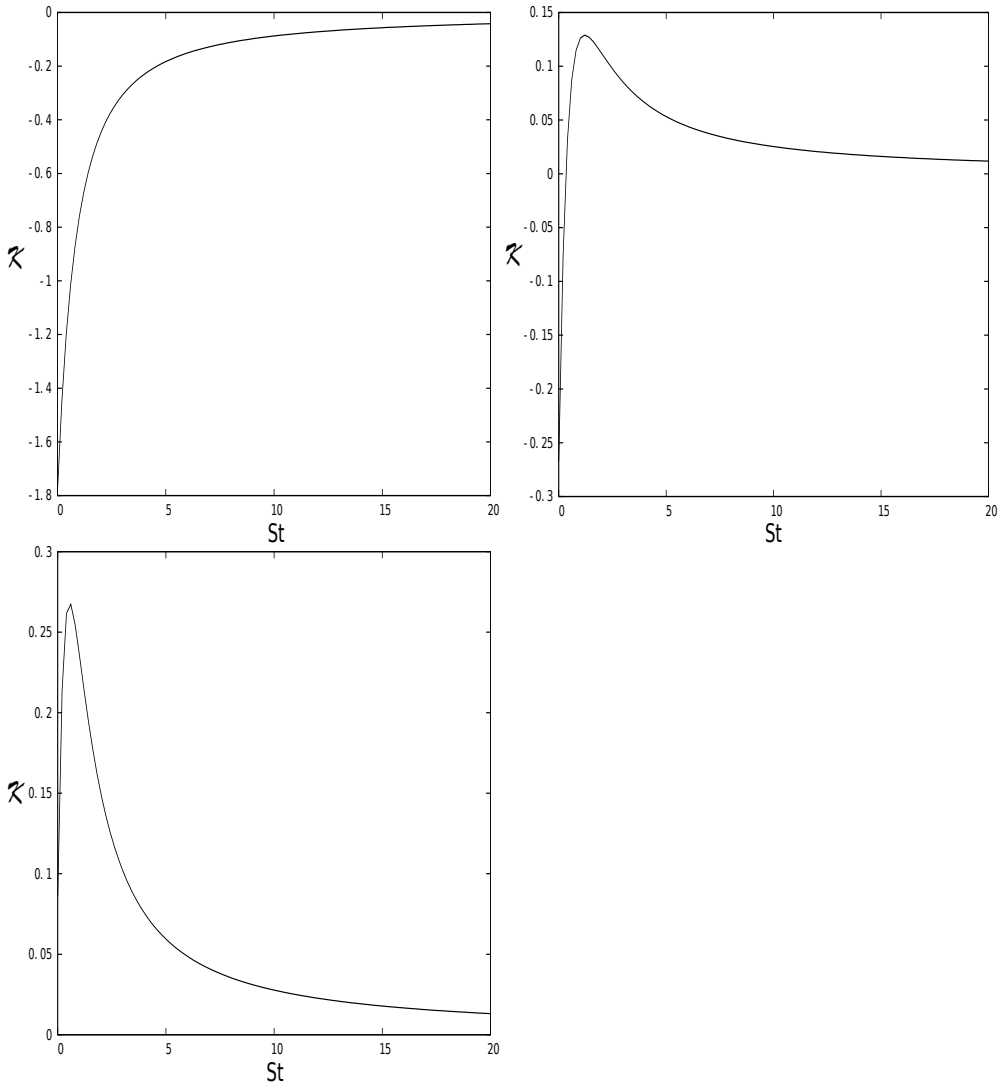

Figure 3.3: $\mathcal{K}$ vs St at $\Omega = 0.2$ (first panel, clockwise sense), $\Omega = 0.8$ (secon panel) and $\Omega = 1.1$ (third panel).

its value thus enhancing transport. For sufficiently large Ω, $\mathcal{K}$ is positive and inertia increases its value up to a certain value of St (corresponding to the intersection with the dotted line of Fig. 3.2) above which transport is reduced by inertia.

The physical explanation of the resulting behavior of $\mathcal{K}$ vs St, for small St, can be traced back to the mechanism of transport enhancement induced by a colored noise discussed in [70]. Indeed, the random contribution to the inertial particle velocity in (3.6) turns out to be a colored noise. The fact that for large Stokes times $\mathcal{K}$ goes to zero is a simple consequence of the fact that in such a limit the contribution of the noise to the transport trivially vanishes as $1/St^2$ as one can see from (3.6). A maximum of transport is thus guaranteed in all cases where $\mathcal{K} > 0$ for $St = 0$.

3.5 Generalization to non-parallel flows: numerical results

Up to now, our results only applies to parallel flows. We now show that our findings actually have a more general character they being valid, at the leading order in a geometric parameter controlling the degree of non parallelism, also for quasi-parallel flows. To show this fact we have to resort to a toy numerical model and perturbation methods later on.

As a toy model, we are going to consider a lagrangian, stochastic, kinematic 2D model of homogeneous turbulence, whose amplitudes decay exponentially as required in the previous section. Namely, we are going to perturbate the parallel flow with unitary wave-vector by adding a new velocity field which mimicks properties of statistically homogenous and quasi-stationary turbulence [34, 35], like below:

$$\begin{aligned} u_1^\epsilon(x,y,t) &= \epsilon A(\boldsymbol{\mathcal{X}}(0),t)\sin(x+\varepsilon\sin(\omega_1 t)+\Theta_1(\boldsymbol{\mathcal{X}}(0))) \\ &\times \cos(y+\varepsilon\sin(\omega_2 t)+\Theta_2(\boldsymbol{\mathcal{X}}(0))) \end{aligned} \tag{3.37}$$

$$\begin{aligned} u_2^\epsilon(x,y,t) &= A(\boldsymbol{\mathcal{X}}(0),t)[\cos(x+\Theta_0(\boldsymbol{\mathcal{X}}(0))) \\ &- \epsilon\cos(x+\varepsilon\sin(\omega_1 t)+\Theta_1(\boldsymbol{\mathcal{X}}(0))) \\ &\times \sin(y+\varepsilon\sin(\omega_2 t)+\Theta_2(\boldsymbol{\mathcal{X}}(0)))] \end{aligned} \tag{3.38}$$

For any diffusing particle, this is a oscillating cellular flow which can develop chaos for sufficiently high ε. Let us analyze briefly in detail this model. Among the random variables involved, $\mathcal{X}(0)$ is meant to stress that we choose independent random processes for each space location (in the following $\mathcal{X}(0)$ will be the initial conditions of Lagrangian particles through which we will investigate the transport problem; each $\mathcal{X}(0)$ will correspond to a given realization of the random process). As to ε, ω_1, and ω_2, these parameter make the convective cell oscillate. If ω_1 and ω_2 are commensurable, the trajectories are periodic. In order to avoid this and facilitate mixing, we choose $\omega_1 = 1,\ \omega_2 = \pi/2$. Convective cells are here squares with side $l_0 = \pi$. To trigger Lagrangian chaos [34, 35], the maximum oscillation amplitude ε is usually $\sim 10^{-1} l_0$. Besides, the pulsations are $\omega_1, \omega_2 \sim 1/t_c$, t_c being the

typical eddy-turnover time $t_c \sim l_0/\langle A^2\rangle$. In order to be in agreement with these conditions, we set $\varepsilon = 0.5$, the pulsations being already coherent with these choices.

The random phases $\Theta_0(\mathcal{X}(0))$ are quenched for each particle. Finally, $A(\boldsymbol{\mathcal{X}}(0), t)$ is the velocity amplitude, a stochastic process fulfilling the sought correlation function. In the pure exponential correlation, it corresponds to an Orstein-Uhlenbeck process with variance equal to 4 and unitary decay time:

$$dA(t) = -A(t)dt + \sqrt{2\langle A^2\rangle}\; d\omega(t) \tag{3.39}$$

where $\langle A^2\rangle$ is the (asymptotically) stationary variance. Setting $\langle A^2\rangle = 4$ guarantees that the unperturbated parallel flow $\boldsymbol{u}^0(\boldsymbol{x}, t)$ has unitary energy [68]. We will choose this value in our numerical simulations. In order to have a further oscillating contribution, with pulsation Ω, we need to complexify the above process and exploit the following SDE:

$$dA(t) = -A(t)(1 - \imath\ \Omega)dt + \sqrt{2\langle(\Re A)^2\rangle}[d\omega_1(t) + \imath\ d\omega_2(t)] \tag{3.40}$$

where $d\omega_1(t), d\omega_2(t)$ are two independent Wiener processes. We are interested in the real part of the solution of this complex SDE:

$$\begin{aligned}
\Re A(t) &= \Re A(t_0)e^{-t}\cos(\Omega t) - \Im A(t_0)e^{-t}\sin(\Omega t) \\
&+ \sqrt{8}\Big[\int_{t_0}^{t} e^{-(t-t_0)}\cos(\Omega(t-t_0))d\omega_1(t) \\
&- \int_{t_0}^{t} e^{-(t-t_0)}\sin(\Omega(t-t_0))d\omega_2(t)\Big]
\end{aligned} \tag{3.41}$$

The above process has clearly zero mean value. By virtue of well known trigonometric Werner formulae, if $A(t_0) = 0$ or, equivalently, waiting a certain thermalization time $>> 1$ for an arbitrary initial condition, we get to the following expression:

$$\langle \Re A(t_1)\Re A(t_2)\rangle = 4e^{-|t_1-t_2|}\cos(\Omega(t_1 - t_2)) \tag{3.42}$$

Therefore, when $\epsilon = 0$, it is sufficient to consider the same model as Eqs. (3.38) where the amplitude are substituted by the process $\Re A(t)$ above, in order to have a stationary correlation function like (3.35) for the parallel flow.

This flow is statistically homogenous due to the random phases [65, 68].

Its two-point correlation function is:

$$\begin{aligned}\langle \boldsymbol{u}(\boldsymbol{x},t)\cdot\boldsymbol{u}(\boldsymbol{x}',t')\rangle = \frac{\langle A(t)A(t')\rangle}{2}\Bigg[&\cos(y-y')\\ +\quad \epsilon^2\quad &\Bigg(\cos\big[x-x'+y'-y'\\ &+\quad \varepsilon\big(\sin(\omega_1 t)+\sin(\omega_2 t)-\sin(\omega_1 t')-\sin(\omega_1 t')\big)\big]\\ +\quad \cos\quad &\big[x-x'-y'+y'\\ &+\quad \varepsilon\big(\sin(\omega_1 t)-\sin(\omega_2 t)-\sin(\omega_1 t')+\sin(\omega_1 t')\big)\big]\Bigg)\Bigg]\end{aligned} \tag{3.43}$$

and we see that the flow tends to be as stationary as $\varepsilon \sim 0$, $\epsilon \sim 0$, or $\omega_1 \sim \omega_2$. Its kinetic energy is $\frac{\langle A(t)^2\rangle}{4}(1+2\epsilon^2)$, then we can consider the oscillating cellular flow a perturbation for some $\epsilon < 0.7$. The flow also turn out to be a superposition of three wavenumbers, which are $\boldsymbol{k}_0 = (0,1)$, $\boldsymbol{k}_{11} = (1,1)$, and $\boldsymbol{k}_{12} = (1,-1)$.

To measure numerically the eddy diffusivity, we certainly need to wait a time >>St, due to the presence of the Stokes transient. Moreover, when $D_0 = 0$, some structures of walength $L >> 2\pi/k_0$ can arise and, velocity being $\sim O(1)$, we nedd to wait a time $t >> L$, to renormalize with respect to the typical times of the structures (for our choices of parameters, $t \sim 100$). Anyway, this problem does not occur when $D_0 > 0$, since molecular diffusivity destroys the trajectory features originating from these structures. To handle this issue, we fit the displacement variance with the function $at+b$, a being $2dD^{\mathrm{ef}}$, for $t > 40$ when $D_0 > 0$ and $t > 100$ when $D_0 = 0$ (see Fig. 3.4).

The numerical results are shown in Fig. 3.5. The interference term $\mathcal{K} = D^{\mathrm{ef}}(D_0 = 0.5) - D_0 - D^{\mathrm{ef}}(D_0 = 0)$ at St=2 turns out to be still destructive or constructive when $\Omega = 0$ or 3 respectively. The conclusions hold true still up to $\epsilon = 1$, therefore quite far from a perturbation regime at $\Omega = 3$. When $\Omega = 0$, at $\epsilon \sim 0.5$ the contribution of frequencies from the perturbating flow becomes relevant and a positive contribution as in the previous case arises, which make the intercerence less destructive and tends to increase the transport with respect to the pure exponentially decaying case ($\epsilon = 0$). However, altogether it remains destructive up to $\epsilon = 1$, which is beyond a perturbation regime.

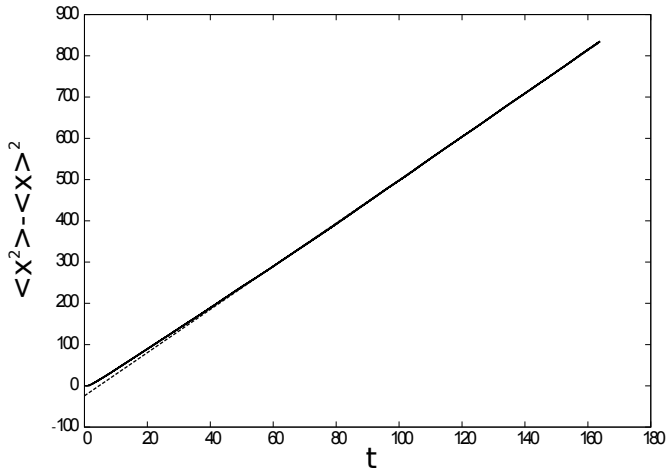

Figure 3.4: Numerical data (continuous line) vs best-fit curve (dashed line) with the function $at + b$, for $t > 100$. Here $D_0 = 0$, $\epsilon = 1$, and $St = 2$. The averages were taken over 90,000 particles starting from a square of side 2π.

3.6 Generalization of Taylor formula for inertial particles

We can exploit the previous analysis to show that the eddy diffusivity for intertial particle can be expressed in a formally identical manner with respect to Taylor's formula for tracers. We recall the simplified Maxey-Riley equations in a given carrier flow $\boldsymbol{u}(\boldsymbol{\mathcal{X}}(t), t)$:

$$\begin{aligned} \mathrm{d}\boldsymbol{\mathcal{X}}(t) &= (\boldsymbol{\mathcal{V}}(t) + \beta \boldsymbol{u}(\boldsymbol{\mathcal{X}}(t), t)\,\mathrm{d}t \\ \mathrm{d}\boldsymbol{\mathcal{V}}(t) &= -\left(\frac{\boldsymbol{\mathcal{V}}(t) - (1-\beta)\boldsymbol{u}(\boldsymbol{\mathcal{X}}(t), t)}{\tau}\right)\mathrm{d}t + \frac{\sqrt{2\,D_0}}{\tau}\,\mathrm{d}\boldsymbol{\omega}(t) \end{aligned} \tag{3.44}$$

The position process now is:

$$\begin{aligned} &\boldsymbol{\mathcal{X}}(t) = \boldsymbol{\mathcal{X}}(t_0) + \tau \boldsymbol{\mathcal{V}}(t_0)(1 - e^{-\frac{t-t_o}{\tau}}) \\ &+(1-\beta)\int_{t_o}^{t} \mathrm{d}s\, \boldsymbol{u}(\boldsymbol{\mathcal{X}}(s), s)\,(1 - e^{-\frac{t-s}{\tau}}) \\ &+\beta \int_{t_o}^{t} \mathrm{d}s\, \boldsymbol{u}(\boldsymbol{\mathcal{X}}(s), s) \\ &+\sqrt{2\,D_0}\int_{t_o}^{t} \mathrm{d}\boldsymbol{\omega}(s)\,(1 - e^{-\frac{t-s}{\tau}}) \end{aligned} \tag{3.45}$$

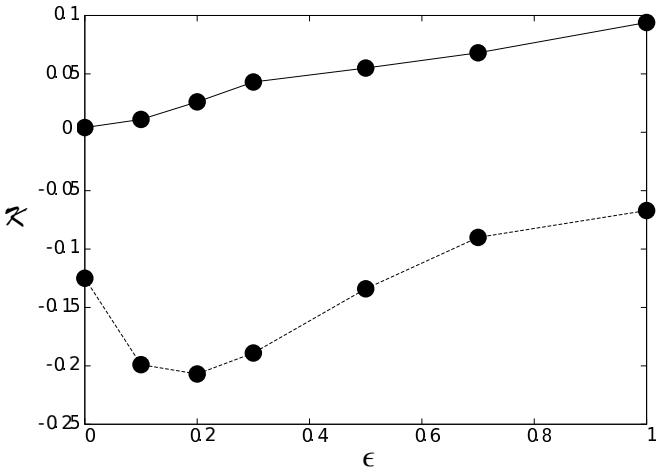

Figure 3.5: Non-perturbative destructive ($\Omega = 0$, dashed line) vs constructive ($\Omega = 3$, continuous line) interference when St=2, for several values of ϵ. We notice a transition in curves when $0.1 < \epsilon < 0.3$, which are the values of ϵ at which we get out of the perturbative regime.

and the *velocity* is:

$$\dot{\boldsymbol{\mathcal{X}}}(t) = \boldsymbol{\mathcal{V}}(t_0)e^{-\frac{t-t_o}{\tau}} + \frac{1-\beta}{\tau}\int_{t_o}^{t} \mathrm{d}s\, \boldsymbol{u}(\boldsymbol{\mathcal{X}}(s),s)\, e^{-\frac{t-s}{\tau}}$$
$$+\beta\, \boldsymbol{u}(\boldsymbol{\mathcal{X}}(t),t) + \frac{\sqrt{2\,D_0}}{\tau}\int_{t_o}^{t} \mathrm{d}\boldsymbol{\omega}(s)\, e^{-\frac{t-s}{\tau}} \tag{3.46}$$

This means that the entire eddy diffusivity now reads:

$$\begin{aligned}
\mathrm{D}^{\mathrm{ef}} &= \lim_{t\uparrow\infty}\frac{1}{d}\langle\dot{\boldsymbol{\mathcal{X}}}(t)\cdot\boldsymbol{\mathcal{X}}(t)\rangle = D_0 \\
+ &\quad \lim_{t\uparrow\infty}\frac{(1-\beta)^2}{\tau\, d}\int_0^{t-t_0}\mathrm{d}t_1\int_0^{t-t_0}\mathrm{d}t_2 e^{-\frac{t_1}{\tau}}(1-e^{-\frac{t_2}{\tau}}) \\
\times &\quad \langle\boldsymbol{u}(\boldsymbol{\mathcal{X}}(t-t_1),t-t_1)\cdot\boldsymbol{u}(\boldsymbol{\mathcal{X}}(t-t_2),t-t_2)\rangle \\
+ &\quad \frac{\beta(1-\beta)}{\tau\, d}\lim_{t\uparrow\infty}\int_0^{t-t_0}\mathrm{d}t_1\int_0^{t-t_0}\mathrm{d}t_2 e^{-\frac{t_1}{\tau}} \\
\times &\quad \langle\boldsymbol{u}(\boldsymbol{\mathcal{X}}(t-t_1),t-t_1)\cdot\boldsymbol{u}(\boldsymbol{\mathcal{X}}(t-t_2),t-t_2)\rangle \\
+ &\quad \frac{\beta(1-\beta)}{d}\lim_{t\uparrow\infty}\int_0^{t-t_0}\mathrm{d}t_1(1-e^{-\frac{t_1}{\tau}}) \\
\times &\quad \langle\boldsymbol{u}(\boldsymbol{\mathcal{X}}(t-t_1),t-t_1)\cdot\boldsymbol{u}(\boldsymbol{\mathcal{X}}(t),t)\rangle \\
+ &\quad \frac{\beta^2}{d}\lim_{t\uparrow\infty}\int_0^{t-t_0}\mathrm{d}t_1\langle\boldsymbol{u}(\boldsymbol{\mathcal{X}}(t-t_1),t-t_1)\cdot\boldsymbol{u}(\boldsymbol{\mathcal{X}}(t),t)\rangle
\end{aligned} \tag{3.47}$$

We now suppose that the process is stationary at least asymptotically after

a certain transient, as done by Pismen and Nir. Thus $\langle \boldsymbol{u}(\boldsymbol{\mathcal{X}}(t-t_1), t-t_1) \cdot \boldsymbol{u}(\boldsymbol{\mathcal{X}}(t-t_2), t-t_2)\rangle = \mathcal{C}(|t_1 - t_2|)$

$$\begin{aligned}
\mathrm{D}^{\mathrm{ef}} &= \lim_{t\uparrow\infty} \frac{1}{d}\langle \dot{\boldsymbol{\mathcal{X}}}(t)\cdot\boldsymbol{\mathcal{X}}(t)\rangle = D_0 \\
&+ \frac{(1-\beta)^2}{\tau\, d}\int_0^\infty \mathrm{d}t_1 \int_0^\infty \mathrm{d}t_2 e^{-\frac{t_1}{\tau}}(1-e^{-\frac{t_2}{\tau}})\mathcal{C}(|t_{12}|) \\
&+ \frac{\beta(1-\beta)}{\tau\, d}\int_0^\infty \mathrm{d}t_1 \int_0^\infty \mathrm{d}t_2 e^{-\frac{t_1}{\tau}}\mathcal{C}(|t_{12}|) \\
&+ \frac{\beta(1-\beta)}{d}\int_0^\infty \mathrm{d}t_1 (1-e^{-\frac{t_1}{\tau}})\mathcal{C}(|t_1|) \\
&+ \frac{\beta^2}{d}\int_0^\infty \mathrm{d}t_1 \mathcal{C}(|t_1|)
\end{aligned} \tag{3.48}$$

Let $\mathcal{C}(t)$ be again a bounded and integrable function vanishing at $t \to \infty$. Then we know that:

$$\begin{aligned}
&\lim_{T\uparrow\infty}\frac{1}{\tau}\int_0^T \mathrm{d}t_1 \int_0^T \mathrm{d}t_2\, e^{-\frac{t_1}{\tau}}\, \mathcal{C}(|t_{12}|)\,(1-e^{-\frac{t_2}{\tau}}) = \\
&\int_0^\infty \mathrm{d}t\mathcal{C}(t)
\end{aligned} \tag{3.49}$$

By applying Eq. (3.49), we can recast Eq. (3.48) after some algebra:

$$\begin{aligned}
\mathrm{D}^{\mathrm{ef}} &= D_0 + \frac{1-\beta+\beta^2}{d}\int_0^\infty \mathrm{d}t_1 \mathcal{C}(|t_1|) \\
&+ \frac{\beta(1-\beta)}{\tau\, d}\int_0^\infty \mathrm{d}t_1 \int_0^\infty \mathrm{d}t_2\, e^{-\frac{t_1}{\tau}}\, \mathcal{C}(|t_{12}|) \\
&- \frac{\beta(1-\beta)}{d}\int_0^\infty \mathrm{d}t_1\, e^{-\frac{t_1}{\tau}}\, \mathcal{C}(|t_1|)
\end{aligned} \tag{3.50}$$

Let us now consider the second addend.

Proposition 3.6.1.

$$\lim_{T\uparrow\infty}\frac{1}{\tau}\int_0^T \mathrm{d}t_1 \int_0^T \mathrm{d}t_2\, e^{-\frac{t_1}{\tau}}\mathcal{C}(|t_{12}|) = \int_0^\infty \mathrm{d}\overline{t}\,\mathcal{C}(|\overline{t}|) + \int_0^\infty \mathrm{d}\overline{t} e^{-\frac{\overline{t}}{\tau}}\,\mathcal{C}(|\overline{t}|) \tag{3.51}$$

Proof. We can again perform the substition $t_1 - t_2 \to \overline{t}$, $t_1 \to t_1$, similarly to what was done for Eq. (3.18). Thus:

$$\lim_{T\uparrow\infty}\frac{1}{\tau}\int_0^T \mathrm{d}t_1\int_0^T \mathrm{d}t_2\, e^{-\frac{t_1}{\tau}}\mathcal{C}(|t_{12}|)$$
$$=\lim_{T\uparrow\infty}\frac{1}{\tau}\int_0^T \mathrm{d}t_1\int_{t_1-T}^{t_1} \mathrm{d}\overline{t}\, e^{-\frac{t_1}{\tau}}\mathcal{C}(|\overline{t}|) \tag{3.52}$$

Looking at Fig. 3.1, we switch the order of integration, performing it with respect to t_1 first:

$$\begin{aligned}
&= \frac{1}{\tau}\int_{-\infty}^0 \mathrm{d}\overline{t}\int_0^{+\infty} \mathrm{d}t_1\, e^{-\frac{t_1}{\tau}}\mathcal{C}(|\overline{t}|)\\
&+ \lim_{T\uparrow\infty}\frac{1}{\tau}\int_0^T \mathrm{d}\overline{t}\int_{\overline{t}}^T \mathrm{d}t_1\, e^{-\frac{t_1}{\tau}}\mathcal{C}(|\overline{t}|)\\
&= \int_0^\infty \mathrm{d}\overline{t}\,\mathcal{C}(|\overline{t}|)+\int_0^\infty \mathrm{d}\overline{t},e^{-\frac{\overline{t}}{\tau}}\,\mathcal{C}(|\overline{t}|)\\
&- \lim_{T\uparrow\infty} e^{-\frac{T}{\tau}}\int_0^T \mathrm{d}\overline{t}\,\mathcal{C}(|\overline{t}|)
\end{aligned} \tag{3.53}$$

If the integral in the last line is bounded, then that term vanishes as $T\to\infty$. □

By plugging Eq. (3.51) into Eq. (3.50), many terms cancel out and we arrive at:

$$\mathrm{D}^{\mathrm{ef}} = D_0+\frac{1}{d}\int_0^\infty \mathrm{d}t_1\mathcal{C}(|t_1|) \tag{3.54}$$

which is the usual Taylor formula.

Appendix

3.A Path integrals and Jannssen-De dominicis action

Let us start off with the Cauchy problem:

$$\begin{aligned} d\boldsymbol{\mathcal{X}} &= \mathbf{u}(\boldsymbol{\mathcal{X}}(t),t)dt \\ \boldsymbol{\mathcal{X}} &= \boldsymbol{\mathcal{X}}_0 \end{aligned} \tag{3.55}$$

We consider here the prepoint discretization over the time-intervals dt and Δt. This is equivalent to the Ito discretization in the case of multiplicative noise. The probability of being at a certain point $\boldsymbol{\mathcal{X}}(t_1)$ at a time $t_1 \to 0$ will be:

$$P(\boldsymbol{\mathcal{X}}(\Delta t_1)|\boldsymbol{\mathcal{X}}_0) = \delta(\boldsymbol{\mathcal{X}}(\Delta t_1) - \boldsymbol{\mathcal{X}}_0 - \mathbf{u}(\boldsymbol{\mathcal{X}}_0,0)\Delta t_1)$$

where $\Delta t_1 = t_1 - t_0$, the latter being set here to 0 for the sake of brevity. If we now consider instead:

$$\begin{aligned} d\boldsymbol{\mathcal{X}} &= \boldsymbol{u}(\boldsymbol{\mathcal{X}}(t),t)dt + d\boldsymbol{\omega}(t) \\ \boldsymbol{\mathcal{X}} &= \boldsymbol{\mathcal{X}}_0 \end{aligned} \tag{3.56}$$

we have:

$$\begin{aligned} P(\boldsymbol{\mathcal{X}}(t_1)|\boldsymbol{\mathcal{X}}_0) &= \int d\boldsymbol{\omega}(0) \int d\Delta\boldsymbol{\omega}_1 P(\Delta\boldsymbol{\omega}_1) P(\boldsymbol{\mathcal{X}}(t_1)|\boldsymbol{\mathcal{X}}_0, \Delta\boldsymbol{\omega}_1)\delta(\boldsymbol{\omega}(0)) \\ &= \int d\Delta\boldsymbol{\omega}_1 \delta(\boldsymbol{\mathcal{X}}(t_1) - \boldsymbol{\mathcal{X}}_0 - \boldsymbol{u}(\boldsymbol{\mathcal{X}}_0,0)\Delta t_1 - \Delta\boldsymbol{\omega}_1) \frac{1}{\sqrt{2\pi\Delta t_1}} e^{-\frac{\Delta\omega_1^2}{2\Delta t_1}} \end{aligned}$$

from the well-known property of Gaussian independent increments of the Wiener process and that $\boldsymbol{\omega}(0) = 0$. Notice that the Wiener initial condition turns obviously out to be irrelevant in the SDE and its value can be ignored. If we now consider the probability of being at a certain point $\boldsymbol{\mathcal{X}}(t_2)$ at a time t_2, with a very small time step $\Delta t_2 = t_2 - t_1$, passing through the point

$\boldsymbol{\mathcal{X}}(t_1)$ at $t = t_1$:

$$
\begin{aligned}
&P(\boldsymbol{\mathcal{X}}(t_2)|\boldsymbol{\mathcal{X}}(t_1)\boldsymbol{\mathcal{X}}_0) = \int d\Delta\boldsymbol{\omega}_1 \int d\Delta\boldsymbol{\omega}_2 \\
&\times P(\boldsymbol{\mathcal{X}}(t_2)|\boldsymbol{\mathcal{X}}(t_1), \Delta\boldsymbol{\omega}_2) P(\Delta\boldsymbol{\omega}_2) P(\boldsymbol{\mathcal{X}}(t_1)|\boldsymbol{\mathcal{X}}_0, \Delta\boldsymbol{\omega}_1) P(\Delta\boldsymbol{\omega}_1) \\
&= \int d\Delta\boldsymbol{\omega}_2 \delta(\boldsymbol{\mathcal{X}}(t_2) - \boldsymbol{\mathcal{X}}(t_1) - \boldsymbol{u}(\boldsymbol{\mathcal{X}}(t_1), t_1)\Delta t_2 - \Delta\boldsymbol{\omega}_2) \frac{1}{\sqrt{2\pi\Delta t_2}} e^{-\frac{\Delta\omega_2^2}{2\Delta t_2}} \\
&\times \int d\Delta\boldsymbol{\omega}_1 \delta(\boldsymbol{\mathcal{X}}(t_1) - \boldsymbol{\mathcal{X}}_0 - \boldsymbol{u}(\boldsymbol{\mathcal{X}}_0, 0)\Delta t_1 - \Delta\boldsymbol{\omega}_1) \frac{1}{\sqrt{2\pi\Delta t_1}} e^{-\frac{\Delta\omega_1^2}{2\Delta t_1}}
\end{aligned} \tag{3.57}
$$

As a consequence:

$$
\begin{aligned}
&P(\boldsymbol{\mathcal{X}}(t_2)|\boldsymbol{\mathcal{X}}_0) = \int d\boldsymbol{\mathcal{X}}(t_1) \int d\Delta\boldsymbol{\omega}_1 \int d\Delta\boldsymbol{\omega}_2 \\
&\times P(\boldsymbol{\mathcal{X}}(t_2)|\boldsymbol{\mathcal{X}}(t_1), \Delta\boldsymbol{\omega}_2) P(\Delta\boldsymbol{\omega}_2) P(\boldsymbol{\mathcal{X}}(t_1)|\boldsymbol{\mathcal{X}}_0, \Delta\boldsymbol{\omega}_1) P(\Delta\boldsymbol{\omega}_1) \\
&= \int d\boldsymbol{\mathcal{X}}(t_1) \int d\Delta\boldsymbol{\omega}_2 \delta(\boldsymbol{\mathcal{X}}(t_2) - \boldsymbol{\mathcal{X}}(t_1) - \boldsymbol{u}(\boldsymbol{\mathcal{X}}(t_1), t_1)\Delta t_2 - \Delta\boldsymbol{\omega}_2) \frac{1}{\sqrt{2\pi\Delta t_2}} e^{-\frac{\Delta\omega_2^2}{2\Delta t_2}} \\
&\times \int d\Delta\boldsymbol{\omega}_1 \delta(\boldsymbol{\mathcal{X}}(t_1) - \boldsymbol{\mathcal{X}}_0 - \boldsymbol{u}(\boldsymbol{\mathcal{X}}_0, 0)\Delta t_1 - \Delta\boldsymbol{\omega}_1) \frac{1}{\sqrt{2\pi\Delta t_1}} e^{-\frac{\Delta\omega_1^2}{2\Delta t_1}}
\end{aligned} \tag{3.58}
$$

Recalling the formal identity $\delta(f(x)) = \int_{-\infty}^{+\infty} dy e^{-\imath y f(x)}$, we can recast the Dirac measures:

$$
\begin{aligned}
&P(\boldsymbol{\mathcal{X}}(t_2)|\boldsymbol{\mathcal{X}}_0) = \int d\boldsymbol{\mathcal{X}}(t_1) \int d\overline{\boldsymbol{\mathcal{X}}}(t_1) \int d\Delta\boldsymbol{\omega}_1 \int d\overline{\boldsymbol{\mathcal{X}}}(t_2) \int d\Delta\boldsymbol{\omega}_2 \\
&e^{-\imath\overline{\boldsymbol{\mathcal{X}}}(t_2)[\boldsymbol{\mathcal{X}}(t_2) - \boldsymbol{\mathcal{X}}(t_1) - \boldsymbol{u}(\boldsymbol{\mathcal{X}}(t_1), t_1)\Delta t_2 - \Delta\boldsymbol{\omega}_2]} \frac{1}{\sqrt{2\pi\Delta t_2}} e^{-\frac{\Delta\omega_2^2}{2\Delta t_2}} \\
&\times e^{-\imath\overline{\boldsymbol{\mathcal{X}}}(t_1)[\boldsymbol{\mathcal{X}}(t_1) - \boldsymbol{\mathcal{X}}_0 - \boldsymbol{u}(\boldsymbol{\mathcal{X}}_0, 0)\Delta t_1 - \Delta\boldsymbol{\omega}_1]} \frac{1}{\sqrt{2\pi\Delta t_1}} e^{-\frac{\Delta\omega_1^2}{2\Delta t_1}}
\end{aligned} \tag{3.59}
$$

We suppose now to apply the previous expressions to a finite time interval $[t_0, t_f]$, after dividing it in fine meshes of N time sub-intervals Δt_i, $i = 1, .., N$, and taking the limit $\{\Delta t_i\} \to 0$, $N \to \infty$ as to have $\sum_{i=1}^{N} \Delta t_i = t_f - t_0$. Then we obtain:

$$
\begin{aligned}
&P(\boldsymbol{\mathcal{X}}(t_f) = \boldsymbol{\mathcal{X}}_f|\boldsymbol{\mathcal{X}}_0) = \lim_{\substack{N\to\infty \\ \{\Delta t_i\}\to 0}} \left[\prod_{i=0}^{N} \int d\boldsymbol{\mathcal{X}}(t_i) \int d\overline{\boldsymbol{\mathcal{X}}}(t_i) \int d\boldsymbol{\omega}_i\right] \\
&\times \left[\prod_{i=1}^{N} e^{-\imath\overline{\boldsymbol{\mathcal{X}}}(t_i)[\boldsymbol{\mathcal{X}}(t_i) - \boldsymbol{\mathcal{X}}(t_{i-1}) - \boldsymbol{u}(\boldsymbol{\mathcal{X}}(t_{i-1}), t_{i-1})\Delta t_i - \Delta\boldsymbol{\omega}_i]} \frac{1}{\sqrt{2\pi\Delta t_i}} e^{-\frac{\Delta\omega_i^2}{2\Delta t_i}}\right] \\
&\times \delta(\boldsymbol{\mathcal{X}}(t_f) - \boldsymbol{\mathcal{X}}_f) \delta(\overline{\boldsymbol{\mathcal{X}}}(t_0))\, \delta(\boldsymbol{\omega}_0)\, \delta(\boldsymbol{\mathcal{X}}(t_0) - \boldsymbol{\mathcal{X}}_0)
\end{aligned} \tag{3.60}
$$

where we have used that the jacobian $d\boldsymbol{\omega}(0)\prod_{i=1}^{N} d\Delta\boldsymbol{\omega}_i = \prod_{i=0}^{N} d\boldsymbol{\omega}_i$ and we have put the initial condition on $\overline{\boldsymbol{\mathcal{X}}} = 0$ for the sake of simplicity, it being inconsequential. Eq. (3.60) is often written as:

$$\begin{aligned} & \int \mathcal{D}\boldsymbol{\mathcal{X}}\mathcal{D}\overline{\boldsymbol{\mathcal{X}}}\mathcal{D}\boldsymbol{\omega} e^{-\imath[\int_{t_0}^{t_f} \overline{\boldsymbol{\mathcal{X}}}(t)(\dot{\boldsymbol{\mathcal{X}}}(t)-\boldsymbol{u}(\boldsymbol{\mathcal{X}}(t),t))dt-\int_{t_0}^{t_f} \overline{\boldsymbol{\mathcal{X}}}(t)d\boldsymbol{\omega}(t)]} \\ \times \quad & \delta(\boldsymbol{\mathcal{X}}(t_f)-\boldsymbol{\mathcal{X}}_f)\,\delta(\boldsymbol{\mathcal{X}}(t_0)-\boldsymbol{\mathcal{X}}_0) \end{aligned} \tag{3.61}$$

where we omitted the not-influential initial condition on the ghost variable and the initial point of the Wiener process; also, we indicated the Gaussian Wiener measure simply by $\mathcal{D}\boldsymbol{\omega}$.

The limit is independent of the discretization because we know the integral form associated to the trajectories of the stochastic differential equation (3.56) is independent of the mesh [11]. In general, however, path integral can be dependent on the discretization, an a prescription has always to be assigned in those cases [10].

We can exploit the well-known results of the Fourier transform of a Gaussian variable to integrale over the Wiener increments in Eq. (3.60), as to obtain:

$$\int \mathcal{D}\overline{\boldsymbol{\mathcal{X}}}\mathcal{D}\boldsymbol{\mathcal{X}}\, e^{-\int_{t_0}^{t_f} \mathrm{d}t\left[\left\|\bar{\boldsymbol{\mathcal{X}}}_t\right\|^2+\imath\bar{\boldsymbol{\mathcal{X}}}_t\cdot(\dot{\boldsymbol{\mathcal{X}}}(t)-\boldsymbol{u}(\boldsymbol{\mathcal{X}}(t),t))\right]} \tag{3.62}$$

The quantity

$$-\int_{t_0}^{t_f} \mathrm{d}t\left[\left\|\bar{\boldsymbol{\mathcal{X}}}_t\right\|^2+\imath\bar{\boldsymbol{\mathcal{X}}}_t\cdot(\dot{\boldsymbol{\mathcal{X}}}(t)-\boldsymbol{u}(\boldsymbol{\mathcal{X}}(t),t))\right]$$

is the Janssen-Dominicis action for a tracer particle.

3.B A free theory reminder

3.B.1 Stochastic method

We consider the stochastic differential equation[1]

$$\mathrm{d}\boldsymbol{\mathcal{X}}_t = (\boldsymbol{u}_0+\bar{\boldsymbol{\jmath}}_t)\,\mathrm{d}t + \sqrt{2D_0}\,\mathrm{d}\boldsymbol{\omega}_t \tag{3.63a}$$

$$\boldsymbol{\mathcal{X}}_{t_0} = \boldsymbol{q} \tag{3.63b}$$

[1] In the rest of this Appendix, we are going to indicate the time dependence of a function $f(t)$ by a low index f_t, in order to have a more compact notation and neater functional formulas.

where $\bar{\boldsymbol{\jmath}}_t \colon \mathbb{R} \mapsto \mathbb{R}^d$ is a smooth response field. The solution is

$$\boldsymbol{\mathcal{X}}_t = \boldsymbol{q} + \boldsymbol{u}_0\,(t - t_0) + \int_{t_0}^{t} \mathrm{d}t_1\,\bar{\boldsymbol{\jmath}}_{t_1} + \sqrt{2D_o}(\boldsymbol{\omega}_t - \boldsymbol{\omega}_{t_0}) \tag{3.64}$$

The field-theoretic partition function is the expectation function of the generating function

$$\begin{aligned} Z &= \left\langle \exp\{\int_0^{t_\mathrm{f}} \mathrm{d}t \boldsymbol{\jmath}_t \cdot \boldsymbol{\mathcal{X}}_t\} \right\rangle = \\ &= \exp\left\{ \int_{t_0}^{t_\mathrm{f}} \mathrm{d}t\, \boldsymbol{\jmath}_t \cdot [\boldsymbol{q} + \boldsymbol{u}_0\,(t - t_0)] + \int_{[t_0,t_\mathrm{f}]^2} \mathrm{d}t_1 \mathrm{d}t_2\, H(t_1 - t_2) \boldsymbol{\jmath}_{t_1} \cdot \bar{\boldsymbol{\jmath}}_{t_2} \right\} \\ &\times \left\langle \exp\left\{ 2D_o \int_{t_0}^{t_\mathrm{f}} \mathrm{d}t\, \boldsymbol{\jmath}_t \cdot (\boldsymbol{\omega}_t - \boldsymbol{\omega}_{t_0}) \right\} \right\rangle \end{aligned} \tag{3.65}$$

The expectation value

$$\begin{aligned} &\left\langle \exp\left\{ D_o \int_{t_0}^{t_\mathrm{f}} \mathrm{d}t \boldsymbol{\jmath}_t \cdot (\boldsymbol{\omega}_t - \boldsymbol{\omega}_{t_0}) \right\} \right\rangle \\ &= \exp\left\{ D_o \int_{[t_0,t_\mathrm{f}]^2} \mathrm{d}t_1 \mathrm{d}t_2\, (\min(t_1,\, t_2) - t_0) \boldsymbol{\jmath}_{t_1} \cdot \boldsymbol{\jmath}_{t_2} \right\} \end{aligned}$$

3.B.2 Field theory method

The partition function in the presence of a constant velocity field is

$$Z = \int_{\mathbb{R}^d} \frac{\mathrm{d}^d \boldsymbol{\lambda}}{(2\,\pi)^d} \int \mathcal{D}[\bar{\boldsymbol{\mathcal{X}}}, \boldsymbol{\mathcal{X}}]\, e^{-\int_{t_0}^{t_\mathrm{f}} \mathrm{d}t \left\{ D_0 \|\dot{\bar{\boldsymbol{\mathcal{X}}}}_t\|^2 + \imath \dot{\bar{\boldsymbol{\mathcal{X}}}}_t \cdot (\dot{\boldsymbol{\mathcal{X}}}_t - \boldsymbol{u}_0 - \bar{\boldsymbol{\jmath}}_t) - \boldsymbol{\jmath}_t \cdot \boldsymbol{\mathcal{X}}_t \right\}} e^{\imath \boldsymbol{\lambda} \cdot (\boldsymbol{\mathcal{X}}_{t_0} - \boldsymbol{q})} \tag{3.66}$$

The integral can be evaluated exactly using the stationary phase approximation. This is done in three steps

- We rotate the integration contour by representing the $\bar{\boldsymbol{\mathcal{X}}}_t$'s as complex variables

$$\bar{\boldsymbol{\mathcal{X}}}_t = \Re \bar{\boldsymbol{\mathcal{X}}}_t + \imath\, \Im \bar{\boldsymbol{\mathcal{X}}}_t \tag{3.67}$$

- We fix the new contour by requiring that the action be real on the contour and the corresponding integral convergent.

- We evaluate the integral by expanding along the stationary value of the action.

Upon performing the rotation (3.67) we get into

$$\Re\mathcal{A} = \int_{t_0}^{t_\mathrm{f}} \mathrm{d}t \left\{ D_o \frac{\|\Re\bar{\boldsymbol{\mathcal{X}}}_t\|^2 - \|\Im\bar{\boldsymbol{\mathcal{X}}}_t\|^2}{2} - (\Im\bar{\boldsymbol{\mathcal{X}}}_t) \cdot \left(\dot{\boldsymbol{\mathcal{X}}}_t - \boldsymbol{u}_0 - \bar{\boldsymbol{\jmath}}_t \right) - \boldsymbol{\jmath} \cdot \boldsymbol{\mathcal{X}}_t \right\} \tag{3.68a}$$

$$\Im\mathcal{A} = \int_{t_0}^{t_\mathrm{f}} \mathrm{d}t\, \Re\bar{\boldsymbol{\mathcal{X}}}_t \cdot \left(D_o\, \Im\bar{\boldsymbol{\mathcal{X}}}_t + \dot{\boldsymbol{\mathcal{X}}}_t - \boldsymbol{u}_0 - \bar{\boldsymbol{\jmath}}_t \right) \tag{3.68b}$$

The vanishing phase condition is satisfied by

$$D_o\, \Im\bar{\boldsymbol{\mathcal{X}}}_t + \dot{\boldsymbol{\mathcal{X}}}_t - \boldsymbol{u}_0 - \bar{\boldsymbol{\jmath}}_t = 0 \tag{3.69}$$

or

$$\Re\bar{\boldsymbol{\mathcal{X}}}_t = 0 \tag{3.70}$$

We rule out the second solution as it yields a diverging integral over $\Im\bar{\boldsymbol{\mathcal{X}}}_t$. Hence minimizing the real part of the action is equivalent to minimizing

$$\begin{aligned} \Re\mathcal{A}_\star = & \min_{\bar{\boldsymbol{\mathcal{X}}}_t, \boldsymbol{\mathcal{X}}_t, \delta_{\boldsymbol{\phi}_t} \Re\mathcal{A}=0} \int_{t_0}^{t_\mathrm{f}} \mathrm{d}t \\ \times & \left\{ D_o \|\Re\bar{\boldsymbol{\mathcal{X}}}_t\|^2 + \|\Im\bar{\boldsymbol{\mathcal{X}}}_t\|^2 - \boldsymbol{\jmath} \cdot \boldsymbol{\mathcal{X}}_t + \boldsymbol{\phi}_t \cdot \left(D_o\, \Im\bar{\boldsymbol{\mathcal{X}}}_t + \dot{\boldsymbol{\mathcal{X}}}_t - \boldsymbol{u}_0 - \bar{\boldsymbol{\jmath}}_t \right) \right\} \end{aligned} \tag{3.71}$$

where the Lagrange multiplier $\boldsymbol{\phi}_t$ linearly enforces the stationary phase condition. This expression allows us to reformulate the extremal problem by a trade off between the ghost field and the Lagrange multiplier

$$\Re\mathcal{A}_\star = \min_{\boldsymbol{\mathcal{X}}_t, \delta_{\boldsymbol{\phi}_t} \Re\mathcal{A}=0} \int_{t_0}^{t_\mathrm{f}} \mathrm{d}t \left\{ -D_o \|\boldsymbol{\phi}_t\|^2 - \boldsymbol{\jmath} \cdot \boldsymbol{\mathcal{X}}_t + \boldsymbol{\phi}_t \cdot \left(\dot{\boldsymbol{\mathcal{X}}}_t - \boldsymbol{u}_0 - \bar{\boldsymbol{\jmath}}_t \right) \right\} \tag{3.72}$$

The variation with respect to $\boldsymbol{\mathcal{X}}_t$ for $\boldsymbol{\mathcal{X}}_{t_0} = \boldsymbol{q}$ yields

$$\dot{\boldsymbol{\phi}}_t + \boldsymbol{\jmath}_t = 0 \tag{3.73a}$$

$$\boldsymbol{\phi}_{t_\mathrm{f}} = 0 \tag{3.73b}$$

which yields, after integrating the term $\boldsymbol{\phi}_t \cdot \dot{\boldsymbol{\mathcal{X}}}_t$:

$$\Re\mathcal{A}_\star = -\boldsymbol{q} \cdot \int_{t_0}^{t_\mathrm{f}} \mathrm{d}t \boldsymbol{\jmath}_t - \int_{t_0}^{t_\mathrm{f}} \mathrm{d}t \left\{ D_o \| \int_t^{t_\mathrm{f}} \mathrm{d}t_1 \boldsymbol{\jmath}_{t_1} \|^2 + (\boldsymbol{u}_0 + \bar{\boldsymbol{\jmath}}_t) \cdot \int_t^{t_\mathrm{f}} \mathrm{d}t_1 \boldsymbol{\jmath}_{t_1} \right\} \tag{3.74}$$

Upon taking into account that

$$\begin{aligned}&\int_{[t_0,t_{\rm f}]^3}{\rm d}t\,{\rm d}t_1\,{\rm d}t_2\,H(t_1-t)\,H(t_2-t)\,\boldsymbol{\jmath}_{t_1}\cdot\boldsymbol{\jmath}_{t_2}\\ =\;&\int_{[t_0,t_{\rm f}]^2}{\rm d}t_1\,{\rm d}t_2{\rm min}(t_1,t_2)\,\boldsymbol{\jmath}_{t_1}\cdot\boldsymbol{\jmath}_{t_2}\end{aligned}\tag{3.75}$$

and that

$$\int_{t_0}^{t_{\rm f}}{\rm d}t\,\boldsymbol{u}_0\cdot\int_t^{t_{\rm f}}{\rm d}t_1\boldsymbol{\jmath}_{t_1}=\int_{t_0}^{t_{\rm f}}{\rm d}t\,\boldsymbol{\jmath}_t\cdot\boldsymbol{u}_0\,(t-t_0)\tag{3.76}$$

we obtain

$$\begin{aligned}\Re\mathcal{A}_\star=&-\int_{t_0}^{t_{\rm f}}{\rm d}t\,\boldsymbol{\jmath}_t\cdot[\boldsymbol{q}+\boldsymbol{u}_0\,(t-t_0)]\\ &-\int_{[t_0,t_{\rm f}]^2}{\rm d}t_1{\rm d}t_2\,\left\{D_0{\rm min}(t_1,t_2)\boldsymbol{\jmath}_{t_1}\cdot\boldsymbol{\jmath}_{t_2}+H(t_1-t_2)\,\boldsymbol{\jmath}_{t_1}\cdot\bar{\boldsymbol{\jmath}}_{t_2}\right\}\end{aligned}\tag{3.77}$$

whence finally

$$\ln Z=-\Re\mathcal{A}_\star\tag{3.78}$$

which is the result used in the main text.

Remark 3.B.1. We notice that the stationary phase approximation is correctly reproduced by finding the extremals of the Janssen-De Dominicis action after preforming the replacement

$$\bar{\boldsymbol{\mathcal{X}}}_t=-\imath\,\boldsymbol{\phi}_t\tag{3.79}$$

This is the shortcut usually adopted to implement perturbative expansions around a Gaussian stationary point [71].

3.C Langevin–Kramers correlation functions

We compute the extremal value of the analytic continuation of the Gaussian De Dominicis-Janssen action (3.130):

$$\begin{aligned}\mathcal{A}=&\int_{t_0}^{t_{\rm f}}{\rm d}t\,\left[-D_0\,\frac{\|\bar{\boldsymbol{\psi}}_t\|^2}{\tau^2}+\bar{\boldsymbol{v}}_t\cdot\left(\dot{\boldsymbol{v}}_t+\frac{\boldsymbol{v}_t-\boldsymbol{u}_0}{\tau}-\bar{\boldsymbol{\jmath}}_t^{(p)}\right)\right.\\ +\;&\left.\bar{\boldsymbol{\mathcal{X}}}_t\cdot\left(\dot{\boldsymbol{\mathcal{X}}}_t-\boldsymbol{v}_t-\bar{\boldsymbol{\jmath}}_t^{(q)}\right)-\left(\boldsymbol{\jmath}_t^{(q)}\cdot\boldsymbol{\mathcal{X}}_t+\boldsymbol{\jmath}_t^{(p)}\cdot\boldsymbol{v}_t\right)\right]\end{aligned}\tag{3.80}$$

The variation with respect to $\boldsymbol{\mathcal{X}}_t$ yields for $\bar{\boldsymbol{\mathcal{X}}}_{t_\mathrm{f}} = 0$

$$\dot{\bar{\boldsymbol{\mathcal{X}}}}_t + \boldsymbol{\jmath}_t^{(q)} = 0 \tag{3.81}$$

Similarly the variation with respect to $\boldsymbol{v}_t$ yields for $\bar{\boldsymbol{v}}_{t_\mathrm{f}} = 0$

$$\dot{\bar{\boldsymbol{v}}}_t - \frac{\bar{\boldsymbol{v}}_t}{\tau} + \bar{\boldsymbol{\mathcal{X}}}_t + \boldsymbol{\jmath}_t^{(p)} = 0 \tag{3.82}$$

which in view of the previous equation becomes

$$\begin{aligned} \dot{\bar{\boldsymbol{v}}}_t - \frac{\bar{\boldsymbol{v}}_t}{\tau} + \boldsymbol{\jmath}_t^{(p)} &= -\int_t^{t_\mathrm{f}} \mathrm{d}t_1\, \boldsymbol{\jmath}_{t_1}^{(q)} \\ \Rightarrow\quad \bar{\boldsymbol{v}}_{\star t} &= \int_t^{t_\mathrm{f}} \mathrm{d}t_1\, e^{\frac{t-t_1}{\tau}} \boldsymbol{\jmath}_{t_1}^{(p)} + \int_t^{t_\mathrm{f}} \mathrm{d}t_1\, e^{\frac{t-t_1}{\tau}} \int_{t_1}^{t_\mathrm{f}} \mathrm{d}t_2\, \boldsymbol{\jmath}_{t_2}^{(q)} \end{aligned} \tag{3.83}$$

Upon inserting into the action functional, after integrating the terms with time derivatives by parts, we get into

$$\begin{aligned} \mathcal{A} &= \int_{t_0}^{t_\mathrm{f}} \mathrm{d}t \left[-D_0 \frac{\|\bar{\boldsymbol{v}}_{\star t}\|^2}{\tau^2} - \bar{\boldsymbol{v}}_{\star t} \cdot \Big(\frac{\boldsymbol{u}_0}{\tau} + \bar{\boldsymbol{\jmath}}_t^{(p)} \Big) - \bar{\boldsymbol{\jmath}}_t^{(q)} \cdot \int_t^{t_\mathrm{f}} \mathrm{d}t_1 \boldsymbol{\jmath}_{t_1}^{(q)} \right] \\ &- \boldsymbol{\mathcal{X}}_{t_0} \cdot \int_{t_0}^{t_\mathrm{f}} \boldsymbol{\jmath}_t^{(q)} \mathrm{d}t - \boldsymbol{v}_{t_0} \cdot \bar{\boldsymbol{v}}_{\star t_0} \end{aligned}$$

3.D Mathematical extension to Gaussian random flows

3.D.1 The tracer case

The scope of this section is to recover the results of [64] working out the details of the calculations not thereby reported.

A Lagrangian particle evolves according to the SDE

$$\mathrm{d}\boldsymbol{\mathcal{X}}_t = \boldsymbol{u}(\boldsymbol{\mathcal{X}}_t, t)\mathrm{d}t + \sqrt{2D_o}\, \mathrm{d}\boldsymbol{\omega}_t \tag{3.84}$$

The De Dominicis–Janssen action for a Lagrangian particle in a flow described by a velocity field $\boldsymbol{u}\colon \mathbb{R}^d \times \mathbb{R} \mapsto \mathbb{R}^d$:

$$\mathcal{A} = \int_{t_0}^{t_\mathrm{f}} \mathrm{d}t\, \Big\{ D_0 \|\bar{\boldsymbol{\mathcal{X}}}_t\|^2 + \imath\, \bar{\boldsymbol{\mathcal{X}}}_t \cdot \Big[\dot{\boldsymbol{\mathcal{X}}}_t - \boldsymbol{u}(\boldsymbol{\mathcal{X}}_t, t) \Big] \Big\} \tag{3.85}$$

The moment generating function (in Statistical Mechanics: partition function) for a diffusion process based at $\boldsymbol{q}$ is

$$Z = \int \mathcal{D}[\bar{\boldsymbol{\mathcal{X}}}, \boldsymbol{\mathcal{X}}]\, e^{-\mathcal{A} + \int_{t_0}^{t_\mathrm{f}} \mathrm{d}t \left(\boldsymbol{\jmath}_t \cdot \boldsymbol{\mathcal{X}}_t + \imath \bar{\boldsymbol{\jmath}} \cdot \bar{\boldsymbol{\mathcal{X}}}_t \right)}\, \delta^{(d)}(\boldsymbol{\mathcal{X}}_{t_0} - \boldsymbol{q}) \tag{3.86}$$

We immediately observe that such a partition function with the external source $\boldsymbol{\jmath} = 0$ is equivalent to a system governed by the following SDE:

$$\mathrm{d}\boldsymbol{\mathcal{X}}_t = (\bar{\boldsymbol{\jmath}}_t + \boldsymbol{u}(\boldsymbol{\mathcal{X}}_t, t))\mathrm{d}t + \sqrt{2D_o}\,\mathrm{d}\boldsymbol{\omega}_t \quad , \tag{3.87}$$

where the external source $\bar{\boldsymbol{\jmath}}$ turns out to be a linear perturbation of the external velocity field.

If the velocity field is space-time constant,

$$\boldsymbol{u}(\boldsymbol{q}, t) = \boldsymbol{u}_o \tag{3.88}$$

the solution of SDE follows immediately:

$$\boldsymbol{\mathcal{X}}_t = \boldsymbol{q} + \int_{t_0}^{t} \bar{\boldsymbol{\jmath}}_{t_1}\,\mathrm{d}t_1 + \boldsymbol{u}\,(t - t_0) + \sqrt{2D_o}\,(\boldsymbol{\omega}_t - \boldsymbol{\omega}_{t_0}) \quad , \tag{3.89}$$

The partition function is specified by the correlation functions we are going to compute. We can obtain directly from the solution (3.89):

$$\langle \boldsymbol{\mathcal{X}}_t \rangle \;=\; \boldsymbol{q} + \boldsymbol{u}_o\,(t - t_0) \tag{3.90a}$$

$$\begin{aligned} \langle \boldsymbol{\mathcal{X}}_{t_1} \otimes \boldsymbol{\mathcal{X}}_{t_2} \rangle \;&=\; (\boldsymbol{q} + \boldsymbol{u}_o\,(t_1 - t_0)\,) \otimes (\boldsymbol{q} + \boldsymbol{u}_o\,(t_2 - t_0)\,) \\ &+\; 2D_o(\min(t_1,\, t_2) - t_0)\mathsf{I} \end{aligned} \tag{3.90b}$$

$$\left\langle \boldsymbol{\mathcal{X}}_{t_1} \otimes \imath\bar{\boldsymbol{\mathcal{X}}}_{t_2} \right\rangle \;=\; \left\langle \frac{\delta \boldsymbol{\mathcal{X}}_{t_1}}{\delta \bar{\boldsymbol{\jmath}}_{t_2}} \right\rangle = H(t_1 - t_2)\,\mathsf{I} \tag{3.90c}$$

where $H(0) = 0$.

In general, one has to compute the moment generating function if interested in deriving the most general statistical observable. From Appendix 3.B.2:

$$Z = e^{\int_{t_0}^{t_\mathrm{f}} \mathrm{d}t\, \boldsymbol{\jmath}_t \cdot [\boldsymbol{q} + \boldsymbol{u}_0\,(t - t_0)] + \int_{[t_0, t_\mathrm{f}]^2} \mathrm{d}t_1 \mathrm{d}t_2 \left\{ D_0(\min(t_1, t_2) - t_0) \boldsymbol{\jmath}_{t_1} \cdot \boldsymbol{\jmath}_{t_2} + H(t_1 - t_2)\, \boldsymbol{\jmath}_{t_1} \cdot \bar{\boldsymbol{\jmath}}_{t_2} \right\}} \tag{3.91}$$

whence we get the following relationships:

$$\left\langle \bar{\boldsymbol{\mathcal{X}}}_t \right\rangle = -\imath \frac{\delta Z}{\delta \bar{\boldsymbol{\jmath}}_t}\bigg|_{\boldsymbol{\jmath} = \bar{\boldsymbol{\jmath}} = 0} = 0 \tag{3.92a}$$

$$\left\langle \bar{\boldsymbol{\mathcal{X}}}_{t_1} \otimes \bar{\boldsymbol{\mathcal{X}}}_{t_2} \right\rangle = -\frac{\delta^2 Z}{\delta \bar{\boldsymbol{\jmath}}_{t_1} \delta \bar{\boldsymbol{\jmath}}_{t_2}}\bigg|_{\boldsymbol{\jmath} = \bar{\boldsymbol{\jmath}} = 0} = 0 \tag{3.92b}$$

Now, let the velocity field field be Gaussian with constant mean

$$\langle \boldsymbol{u}(\boldsymbol{q},t)\rangle_{(u)} = \boldsymbol{u}_o \tag{3.93}$$

and correlation

$$\begin{aligned} & \langle (\boldsymbol{u}(\boldsymbol{q}_2,t_2)-\boldsymbol{u}_0)\otimes(\boldsymbol{u}(\boldsymbol{q}_1,t_1)-\boldsymbol{u}_0)\rangle_{(u)} \\ = \quad & \mathsf{B}(\boldsymbol{q}_1-\boldsymbol{q}_2,|t_1-t_2|)\equiv \mathsf{B}(\boldsymbol{q}_{12},|t_{12}|) \end{aligned}$$

We wish to compute the perturbative expression of the eddy-diffusivity:

$$\mathrm{D}^{\mathrm{ef}} \equiv \frac{1}{2d}\lim_{t\uparrow\infty}\frac{d}{dt}\left\langle \|\boldsymbol{\mathcal{X}}_t - \langle \boldsymbol{\mathcal{X}}_t\rangle^{(u)}\|^2\right\rangle_{(u)} \tag{3.94}$$

We can evaluate (3.94) by averaging the generating function over the velocity ensemble

$$\begin{aligned} \langle Z\rangle_{(u)} \quad = \quad & \int \mathcal{D}[\boldsymbol{\mathcal{X}},\bar{\boldsymbol{\mathcal{X}}}] \\ & \times \quad \exp\left\{-\int_{t_0}^{t_{\mathrm{f}}}\mathrm{d}t\left[D_o\|\bar{\boldsymbol{\mathcal{X}}}_t\|^2 - \boldsymbol{\jmath}_t\cdot\boldsymbol{\mathcal{X}}_t + \imath\,\bar{\boldsymbol{\mathcal{X}}}_t\cdot\left(\dot{\boldsymbol{\mathcal{X}}}_t-\bar{\boldsymbol{\jmath}}_t\right)\right]\right\}\langle\mathcal{I}\rangle_{(u)} \end{aligned} \tag{3.95}$$

where

$$\begin{aligned} \langle\mathcal{I}\rangle_{(u)} \equiv \exp\left\{-\frac{1}{2}\int_{[t_0,t_{\mathrm{f}}]^2}\mathrm{d}t_1\mathrm{d}t_2\,\bar{\boldsymbol{\mathcal{X}}}_{t_1}\cdot\mathsf{B}(\boldsymbol{\mathcal{X}}_{t_1}-\boldsymbol{\mathcal{X}}_{t_2},|t_{12}|)\cdot\bar{\boldsymbol{\mathcal{X}}}_{t_2}\right\} = \\ \exp\left\{\int_{[t_0,t_{\mathrm{f}}]}\mathrm{d}t\left(\boldsymbol{\mathcal{X}}_t\cdot\frac{\delta}{\delta\boldsymbol{\phi}_t}+\bar{\boldsymbol{\mathcal{X}}}_t\cdot\frac{\delta}{\delta\bar{\boldsymbol{\phi}}_t}\right)\right\}. \\ \times\ \exp\left\{-\frac{1}{2}\int_{[t_0,t_{\mathrm{f}}]^2}\mathrm{d}t_1\mathrm{d}t_2\,\bar{\boldsymbol{\phi}}_{t_1}\cdot\mathsf{B}(\boldsymbol{\phi}_{t_1}-\boldsymbol{\phi}_{t_2},|t_{12}|)\cdot\bar{\boldsymbol{\phi}}_{t_2}\right\}\Bigg|_{\bar{\boldsymbol{\phi}}=\boldsymbol{\phi}=0} \end{aligned} \tag{3.96}$$

The formal expression of the path integral becomes

$$\begin{aligned} & \langle Z\rangle_{(u)} \\ & = e^{\int_{t_0}^{t_{\mathrm{f}}}\mathrm{d}t\,[\boldsymbol{q}+\boldsymbol{u}_o\,(t-t_0)]\cdot\left(\boldsymbol{\jmath}_t+\frac{\delta}{\delta\boldsymbol{\phi}_t}\right)+\int_{[t_{\mathrm{f}},t_0]^2}\mathrm{d}t_1\mathrm{d}t_2\,D_0(\min(t_1,t_2)-t_0)\left(\boldsymbol{\jmath}_{t_1}+\frac{\delta}{\delta\boldsymbol{\phi}_{t_1}}\right)\cdot\left(\boldsymbol{\jmath}_{t_2}+\frac{\delta}{\delta\boldsymbol{\phi}_{t_2}}\right)} \\ & \times e^{\int_{[t_{\mathrm{f}},t_0]^2}\mathrm{d}t_1\mathrm{d}t_2\,H(t_1-t_2)\left(\boldsymbol{\jmath}_{t_1}+\frac{\delta}{\delta\boldsymbol{\phi}_{t_1}}\right)\cdot\left(\bar{\boldsymbol{\jmath}}_{t_2}+\frac{1}{\imath}\frac{\delta}{\delta\bar{\boldsymbol{\phi}}_{t_2}}\right)} \\ & \times e^{-\frac{1}{2}\int_{[t_0,t_{\mathrm{f}}]^2}\mathrm{d}t_1\mathrm{d}t_2\,\bar{\boldsymbol{\phi}}_{t_1}\cdot\mathsf{B}(\boldsymbol{\phi}_{t_1}-\boldsymbol{\phi}_{t_2},|t_{12}|)\cdot\bar{\boldsymbol{\phi}}_{t_2}}\Big|_{\boldsymbol{\phi}_t=\bar{\boldsymbol{\phi}}_t=0} \end{aligned} \tag{3.97}$$

The expression is amenable to the conceptually more transparent form

$$\begin{aligned}\langle Z\rangle_{(u)} &= e^{W_0}\,\mathfrak{T}(\boldsymbol{\phi},\imath\bar{\boldsymbol{\phi}})\,e^{\mathfrak{O}(\boldsymbol{\phi},\imath\bar{\boldsymbol{\phi}})}\,e^{-F(\boldsymbol{\phi},\bar{\boldsymbol{\phi}})}\Big|_{\boldsymbol{\phi}_t=\bar{\boldsymbol{\phi}}_t=0}\\ &\equiv e^{W_0}\,\mathfrak{T}(\boldsymbol{\phi},\imath\bar{\boldsymbol{\phi}})\,e^{\mathfrak{O}(\boldsymbol{\phi},\imath\bar{\boldsymbol{\phi}})}\\ &\times \exp\left\{-\frac{1}{2}\int_{[t_0,t_{\rm f}]^2}\mathrm{d}t_1\mathrm{d}t_2\,\bar{\boldsymbol{\phi}}_{t_1}\cdot\mathsf{B}(\boldsymbol{\phi}_{t_1}-\boldsymbol{\phi}_{t_2},|t_{12}|)\cdot\bar{\boldsymbol{\phi}}_{t_2}\right\}\Big|_{\boldsymbol{\phi}_t=\bar{\boldsymbol{\phi}}_t=0}\end{aligned} \tag{3.98}$$

where

$$\begin{aligned}W_0 &= \int_{t_0}^{t_{\rm f}}\mathrm{d}t\,[\boldsymbol{q}+\boldsymbol{u}_o\,(t-t_0)]\cdot\boldsymbol{\jmath}_t\\ &+ \int_{[t_{\rm f},t_0]^2}\mathrm{d}t_1\mathrm{d}t_2\,\left\{D_0\,(\min(t_1,\,t_2)-t_0)\boldsymbol{\jmath}_{t_1}\cdot\boldsymbol{\jmath}_{t_2}+H(t_1-t_2)\,\boldsymbol{\jmath}_{t_1}\cdot\bar{\boldsymbol{\jmath}}_{t_2}\right\}\end{aligned} \tag{3.99}$$

Furthermore $\mathfrak{T}$ is the translation operator

$$\begin{aligned}&\mathfrak{T}(\boldsymbol{\phi},\imath\bar{\boldsymbol{\phi}})\\ &=\exp\left\{\int_{t_0}^{t_{\rm f}}\mathrm{d}t\,\left[(\boldsymbol{q}+\boldsymbol{u}_o(t-t_0)+G\cdot\boldsymbol{\jmath}_t+R\circ\bar{\boldsymbol{\jmath}}_t)\cdot\frac{\delta}{\delta\boldsymbol{\phi}_t}+\frac{(R^\dagger\circ\boldsymbol{\jmath})_t}{\imath}\cdot\frac{\delta}{\delta\bar{\boldsymbol{\phi}}_t}\right]\right\}\end{aligned} \tag{3.100}$$

where we defined

$$R^\dagger\circ\boldsymbol{\jmath}_t=\int_{t_0}^{t_{\rm f}}\mathrm{d}t_1\,H(t_1-t)\boldsymbol{\jmath}_{t_1} \tag{3.101}$$

$$R\circ\bar{\boldsymbol{\jmath}}_t=\int_{t_0}^{t_{\rm f}}\mathrm{d}t_1\,H(t-t_1)\bar{\boldsymbol{\jmath}}_{t_1} \tag{3.102}$$

and

$$G\circ\boldsymbol{\jmath}_t=2D_0\int_{t_0}^{t_{\rm f}}\mathrm{d}t_1\,(\min(t_1,t)-t_0)\,\boldsymbol{\jmath}_{t_1} \tag{3.103}$$

Finally in (3.98) the exponential of the operator

$$\begin{aligned}&\mathfrak{O}(\boldsymbol{\phi},\imath\,\bar{\boldsymbol{\phi}})\\ &=\int_{[t_{\rm f},t_0]^2}\mathrm{d}t_1\mathrm{d}t_2\,\left\{D_0(\min(t_1,\,t_2)-t_0)\frac{\delta}{\delta\boldsymbol{\phi}_{t_1}}\cdot\frac{\delta}{\delta\boldsymbol{\phi}_{t_2}}+\frac{H(t_{12})}{\imath}\frac{\delta}{\delta\boldsymbol{\phi}_{t_1}}\cdot\frac{\delta}{\delta\bar{\boldsymbol{\phi}}_{t_2}}\right\}\end{aligned} \tag{3.104}$$

acts on the the interaction term. We now can re-absorb the imaginary factor at the price of a redefinition of the ghost field:

$$\bar{\boldsymbol{\phi}} \mapsto -\imath\, \bar{\boldsymbol{\phi}} \tag{3.105}$$

so that the loop expansion of the cumulant generating function (in Statistical Mechanics: Helmholtz free energy) stems from the *formula*

$$W = W_0 + \ln \left\{ \mathfrak{T}(\boldsymbol{\phi}, \bar{\boldsymbol{\phi}})\, e^{\mathfrak{O}(\boldsymbol{\phi},\bar{\boldsymbol{\phi}})}\, e^{F(\boldsymbol{\phi},\bar{\boldsymbol{\phi}})} \right\}\Big|_{\boldsymbol{\phi}_t=\bar{\boldsymbol{\phi}}_t=0} \tag{3.106}$$

which involves only real quantities. The formula (3.106) is the one usually applied in the field theoretic systematic analysis of perturbation theory [71]. Having fixed the conventions (3.105) and (3.106), we will omit in what follows any explicit reference to the functional dependence on $\boldsymbol{\phi}, \bar{\boldsymbol{\phi}}$. We generate the perturbative expansion in powers of the scalar functional F:

$$\mathfrak{T}\, e^{\mathfrak{O}}\, e^{F} = \mathfrak{T}\, e^{\mathfrak{O}}\, (1 + F + \dots) = 1 + \mathfrak{T}\, e^{\mathfrak{O}}\, F + \dots \tag{3.107}$$

Consequently, at the lowest order in F it also holds that:

$$\begin{aligned} W &= W_0 + \ln \left(1 + \left\{ \mathfrak{T}\, e^{\mathfrak{O}}\, F \right\}_{\boldsymbol{\phi}_t \bar{\boldsymbol{\phi}}_t = 0} \right) + \dots \\ &= W_0 + \left\{ \mathfrak{T}\, e^{\mathfrak{O}}\, F \right\}_{\boldsymbol{\phi}_t=\bar{\boldsymbol{\phi}}_t=0} + \dots \end{aligned} \tag{3.108}$$

In order to proceed further we write

$$\begin{aligned} F &= \frac{1}{2} \int \frac{\mathrm{d}^d \boldsymbol{k}}{(2\,\pi)^d} \int_{[t_0,t_{\mathrm{f}}]^2} \mathrm{d}t_1 \mathrm{d}t_2\, e^{\imath\, \boldsymbol{k}\cdot(\boldsymbol{\phi}_{t_1} - \boldsymbol{\phi}_{t_2})} \bar{\boldsymbol{\phi}}_{t_1} \cdot \check{\mathsf{B}}(\boldsymbol{k}, |t_{12}|) \cdot \bar{\boldsymbol{\phi}}_{t_2} \\ &= \frac{1}{2} \partial_{\boldsymbol{a}_1} \otimes \partial_{\boldsymbol{a}_2} \Big|_{\boldsymbol{a}_1=\boldsymbol{a}_2=0} \\ &: \int \frac{\mathrm{d}^d \boldsymbol{k}}{(2\,\pi)^d} \int_{[t_0,t_{\mathrm{f}}]^2} \mathrm{d}t_1 \mathrm{d}t_2\, e^{\imath\, \boldsymbol{k}\cdot(\boldsymbol{\phi}_{t_1} - \boldsymbol{\phi}_{t_2})}\, e^{\sum_{i=1}^2 \boldsymbol{a}_i \bar{\boldsymbol{\phi}}_{t_i}} \check{\mathsf{B}}(\boldsymbol{k}, |t_{12}|) \end{aligned} \tag{3.109}$$

The latter representation is useful once we recognize that $\mathfrak{O}$ is the generator of the Gaussian measure. Namely we recall that

Proposition 3.D.1.

$$\begin{aligned} & e^{\mathfrak{O}} e^{\int_{t_0}^{t_{\mathrm{f}}} \mathrm{d}t \left(\boldsymbol{\jmath}_t \cdot \boldsymbol{\phi}_t + \bar{\boldsymbol{\jmath}}_t \cdot \bar{\boldsymbol{\phi}}_t \right)} \\ = \; & e^{\int_{t_0}^{t_{\mathrm{f}}} \mathrm{d}t \left(\boldsymbol{\jmath}_t \cdot \boldsymbol{\phi}_t + \bar{\boldsymbol{\jmath}}_t \cdot \bar{\boldsymbol{\phi}}_t \right) + \int_{[t_{\mathrm{f}},t_0]^2} \mathrm{d}t_1 \mathrm{d}t_2 \left\{ D_0(\min(t_1,t_2) - t_0) \boldsymbol{\jmath}_{t_1} \cdot \boldsymbol{\jmath}_{t_2} + H(t_1 - t_2)\, \boldsymbol{\jmath}_{t_1} \cdot \bar{\boldsymbol{\jmath}}_{t_2} \right\}} \end{aligned} \tag{3.110}$$

Proof. The proof stems from the definition of $\exp \mathfrak{O}$ as Gaussian average of a translation operator:

$$
\begin{aligned}
& e^{\mathfrak{O}} e^{\int_{t_0}^{t_\mathrm{f}} \mathrm{d}t \left(\boldsymbol{\jmath}_t \cdot \boldsymbol{\phi}_t + \bar{\boldsymbol{\jmath}}_t \cdot \bar{\boldsymbol{\phi}}_t \right)} = \int \limits_{\boldsymbol{\mathcal{X}}_{t_0} = \bar{\boldsymbol{\mathcal{X}}}_{t_\mathrm{f}} = 0} \mathcal{D}[\boldsymbol{\mathcal{X}}, \bar{\boldsymbol{\mathcal{X}}}] \\
\times \quad & \exp \left\{ - \int_{t_0}^{t_\mathrm{f}} \mathrm{d}t \left[D_o \| \bar{\boldsymbol{\mathcal{X}}}_t \|^2 + \bar{\boldsymbol{\mathcal{X}}}_t \cdot \dot{\boldsymbol{\mathcal{X}}}_t \right] \right\} \\
\times \quad & \exp \left\{ - \int_{t_0}^{t_\mathrm{f}} \mathrm{d}t \left[- \boldsymbol{\mathcal{X}}_t \cdot \frac{\delta}{\delta \boldsymbol{\phi}_t} - \bar{\boldsymbol{\mathcal{X}}}_t \cdot \frac{\delta}{\delta \bar{\boldsymbol{\phi}}_t} - \int_t^{t_\mathrm{f}} \mathrm{d}t_1 \bar{\boldsymbol{\mathcal{X}}}_{t_1} \cdot \frac{\delta}{\delta \boldsymbol{\phi}_t} \right] \right\} \\
\times \quad & \exp \left\{ \int_{t_0}^{t_\mathrm{f}} \mathrm{d}t \left(\boldsymbol{\jmath}_t \cdot \boldsymbol{\phi}_t + \bar{\boldsymbol{\jmath}}_t \cdot \bar{\boldsymbol{\phi}}_t \right) \right\} \\
= \quad & e^{\int_{t_0}^{t_\mathrm{f}} \mathrm{d}t \left(\boldsymbol{\jmath}_t \cdot \boldsymbol{\phi}_t + \bar{\boldsymbol{\jmath}}_t \cdot \bar{\boldsymbol{\phi}}_t \right)} \int \limits_{\boldsymbol{\mathcal{X}}_{t_0} = \bar{\boldsymbol{\mathcal{X}}}_{t_\mathrm{f}} = 0} \mathcal{D}[\boldsymbol{\mathcal{X}}, \bar{\boldsymbol{\mathcal{X}}}] \\
\times \quad & \exp \left\{ - \int_{t_0}^{t_\mathrm{f}} \mathrm{d}t \left[D_o \| \bar{\boldsymbol{\mathcal{X}}}_t \|^2 + \bar{\boldsymbol{\mathcal{X}}}_t \cdot \dot{\boldsymbol{\mathcal{X}}}_t - \boldsymbol{\mathcal{X}}_t \cdot \boldsymbol{\jmath}_t - \bar{\boldsymbol{\mathcal{X}}}_t \cdot \left(\bar{\boldsymbol{\jmath}}_t - \int_{t_0}^{t} \mathrm{d}t_1 \boldsymbol{\jmath}_{t_1} \right) \right] \right\}
\end{aligned}
$$

whence the claim. □

If we now set

$$\boldsymbol{\jmath}_t = \imath \, \boldsymbol{k} \left[\delta(t - t_1) - \delta(t - t_2) \right] \tag{3.111a}$$

$$\bar{\boldsymbol{\jmath}}_t = \boldsymbol{a}_1 \delta(t - t_1) + \boldsymbol{a}_2 \delta(t - t_2) \tag{3.111b}$$

Since we assume $H(0) = 0$, it is straightforward to obtain

$$
\begin{aligned}
e^{\mathfrak{O}} \, F \quad = \quad & \partial_{\boldsymbol{a}_1} \otimes \partial_{\boldsymbol{a}_2} |_{\boldsymbol{a}_1 = \boldsymbol{a}_2 = 0} : \int \frac{\mathrm{d}^d \boldsymbol{k}}{(2\,\pi)^d} \int_{[t_0, t_\mathrm{f}]^2} \mathrm{d}t_1 \mathrm{d}t_2 \\
& \times \quad e^{\imath \, \boldsymbol{k} \cdot (\boldsymbol{\phi}_{t_1} - \boldsymbol{\phi}_{t_2}) - D_o \| \boldsymbol{k} \|^2 |t_{12}|} \, e^{\sum_{i=1}^2 \boldsymbol{a}_i \cdot \bar{\boldsymbol{\phi}}_{t_i} + \imath \, \boldsymbol{k} \cdot [\boldsymbol{a}_2 H(t_{12}) - \boldsymbol{a}_1 H(t_{21})]} \frac{\check{\mathsf{B}}(\boldsymbol{k}, |t_{12}|)}{2} \\
& = \quad \frac{1}{2} \int \frac{\mathrm{d}^d \boldsymbol{k}}{(2\,\pi)^d} \int_{[t_0, t_\mathrm{f}]^2} \mathrm{d}t_1 \mathrm{d}t_2 \, e^{\imath \, \boldsymbol{k} \cdot (\boldsymbol{\phi}_{t_1} - \boldsymbol{\phi}_{t_2}) - D_o \| \boldsymbol{k} \|^2 |t_{12}|} \\
& \times \quad \left[\bar{\boldsymbol{\phi}}_{t_1} - \imath \, \boldsymbol{k} \, H(t_{21}) \right] \cdot \check{\mathsf{B}}(\boldsymbol{k}, |t_{12}|) \left[\bar{\boldsymbol{\phi}}_{t_2} + \imath \, \boldsymbol{k} \, H(t_{12}) \right] \cdot
\end{aligned}
\tag{3.112}
$$

Upon applying the translation operator $\mathfrak{T}$ we find then

$$
\begin{aligned}
& \left\{ \mathfrak{T} \, e^{\mathfrak{O}} \, e^F \right\}_{\boldsymbol{\phi}_t = \bar{\boldsymbol{\phi}}_t = 0} \\
= \quad & \frac{1}{2} \int \frac{\mathrm{d}^d \boldsymbol{k}}{(2\,\pi)^d} \int_{[t_0, t_\mathrm{f}]^2} \mathrm{d}t_1 \mathrm{d}t_2 \, e^{\imath \, \boldsymbol{k} \cdot \sum_{i=1}^2 (-)^{1+i} (G \circ \boldsymbol{\jmath}_{t_i} + R \circ \bar{\boldsymbol{\jmath}}_{t_i} + \boldsymbol{u}_o \, t_i) - D_o \| \boldsymbol{k} \|^2 |t_{12}|} \\
\times \quad & \left[R^\dagger \circ \boldsymbol{\jmath}_{t_1} - \imath \, \boldsymbol{k} \, H(t_{21}) \right] \cdot \mathsf{B}(\boldsymbol{k}, |t_{12}|) \cdot \left[R^\dagger \circ \boldsymbol{\jmath}_{t_2} + \imath \, \boldsymbol{k} \, H(t_{12}) \right] + \ldots
\end{aligned}
\tag{3.113}
$$

3.D.2 Explicit expression of the diffusion constant up to leading order

In order to compute the eddy diffusivity we first need the second order position cumulant:

$$\begin{aligned}
&\left.\frac{\delta^2 W}{\delta \boldsymbol{\jmath}_{t_3} \cdot \delta \boldsymbol{\jmath}_{t_3}}\right|_{\boldsymbol{\jmath}_{\boldsymbol{t}}=\bar{\boldsymbol{\jmath}}_{\boldsymbol{t}}=0} = 2d\, D_o\, t_{30} \\
&+ \int_{[t_0,t_3]^2} \mathrm{d}t_1 \mathrm{d}t_2 \int \frac{\mathrm{d}^d \boldsymbol{k}}{(2\,\pi)^d} e^{\imath\, \boldsymbol{k}\cdot\boldsymbol{u}_o\, t_{12} - D_o \|\boldsymbol{k}\|^2 |t_{12}|}\ \mathrm{tr}\,\mathsf{B}\,(\boldsymbol{k}, |t_{12}|) \\
&+ 2D_o \int_{[t_0,t_3]^2} \mathrm{d}t_1 \mathrm{d}t_2\, H(t_{12})\, t_{12} \int \frac{\mathrm{d}^d \boldsymbol{k}}{(2\,\pi)^d} e^{\imath\, \boldsymbol{k}\cdot\boldsymbol{u}_o\, t_{12} - D_o \|\boldsymbol{k}\|^2 |t_{12}|} \\
&\times\ (\imath\, \boldsymbol{k}) \cdot \mathsf{B}\,(\boldsymbol{k}, |t_{12}|) \cdot (\imath\, \boldsymbol{k}) + \ldots
\end{aligned} \tag{3.114}$$

Whence:

$$\begin{aligned}
&\mathrm{D}^{\mathrm{ef}} = \frac{1}{2d} \lim_{t_3 \uparrow \infty} \frac{d}{dt_3} \left.\frac{\delta^2 W}{\delta \boldsymbol{\jmath}_{t_3} \cdot \delta \boldsymbol{\jmath}_{t_3}}\right|_{\boldsymbol{\jmath}_{\boldsymbol{t}}=\bar{\boldsymbol{\jmath}}_{\boldsymbol{t}}=0} = \\
&D_o + \lim_{t_3 \uparrow \infty} \frac{1}{d} \int_{[t_0,t_3]} \mathrm{d}t \int \frac{\mathrm{d}^d \boldsymbol{k}}{(2\,\pi)^d} e^{\imath\, \boldsymbol{k}\cdot\boldsymbol{u}_o\, (t_3 - t) - D_o \|\boldsymbol{k}\|^2 |t_3 - t|}\ \mathrm{tr}\,\mathsf{B}\,(\boldsymbol{k}, |t_3 - t|) \\
&+ \lim_{t_3 \uparrow \infty} \frac{D_o}{d} \int_{[t_0,t_3]} \mathrm{d}t\, (t_3 - t) \int \frac{\mathrm{d}^d \boldsymbol{k}}{(2\,\pi)^d} e^{\imath\, \boldsymbol{k}\cdot\boldsymbol{u}_o\, (t_3 - t) - D_o \|\boldsymbol{k}\|^2 |t_3 - t|} \\
&\times (\imath\, \boldsymbol{k}) \cdot \mathsf{B}\,(\boldsymbol{k}, |t_3 - t|) \cdot (\imath\, \boldsymbol{k}) + \ldots
\end{aligned} \tag{3.115}$$

After performing the substitution $t_3 - t \to T$ in the integrals, one obtains:

$$\begin{aligned}
&D_o + \lim_{t_3 \uparrow \infty} \frac{1}{d} \int_0^{t_3 - t_0} \mathrm{d}T \int \frac{\mathrm{d}^d \boldsymbol{k}}{(2\,\pi)^d} e^{\imath\, \boldsymbol{k}\cdot\boldsymbol{u}_o\, T - D_o \|\boldsymbol{k}\|^2 |T|}\ \mathrm{tr}\,\mathsf{B}\,(\boldsymbol{k}, |T|) \\
&\quad + \lim_{t_3 \uparrow \infty} \frac{D_o}{d} \int_0^{t_3 - t_0} T \mathrm{d}T \int \frac{\mathrm{d}^d \boldsymbol{k}}{(2\,\pi)^d} e^{\imath\, \boldsymbol{k}\cdot\boldsymbol{u}_o\, T - D_o \|\boldsymbol{k}\|^2 |T|} \\
&\quad \times\ \ (\imath\, \boldsymbol{k}) \cdot \mathsf{B}\,(\boldsymbol{k}, |T|) \cdot (\imath\, \boldsymbol{k}) + \ldots \\
&\quad = D_o + \frac{1}{d} \int_0^{\infty} \mathrm{d}T \int \frac{\mathrm{d}^d \boldsymbol{k}}{(2\,\pi)^d} e^{\imath\, \boldsymbol{k}\cdot\boldsymbol{u}_o\, T - D_o \|\boldsymbol{k}\|^2 |T|} \\
&\quad \times \int \mathrm{d}^d \boldsymbol{\mathcal{X}}\, e^{-\imath \boldsymbol{k}\cdot\boldsymbol{\mathcal{X}}}\, \langle \boldsymbol{u}(\boldsymbol{q} + \boldsymbol{\mathcal{X}}, T) \cdot \boldsymbol{u}(\boldsymbol{q}, 0) \rangle \\
&\quad + \frac{D_o}{d} \int_0^{\infty} T \mathrm{d}T \int \frac{\mathrm{d}^d \boldsymbol{k}}{(2\,\pi)^d} e^{\imath\, \boldsymbol{k}\cdot\boldsymbol{u}_o\, T - D_o \|\boldsymbol{k}\|^2 |T|} \\
&\quad \times \int \mathrm{d}^d \boldsymbol{\mathcal{X}}\, e^{-\imath \boldsymbol{k}\cdot\boldsymbol{\mathcal{X}}} \partial_{\boldsymbol{\mathcal{X}}} \otimes \partial_{\boldsymbol{\mathcal{X}}} : \langle \boldsymbol{u}(\boldsymbol{q} + \boldsymbol{\mathcal{X}}, T) \otimes \boldsymbol{u}(\boldsymbol{q}, 0) \rangle + \ldots
\end{aligned} \tag{3.116}$$

We now focus on the case $\boldsymbol{u}_o = 0$, and expand this expression up to the first order in D_o:

$$
\begin{aligned}
D_o &+ \frac{1}{d}\int_0^\infty \mathrm{d}T \int \frac{\mathrm{d}^d\boldsymbol{k}}{(2\,\pi)^d}\int \mathrm{d}^d\boldsymbol{\mathcal{X}}\, e^{-\imath\boldsymbol{k}\cdot\boldsymbol{\mathcal{X}}}\,\langle \boldsymbol{u}(\boldsymbol{q}+\boldsymbol{\mathcal{X}},T)\cdot\boldsymbol{u}(\boldsymbol{q},0)\rangle \\
&+\frac{D_0}{d}\int_0^\infty T\mathrm{d}T \int \frac{\mathrm{d}^d\boldsymbol{k}}{(2\,\pi)^d}\int \mathrm{d}^d\boldsymbol{\mathcal{X}}\, e^{-\imath\boldsymbol{k}\cdot\boldsymbol{\mathcal{X}}}\partial_{\boldsymbol{\mathcal{X}}}\cdot\partial_{\boldsymbol{\mathcal{X}}} \\
&\times \qquad \langle \boldsymbol{u}(\boldsymbol{q}+\boldsymbol{\mathcal{X}},T)\cdot\boldsymbol{u}(\boldsymbol{q},0)\rangle \\
&+\frac{D_o}{d}\int_0^\infty T\mathrm{d}T \int \frac{\mathrm{d}^d\boldsymbol{k}}{(2\,\pi)^d}\int \mathrm{d}^d\boldsymbol{\mathcal{X}}\, e^{-\imath\boldsymbol{k}\cdot\boldsymbol{\mathcal{X}}} \\
&\times \qquad \partial_{\boldsymbol{\mathcal{X}}}\otimes\partial_{\boldsymbol{\mathcal{X}}} : \langle \boldsymbol{u}(\boldsymbol{q}+\boldsymbol{\mathcal{X}},T)\otimes\boldsymbol{u}(\boldsymbol{q},0)\rangle \\
&+ \qquad \ldots \\
&= D_o + \frac{1}{d}\int_0^\infty \mathrm{d}T\ \langle \boldsymbol{u}(\boldsymbol{q},T)\cdot\boldsymbol{u}(\boldsymbol{q},0)\rangle \\
&+\frac{D_0}{d}\int_0^\infty T\mathrm{d}T\ \left\langle [\partial_{\mathcal{X}_\alpha}\partial_{\mathcal{X}_\alpha}u_\beta(\boldsymbol{q}+\boldsymbol{\mathcal{X}},T)]\big|_{\boldsymbol{\mathcal{X}}=0}\cdot u_\beta(\boldsymbol{q},0)\right\rangle \\
&+\frac{D_o}{d}\int_0^\infty T\mathrm{d}T\ \left\langle [\partial_{\mathcal{X}_\alpha}\partial_{\mathcal{X}_\beta}u_\alpha(\boldsymbol{q}+\boldsymbol{\mathcal{X}},T)]\big|_{\boldsymbol{\mathcal{X}}=0}\, u_\beta(\boldsymbol{q},0)\right\rangle + \ldots
\end{aligned}
\tag{3.117}
$$

Observing that $[\partial_{\boldsymbol{\mathcal{X}}}\boldsymbol{u}(\boldsymbol{q}+\boldsymbol{\mathcal{X}},T)]\big|_{\boldsymbol{\mathcal{X}}=0} = \partial_{\boldsymbol{q}}\boldsymbol{u}(\boldsymbol{q},T)$, and due to the homogeneity and stationarity of the two-point velocity correlation function, by simply using the chain rule:

$$
\begin{aligned}
&\langle [\partial_{q_\alpha}\partial_{q_\alpha}u_\beta(\boldsymbol{q},T)]\, u_\beta(\boldsymbol{q},0)\rangle = \partial_{\mathcal{X}_\alpha}\partial_{\mathcal{X}_\alpha}\left\langle [u_\beta(\boldsymbol{q}+\boldsymbol{\mathcal{X}},T)]\, u_\beta(\boldsymbol{q},0)\right\rangle\big|_{\boldsymbol{\mathcal{X}}=0} \\
&= \partial_{\mathcal{X}_\alpha}\partial_{\mathcal{X}_\alpha}\left\langle [u_\beta(\boldsymbol{q}+\boldsymbol{\mathcal{X}},0)]\, u_\beta(\boldsymbol{q},T)\right\rangle\big|_{\boldsymbol{\mathcal{X}}=0} = \langle [\partial_{q_\alpha}\partial_{q_\alpha}u_\beta(\boldsymbol{q},0)]\, u_\beta(\boldsymbol{q},T)\rangle
\end{aligned}
\tag{3.118}
$$

$$
\begin{aligned}
&\langle [\partial_{q_\alpha}\partial_{q_\alpha}u_\beta(\boldsymbol{q},T)]\, u_\beta(\boldsymbol{q},0)\rangle \\
&= \partial_{q_\alpha}\left\langle [\partial_{q_\alpha}u_\beta(\boldsymbol{q},T)]\, u_\beta(\boldsymbol{q},0)\right\rangle - \langle [\partial_{q_\alpha}u_\beta(\boldsymbol{q},T)][\partial_{q_\alpha}u_\beta(\boldsymbol{q},0)]\rangle \\
&= \partial_{q_\alpha}\partial_{q_\alpha}\left\langle u_\beta(\boldsymbol{q},T)\, u_\beta(\boldsymbol{q},0)\right\rangle - \partial_{q_\alpha}\left\langle u_\beta(\boldsymbol{q},T)\,[\partial_{q_\alpha}u_\beta(\boldsymbol{q},0)]\right\rangle \\
&- \langle [\partial_{q_\alpha}u_\beta(\boldsymbol{q},T)][\partial_{q_\alpha}u_\beta(\boldsymbol{q},0)]\rangle \\
&= -\left\langle u_\beta(\boldsymbol{q},T)\,[\partial_{q_\alpha}\partial_{q_\alpha}u_\beta(\boldsymbol{q},0)]\right\rangle - 2\,\langle [\partial_{q_\alpha}u_\beta(\boldsymbol{q},T)][\partial_{q_\alpha}u_\beta(\boldsymbol{q},0)]\rangle
\end{aligned}
\tag{3.119}
$$

Upon taking into account all of this, for an incompressible velocity field we end up with:

$$
\langle [\partial_{q_\alpha}\partial_{q_\alpha}u_\beta(\boldsymbol{q},T)]\, u_\beta(\boldsymbol{q},0)\rangle = -\,\langle [\partial_{q_\alpha}u_\beta(\boldsymbol{q},T)][\partial_{q_\alpha}u_\beta(\boldsymbol{q},0)]\rangle \tag{3.120a}
$$

$$
\left\langle [\partial_{q_\alpha}\partial_{q_\beta}u_\alpha(\boldsymbol{q},T)]\, u_\beta(\boldsymbol{q},0)\right\rangle = 0 \qquad (\text{since } \partial_{q_\alpha}u_\alpha = 0) \tag{3.120b}
$$

If we substitute these two identities in (3.117), we finally get the eddy-diffusivity espression presented by Mazzino and Vergassola in 1997:

$$\begin{aligned}\mathrm{D}^{\mathrm{ef}} &= D_o + \frac{1}{d}\int_0^\infty \mathrm{d}T\ \langle \boldsymbol{u}(\boldsymbol{q},T)\cdot\boldsymbol{u}(\boldsymbol{q},0)\rangle \\ &-\frac{D_o}{d}\int_0^\infty T\mathrm{d}T\ \langle[\partial_{q_\alpha}u_\beta(\boldsymbol{q},T)][\partial_{q_\alpha}u_\beta(\boldsymbol{q},0)]\rangle + \dots\end{aligned} \tag{3.121}$$

3.D.3 The inertial case: Gaussian Langevin-Kramers model

We now consider the simplified Maxey-Riley equations for the inertial particles:

$$\mathrm{d}\boldsymbol{\mathcal{X}}_t = \boldsymbol{v}_t\,\mathrm{d}t \tag{3.122a}$$

$$\mathrm{d}\boldsymbol{v}_t = -\left(\frac{\boldsymbol{v}_t-\boldsymbol{u}}{\tau}\right)\mathrm{d}t + \frac{\sqrt{2\,D_0}}{\tau}\,\mathrm{d}\boldsymbol{\omega}_t \tag{3.122b}$$

When the velocity is a costant $\boldsymbol{u}_0$, particle velocity along the shear components evolves according to a $d-1$-dimensional Ornstein–Uhlenbeck process

$$\boldsymbol{v}_t = e^{-\frac{t-t_o}{\tau}}\,\boldsymbol{v}_{t_0} + \boldsymbol{u}_0\,(1-e^{-\frac{t-t_o}{\tau}}) + \frac{\sqrt{2\,D_0}}{\tau}\int_{t_o}^t \mathrm{d}\boldsymbol{\omega}_s\,e^{-\frac{t-s}{\tau}} \tag{3.123}$$

the position process is

$$\begin{aligned}\boldsymbol{\mathcal{X}}_t &= \boldsymbol{\mathcal{X}}_{t_0} + \boldsymbol{v}_{t_0}(1-e^{-\frac{t-t_o}{\tau}}) + \boldsymbol{u}_0\,[t-t_o-\tau\,(1-e^{-\frac{t-t_o}{\tau}})] \\ &+ \sqrt{2\,D_0}\int_{t_o}^t \mathrm{d}\boldsymbol{\omega}_s\,(1-e^{-\frac{t-s}{\tau}})\end{aligned} \tag{3.124}$$

Let $\boldsymbol{\chi}_t = \boldsymbol{\mathcal{X}}_t \oplus \boldsymbol{v}_t$ the phase space Gaussian process. Its initial data conditioned is specified by

$$\langle\boldsymbol{\mathcal{X}}_t\rangle = \boldsymbol{\mathcal{X}}_{t_0} + \boldsymbol{v}_{t_0}\,(1-e^{-\frac{t-t_o}{\tau}}) + \boldsymbol{u}_0\,[t-t_0-\tau\,(1-e^{-\frac{t-t_0}{\tau}})] \tag{3.125}$$

$$\langle\boldsymbol{v}_t\rangle = e^{-\frac{t-t_o}{\tau}}\,\boldsymbol{v}_{t_0} + \boldsymbol{u}_0\,(1-e^{-\frac{t-t_o}{\tau}}) \tag{3.126}$$

The covariance matrix has instead components in position space

$$\begin{aligned}&\langle(\boldsymbol{\mathcal{X}}_{t_1}-\langle\boldsymbol{\mathcal{X}}_{t_1}\rangle)\otimes(\boldsymbol{\mathcal{X}}_{t_2}-\langle\boldsymbol{\mathcal{X}}_{t_2}\rangle)\rangle \\ &\quad= 2\,D_0\,\tau\,\mathsf{I}\left(e^{-\frac{t_{10}}{\tau}} + e^{-\frac{t_{20}}{\tau}} - \frac{e^{-\frac{|t_{12}|}{\tau}} + e^{-\frac{t_{10}+t_{20}}{\tau}}}{2} + \frac{\min(t_1,t_2)-t_0-\tau}{\tau}\right) \\ &\quad\equiv \mathsf{G}^{(qq)}(t_1,t_2;t_0)\end{aligned} \tag{3.127}$$

in momentum space

$$\langle (\boldsymbol{v}_{t_1} - \langle \boldsymbol{v}_{t_1} \rangle) \otimes (\boldsymbol{v}_{t_2} - \langle \boldsymbol{v}_{t_2} \rangle) \rangle = \frac{D_0 \, \mathsf{I}}{\tau} \left(e^{-\frac{|t_{12}|}{\tau}} - e^{-\frac{t_{10}+t_{20}}{\tau}} \right) \equiv \mathsf{G}^{(pp)}(t_1, t_2; t_o) \tag{3.128}$$

and cross correlation

$$\begin{aligned} \mathsf{G}^{(qp)}(t_1, t_2; t_0) &\equiv \langle (\boldsymbol{\mathcal{X}}_{t_1} - \langle \boldsymbol{\mathcal{X}}_{t_1} \rangle) \otimes (\boldsymbol{v}_{t_2} - \langle \boldsymbol{v}_{t_2} \rangle) \rangle \\ &= 2 \, D_0 \, \mathsf{I} \left[1 - e^{-\frac{t_{20}}{\tau}} - e^{-\frac{t_{10}}{\tau}} \sinh \frac{t_{20}}{\tau} \right] H(t_{12}) \\ &\quad -2 \, D_0 \, \mathsf{I} \, e^{-\frac{t_{20}}{\tau}} \left[1 + e^{\frac{t_{10}}{\tau}} - 2 \, e^{-\frac{t_{10}}{\tau}} \right] H(t_{21}) \end{aligned} \tag{3.129}$$

We now consider the situation when $\boldsymbol{u}$ is a general Gaussian field. The action is:

$$\begin{aligned} \mathcal{A} = &\int_{t_0}^{t_\mathrm{f}} \mathrm{d}t \, \left[D_0 \, \frac{\|\bar{\boldsymbol{v}}_t\|^2}{\tau^2} + \imath \, \bar{\boldsymbol{v}}_t \cdot \left(\dot{\boldsymbol{v}}_t + \frac{\boldsymbol{v}_t - \boldsymbol{u}_0}{\tau} - \bar{\boldsymbol{\jmath}}_t^{(p)} \right) + \imath \, \bar{\boldsymbol{\mathcal{X}}}_t \cdot \left(\dot{\boldsymbol{\mathcal{X}}}_t - \boldsymbol{v}_t - \bar{\boldsymbol{\jmath}}_t^{(q)} \right) \right] \\ &- \int_{t_0}^{t_\mathrm{f}} \mathrm{d}t \left(\boldsymbol{\jmath}_t^{(q)} \cdot \boldsymbol{\mathcal{X}}_t + \boldsymbol{\jmath}_t^{(p)} \cdot \boldsymbol{v}_t \right) + \int_{[t_0, t_\mathrm{f}]^2} \mathrm{d}t_1 \mathrm{d}t_2 \, \bar{\boldsymbol{v}}_{t_1} \cdot \frac{\mathsf{B}\left(\boldsymbol{\mathcal{X}}_{t_1} - \boldsymbol{\mathcal{X}}_{t_2}, |t_{12}| \right)}{2\tau^2} \cdot \bar{\boldsymbol{v}}_{t_2} \end{aligned} \tag{3.130}$$

Let us preliminarily consider the test case when the flow is $\delta-$correlated, i. e. $\mathsf{B}\left(\boldsymbol{q}_1 - \boldsymbol{q}_2, |t_{12}| \right) = 4\pi \mathsf{F}\left(\boldsymbol{q}_1 - \boldsymbol{q}_2 \right) \delta(t_1 - t_2)$. In that case the previous action becomes:

$$\begin{aligned} \mathcal{A} = &\int_{t_0}^{t_\mathrm{f}} \mathrm{d}t \, \left[(D_0 \, + 2\pi \, \mathrm{tr} \, \mathsf{F}(0)) \frac{\|\bar{\boldsymbol{v}}_t\|^2}{\tau^2} + \imath \, \bar{\boldsymbol{v}}_t \cdot \left(\dot{\boldsymbol{v}}_t + \frac{\boldsymbol{v}_t - \boldsymbol{u}_0}{\tau} - \bar{\boldsymbol{\jmath}}_t^{(p)} \right) \right] \\ &+ \int_{t_0}^{t_\mathrm{f}} \mathrm{d}t \left[\imath \, \bar{\boldsymbol{\mathcal{X}}}_t \cdot \left(\dot{\boldsymbol{\mathcal{X}}}_t - \boldsymbol{v}_t - \bar{\boldsymbol{\jmath}}_t^{(q)} \right) - \boldsymbol{\jmath}_t^{(q)} \cdot \boldsymbol{\mathcal{X}}_t + \boldsymbol{\jmath}_t^{(p)} \cdot \boldsymbol{v}_t \right] \end{aligned} \tag{3.131}$$

This action, withouth any source, makes the functional integral easily computable since it has the same form as the free theory with the substitiution $D_0 \to D_0 + 2\pi \, \mathrm{tr} \, \mathsf{F}(0)$, which turns out to be the very eddy-diffusivity. That is the same expression as the one in the tracer case, as proved in a different way by Boi, Martins and Mazzino in 2015.

The knowledge of the foregoing indicators, specifies the perturbative algorithm around the Gaussian theory. The response functions are then easily computed from the solutions of the SDEs associated to the free part of the above action (3.130) including the new external sources $\bar{\boldsymbol{\jmath}}_t^{(q)}$ and $\bar{\boldsymbol{\jmath}}_t^{(p)}$.

$$\mathrm{d}\boldsymbol{\mathcal{X}}_t = \left(\boldsymbol{v}_t + \bar{\boldsymbol{\jmath}}_t^{(q)} \right) \mathrm{d}t \tag{3.132a}$$

$$\mathrm{d}\boldsymbol{v}_t = - \left(\frac{\boldsymbol{v}_t - \boldsymbol{u}_0}{\tau} - \bar{\boldsymbol{\jmath}}_t^{(p)} \right) \mathrm{d}t + \frac{\sqrt{2 \, D_0}}{\tau} \, \mathrm{d}\boldsymbol{\omega}_t \tag{3.132b}$$

The solutions are given by Eq. (3.123)-(3.124) after substituting $\frac{\sqrt{2\,D_0}}{\tau}\,\mathrm{d}\boldsymbol{\omega}_s \to \frac{\sqrt{2\,D_0}}{\tau}\,\mathrm{d}\boldsymbol{\omega}_t + \bar{\boldsymbol{\jmath}}_t^{(p)}\mathrm{d}t$ and $\boldsymbol{\mathcal{X}}_t \to \boldsymbol{\mathcal{X}}_t + \int_{t_0}^{t}\bar{\boldsymbol{\jmath}}_{t_1}^{(q)}\mathrm{d}t_1$. Consequently:

$$\left\langle \boldsymbol{\mathcal{X}}_{t_1} \otimes \imath\,\bar{\boldsymbol{\mathcal{X}}}_{t_2}\right\rangle = \left\langle \frac{\delta\boldsymbol{\mathcal{X}}_{t_1}}{\delta\bar{\boldsymbol{\jmath}}_{t_2}^{(q)}}\right\rangle = H(t_{12})\,\mathsf{I} \equiv \mathsf{R}^{(qq)}(t_{12}) \tag{3.133a}$$

$$\left\langle \boldsymbol{\mathcal{X}}_{t_1} \otimes \imath\,\bar{\boldsymbol{v}}_{t_2}\right\rangle = \left\langle \frac{\delta\boldsymbol{\mathcal{X}}_{t_1}}{\delta\bar{\boldsymbol{\jmath}}_{t_2}^{(p)}}\right\rangle = \tau\,(1-e^{-\frac{t_{12}}{\tau}})\,H(t_{12})\,\mathsf{I} \equiv \mathsf{R}^{(qp)}(t_{12}) \tag{3.133b}$$

$$\left\langle \boldsymbol{v}_{t_1} \otimes \imath\,\bar{\boldsymbol{\mathcal{X}}}_{t_2}\right\rangle = \left\langle \frac{\delta\boldsymbol{\mathcal{X}}_{t_1}}{\delta\bar{\boldsymbol{\jmath}}_{t_2}^{(q)}}\right\rangle = 0 \equiv \mathsf{R}^{(pq)}(t_{12}) \tag{3.133c}$$

$$\left\langle \boldsymbol{v}_{t_1} \otimes \imath\,\bar{\boldsymbol{v}}_{t_2}\right\rangle = \left\langle \frac{\delta\boldsymbol{\mathcal{X}}_{t_1}}{\delta\bar{\boldsymbol{\jmath}}_{t_2}^{(p)}}\right\rangle = e^{-\frac{t_{12}}{\tau}}\,H(t_{12})\,\mathsf{I} \equiv \mathsf{R}^{(pp)}(t_{12}) \tag{3.133d}$$

We generate the perturbative expansion from the functional

$$W = W_0 + \ln\left\{\mathfrak{T}\,e^{\mathfrak{D}}\,e^{F}\right\}_{\boldsymbol{\Phi}_t=\bar{\boldsymbol{\Phi}}_t=0} \tag{3.134}$$

where upon defining $\boldsymbol{J} = [\boldsymbol{\jmath}^{(q)}, \boldsymbol{\jmath}^{(p)}]$ and $\bar{\boldsymbol{J}} = [\bar{\boldsymbol{\jmath}}^{(q)}, \bar{\boldsymbol{\jmath}}^{(p)}]$ we write

$$W_0 = \int_{t_0}^{t_{\mathrm{f}}}\mathrm{d}t\,\boldsymbol{J}_t\cdot\langle\boldsymbol{\chi}_t\rangle + \int_{[t_{\mathrm{f}},t_0]^2}\mathrm{d}t_1\mathrm{d}t_2\,\left\{\boldsymbol{J}_{t_1}\cdot\frac{\mathsf{G}}{2}\cdot\boldsymbol{J}_{t_2} + \boldsymbol{J}_{t_1}\cdot\mathsf{R}\cdot\bar{\boldsymbol{J}}_{t_2}\right\} \tag{3.135}$$

and

$$F = \int_{[t_0,t_{\mathrm{f}}]^2}\mathrm{d}t_1\mathrm{d}t_2\,\bar{\boldsymbol{v}}_{t_1}\cdot\frac{\mathsf{B}\,(\boldsymbol{\mathcal{X}}_{t_1}-\boldsymbol{\mathcal{X}}_{t_2},|t_{12}|)}{2\tau^2}\cdot\bar{\boldsymbol{v}}_{t_2} \tag{3.136}$$

In order to define the functional translation operator we observe that

$$\begin{aligned}\mathsf{G}\circ\boldsymbol{J}_{t_1} + \mathsf{R}\circ\bar{\boldsymbol{J}}_{t_1} &= \int_{t_0}^{t_{\mathrm{f}}}\mathrm{d}t_2 \\ \times&\begin{bmatrix}\mathsf{G}^{(qq)}(t_1,t_2,t_0)\cdot\boldsymbol{\jmath}_{t_2}^{(q)} + \mathsf{G}^{(qp)}(t_1,t_2,t_0)\cdot\boldsymbol{\jmath}_{t_2}^{(p)} + \mathsf{R}^{(qq)}(t_{12})\cdot\bar{\boldsymbol{\jmath}}_{t_2}^{(q)} + \mathsf{R}^{(qp)}(t_{12})\cdot\bar{\boldsymbol{\jmath}}_{t_2}^{(p)} \\ \mathsf{G}^{(pq)}(t_1,t_2,t_0)\cdot\boldsymbol{\jmath}_{t_2}^{(q)} + \mathsf{G}^{(pp)}(t_1,t_2,t_0)\cdot\boldsymbol{\jmath}_{t_2}^{(p)} + \mathsf{R}^{(pp)}(t_{12})\cdot\bar{\boldsymbol{\jmath}}_{t_2}^{(p)}\end{bmatrix}\end{aligned} \tag{3.137}$$

and

$$\mathsf{R}^{\dagger}\circ\boldsymbol{J}_{t_1} = \int_{t_0}^{t_{\mathrm{f}}}\mathrm{d}t_2\begin{bmatrix}\boldsymbol{\jmath}_{t_2}^{(q)}\cdot\mathsf{R}^{(qq)}(t_{21}) \\ \boldsymbol{\jmath}_{t_2}^{(q)}\cdot\mathsf{R}^{(qp)}(t_{21}) + \boldsymbol{\jmath}_{t_2}^{(p)}\cdot\mathsf{R}^{pp}(t_{21})\end{bmatrix} \tag{3.138}$$

so that we can write

$$\mathfrak{T} = \exp\left\{\int_{[t_{\mathrm{f}},t_0]} \mathrm{d}t\, \left[\left(\langle\boldsymbol{\chi}_t\rangle + \mathsf{G}\circ\boldsymbol{J}_t + \mathsf{R}\circ\bar{\boldsymbol{J}}_t\right)\cdot\frac{\delta}{\delta\boldsymbol{\Phi}_t} + \mathsf{R}^\dagger\circ\boldsymbol{J}_t\cdot\frac{\delta}{\delta\bar{\boldsymbol{\Phi}}_t}\right]\right\} \tag{3.139}$$

Finally the generator of Gaussian fluctuations is now

$$\mathfrak{O} = \int_{[t_{\mathrm{f}},t_0]^2} \mathrm{d}t_1\mathrm{d}t_2\, \left[\frac{\delta}{\delta\boldsymbol{\Phi}_{t_1}}\cdot\frac{\mathsf{G}}{2}\cdot\frac{\delta}{\delta\boldsymbol{\Phi}_{t_2}} + \frac{\delta}{\delta\boldsymbol{\Phi}_{t_1}}\cdot\mathsf{R}\cdot\frac{\delta}{\delta\bar{\boldsymbol{\Phi}}_{t_2}}\right] \tag{3.140}$$

With these conventions, we see that the tree level correction to the free energy

$$\begin{aligned} e^{\mathfrak{O}}F &= \frac{1}{2}\,\partial_{\boldsymbol{a}_1}\otimes\partial_{\boldsymbol{a}_2}|_{\boldsymbol{a}_1=\boldsymbol{a}_2=0} : e^{\mathfrak{O}}\int\frac{\mathrm{d}^d\boldsymbol{k}}{(2\,\pi)^d}\int_{[t_0,t_{\mathrm{f}}]^2}\mathrm{d}t_1\mathrm{d}t_2 \\ &\times\quad e^{\imath\,\boldsymbol{k}\cdot(\boldsymbol{\phi}^{(q)}_{t_1}-\boldsymbol{\phi}^{(q)}_{t_2})}\, e^{\sum_{i=1}^2\boldsymbol{a}_i\bar{\boldsymbol{\phi}}^{(p)}_{t_i}}\,\frac{\check{\mathsf{B}}}{\tau^2}(\boldsymbol{k},|t_{12}|) \end{aligned} \tag{3.141}$$

Upon introducing the currents

$$\boldsymbol{J}_t = \begin{bmatrix}\imath\,\boldsymbol{k}\,[\delta(t-t_1)-\delta(t-t_2)]\\ 0\end{bmatrix} \tag{3.142a}$$

$$\bar{\boldsymbol{J}}_t = \begin{bmatrix}0\\ \boldsymbol{a}_1\delta(t-t_1)+\boldsymbol{a}_2\,\delta(t-t_2)\end{bmatrix} \tag{3.142b}$$

we get into

$$\begin{aligned} e^{\mathfrak{O}}F = \frac{1}{2}\,\partial_{\boldsymbol{a}_1}\otimes\partial_{\boldsymbol{a}_2}|_{\boldsymbol{a}_1=\boldsymbol{a}_2=0} : \int\frac{\mathrm{d}^d\boldsymbol{k}}{(2\,\pi)^d}\int_{[t_0,t_{\mathrm{f}}]^2}\mathrm{d}t_1\mathrm{d}t_2 \\ \times e^{\imath\,\boldsymbol{k}\cdot(\boldsymbol{\phi}^{(q)}_{t_1}-\boldsymbol{\phi}^{(q)}_{t_2})-\frac{\tilde{G}^{(qq)}(t_1,t_2,t_0)\|\boldsymbol{k}\|^2}{2}}\, e^{\sum_{i=1}^2\boldsymbol{a}_i\cdot\bar{\boldsymbol{\phi}}^{(p)}_{t_i}+\imath\,\boldsymbol{k}\cdot[\boldsymbol{a}_2R^{(qp)}(t_{12})-\boldsymbol{a}_1R^{(qp)}(t_{21})]}\frac{\check{\mathsf{B}}}{\tau^2}(\boldsymbol{k},|t_{12}|) \end{aligned} \tag{3.143}$$

where

$$\begin{aligned} &\tilde{G}^{(qq)}(t_1,t_2,t_0) \\ &= G^{(qq)}(t_1,t_1,t_0)+G^{(qq)}(t_2,t_2,t_0)-G^{(qq)}(t_1,t_2,t_0)-G^{(qq)}(t_2,t_1,t_0) \\ &= 2\,D_0\,\tau\left(1-e^{-\frac{|t_{12}|}{\tau}}+e^{-\frac{t_{10}+t_{20}}{\tau}}-\frac{e^{-\frac{2t_{10}}{\tau}}+e^{-\frac{2t_{20}}{\tau}}}{2}+\frac{|t_{12}|}{\tau}\right) \end{aligned} \tag{3.144}$$

Upon evaluating the derivatives we get into

$$e^{\mathfrak{D}}F = \frac{1}{2}\int \frac{\mathrm{d}^d\boldsymbol{k}}{(2\,\pi)^d}\int_{[t_0,t_\mathrm{f}]^2}\mathrm{d}t_1\mathrm{d}t_2\, e^{\imath\,\boldsymbol{k}\cdot(\boldsymbol{\phi}^{(q)}_{t_1}-\boldsymbol{\phi}^{(q)}_{t_2})-\frac{\tilde{G}^{(qq)}(t_1,t_2,t_0)\|\boldsymbol{k}\|^2}{2}}$$
$$\times\left[\bar{\boldsymbol{\phi}}^{(p)}_{t_1}-\imath\,R^{(qp)}(t_{21})\boldsymbol{k}\right]\cdot\frac{\check{\mathsf{B}}}{\tau^2}(\boldsymbol{k},|t_{12}|)\cdot\left[\bar{\boldsymbol{\phi}}^{(p)}_{t_2}+\imath\,R^{(qp)}(t_{12})\boldsymbol{k}\right] \tag{3.145}$$

In order to derive the tree level contribution to the free energy we need to apply the translation operator to the expression above:

$$\begin{aligned}\mathfrak{T}e^{\mathfrak{D}}F|_{\boldsymbol{\Phi}=\bar{\boldsymbol{\Phi}}=0} &= \frac{1}{2}\int\frac{\mathrm{d}^d\boldsymbol{k}}{(2\,\pi)^d}\int_{[t_0,t_\mathrm{f}]^2}\mathrm{d}t_1\mathrm{d}t_2\\
&\times e^{\imath\,\boldsymbol{k}\cdot[\sum_{i=1}^2(-)^{i+1}[\langle\boldsymbol{\mathcal{X}}_{t_i}\rangle+G^{(qq)}\circ\boldsymbol{\jmath}^{(q)}_{t_i}+G^{(qp)}\circ\boldsymbol{\jmath}^{(p)}_{t_i}+R^{(qq)}\circ\bar{\boldsymbol{\jmath}}^{(q)}_{t_i}+R^{(qp)}\circ\bar{\boldsymbol{\jmath}}^{(p)}_{t_2}]-\frac{\tilde{G}^{(qq)}(t_1,t_2,t_0)\|\boldsymbol{k}\|^2}{2}}\\
&\times\left[R^{(qp)\dagger}\circ\boldsymbol{\jmath}^{(q)}_{t_1}+R^{(pp)}\circ\boldsymbol{\jmath}^{(p)}_{t_1}-\imath\,R^{(qp)}(t_{21})\boldsymbol{k}\right]\\
&\cdot\frac{\check{\mathsf{B}}}{\tau^2}(\boldsymbol{k},|t_{12}|)\cdot\left[R^{(qp)\dagger}\circ\boldsymbol{\jmath}^{(q)}_{t_2}+R^{(pp)}\circ\boldsymbol{\jmath}^{(p)}_{t_2}+\imath\,R^{(qp)}(t_{12})\boldsymbol{k}\right]\end{aligned} \tag{3.146}$$

3.D.4 Explicit espression for the diffusion constant at the leading order

The second cumulant is:

$$\begin{aligned}\left.\frac{\delta^2 W}{\delta\boldsymbol{\jmath}^{(q)}_{t_3}\cdot\delta\boldsymbol{\jmath}^{(q)}_{t_3}}\right|_{\boldsymbol{\jmath}_{\boldsymbol{t}}=\bar{\boldsymbol{\jmath}}_{\boldsymbol{t}}=0} &= G^{(qq)}(t_3,t_3,t_0)+\int\frac{\mathrm{d}^d\boldsymbol{k}}{(2\,\pi)^d}\\
&\times\left\{\int_{[t_0,t_\mathrm{f}]^2}\mathrm{d}t_1\mathrm{d}t_2\, e^{\imath\,\boldsymbol{k}\cdot\langle\boldsymbol{\mathcal{X}}_{t_1}-\boldsymbol{\mathcal{X}}_{t_2}\rangle-\frac{\tilde{G}^{(qq)}(t_1,t_2,t_0)\|\boldsymbol{k}\|^2}{2}}\,R^{(qp)\dagger}(t_{31})\,\mathrm{tr}\,\frac{\check{\mathsf{B}}}{\tau^2}(\boldsymbol{k},|t_{12}|)\,R^{(qp)\dagger}(t_{32})\right.\\
&+\int_{[t_0,t_\mathrm{f}]^2}\mathrm{d}t_1\mathrm{d}t_2\, e^{\imath\,\boldsymbol{k}\cdot\langle\boldsymbol{\mathcal{X}}_{t_1}-\boldsymbol{\mathcal{X}}_{t_2}\rangle-\frac{\tilde{G}^{(qq)}(t_1,t_2,t_0)\|\boldsymbol{k}\|^2}{2}}\,(\imath\,\boldsymbol{k})\cdot\frac{\check{\mathsf{B}}}{\tau^2}(\boldsymbol{k},|t_{12}|)\cdot(\imath\,\boldsymbol{k})\\
&\left.\times\left[G^{(qq)}(t_1,t_3)-G^{(qq)}(t_2,t_3)\right]\left[R^{(qp)\dagger}(t_{31})R^{(qp)}(t_{12})-R^{(qp)}(t_{21})R^{(qp)\dagger}(t_{32})\right]\right\}\end{aligned} \tag{3.147}$$

We notice that

$$\langle\boldsymbol{\mathcal{X}}_{t_1}-\boldsymbol{\mathcal{X}}_{t_2}\rangle=\boldsymbol{v}_{t_0}\tau\,(e^{-\frac{t_{20}}{\tau}}-e^{-\frac{t_{10}}{\tau}})+\boldsymbol{u}_0\,[t_{12}+\tau\,(e^{-\frac{t_{20}}{\tau}}-e^{-\frac{t_{10}}{\tau}})] \tag{3.148}$$

hence the correlation depends in principle of the initial momentum average although memory of it is exponentially lost, as already proven in Prop. 3.2.1. We also notice that for an incompressible flow (the limit we are interested in), the last addend in (3.147) cancels out. If we also consider a zero-mean flow, we end up with the same first-order expression 3.16 for the eddy diffusivity

as in the parallel flow, which holds for any β. This means that a further perturbation expansion in the neighbourhood of $\beta = 1$ would give some non-zero result at least starting from the next-to-leading order of this theory with respect to the Brownian trajectories. That would be indeed the order where the geometry of the flow plays an active role in determining the trajectories.

Conclusions

In this PhD thesis we have investigated general large-scale properties of particle transport. In particular, herein we have dedicated the treatment to those processes to which Central Limit Theorem applies and the corresponding large-scale dynamics consists of a Gaussian random process. In these cases, standard advection/diffusion equation describes correctly the large-scale evolution of the probability distribution function of the particles - or, equivalently, their concentration field. Such a dynamics is then completely identified by an effective diffusivity, which is a tensor field in general and enters into the effective advection/diffusion equation. Such a tensor field is called eddy-diffusivity.

To study the probabilistic behaviour of several stochastic systems typically including a chaotic flow plus a possible white noise contribution, we have exploited both numerical and analytic methods. The former were used preliminarily in Chapter 1 to confute a perturbative result in literature [25], about the possibility of having a non-Gaussian large-scale regime which would give rise to an infinite eddy-diffusivity tensor. The two main ingredients considered in that analysis were the inertia of particles and the shape of the flow spectrum in the infra-red zone. This was of potential interest for applications because that region of the spectrum has not universal behaviour. It is indeed affected by the boundary presence and the external forces, contrarily to sufficiently-small-scale turbulence [58].

As for the numerical method, it consisted of measuring eddy-diffusivity in Lagrangian simulations of a large number of particles in a flow whose statistical properties (mean value, correlation functions, stationarity, homogeneity,...) were set *a priori*, thanks to suitable Fourier analysis along with stochastic methods which were explained in Chapter 1. This gave us a twofold advantage. Firstly, having a full control on the statistical behaviour of our system allowed us to be sure that any result was totally genuine, rather than a consequence of too short a spectral range such as the -5/3 range one usually obtains in DNS of Navier-Stokes equations at high Reynolds number. Secondly, we were allowed to construct an arbitrarily shape of the infrared spectrum.

This numerical method was afterwards used to mimic small scall turbulence properties according to theory of ideal turbulence [58, 67]. On such a

model, we were able to assess the reliability of some perturbative expressions we had achieved by means of multiple-scale methods. In this manner, we obtained explicit effective expressions for eddy-diffusivity tensor fields and effective advective velocity fields to insert into a possible effective transport equation. This problem was of interest because in pollutant transport applications for Oceanography and Atmosphere Physics the unresolved small-scale flow still gives a contribution to the mixing. Thanks to a comparison between numerical measures in our effective model and the "exact" fully-resolved field, those expressions turned out to be more accurate than other possible closures, so long as the small-scales are incompressible, ergodic and in general fulfill the several properties of ideal turbulence.

In Chapter 3 we leveraged analytic methods to obtain exact expression of the eddy diffusivity for inertial particles. Such a result let us give an analytic explaination for the numerical results of Chapter 1. To do that, first we exploited the class of parallel flows, which originates an exactly solvable problem for inertial particle diffusion. This model could have application for example in microchannel mixing. Indeed, there flow velocity is small and typically width of the system is $100-1000\,\mu m$. Reynolds and Pèclet numbers are thus quite low, and molecular diffusivity becomes important for mixing process. On the other hand, suitable polymer solution can bring about chaotic and fully mixing flows even at arbitrarily small Reynolds numbers [73]. This system can be modelled to a first approximation with a random, statistically stationary and homogenous parallel flow.

Successively, we showed those results about the role of inertia are useful in more general application. Namely, they apply as a leading order expansion every time molecular diffusivity plays an important role, no matter the form of the carrier flow is. Another valid application is to parallel flows plus possible small perturbations (which could represent instabilities in transition to turbulence). Systems of inertial particles in such flows eventually turned out to be equivalent to tracer particles in the same flow plus coloured white noise [70].

Finally, we proved the generality of Taylor's formula from 1921, by demonstrating that it turns out to be applicable to inertial particles everytime the conditions for the simplified Maxey-Riley equation holds true. The consequence of this fact could be potentially of interest in both numerical and perturbation applications, because every technique which has been applied for tracer particles so far is also applicable to inertial particles. The result is an exact one when particles are much denser with respect to the fluid , i. e. $\beta \sim 0$, and everytime $\mathrm{St}\beta \ll 1$ - typically $\lesssim 10^{-3}$. In the latter case, neglecting Basset term in chaotic and fully mixing flows term does not seem to entail such a great change in the trend of the values of eddy diffusivity, although these values are still different.

All of the above results about tracers and inertial particles therefore represent analytical properties. They were corroborated numerically, and

help understand the behaviour of such physical systems in the situations where chaotic dynamics is statistically equivalent to an ergodic stochastic flow plus white noise.

To conclude this section, we briefly list some possible perspectives one could try to carry on about these projects:

- evaluating the performance of the closure for tracer pre-asymptotic transport in real cases, such as RaDAR data, RANS numerical models in ocean and atmosphere, whenever the small-scale flow can be considered ideally turbulent and incompressible;
- evaluating a new closure for compressible cases, by exploiting the first order perturbation results in the Appendix of Chapter 3, and then assessing its performance in a compressible 2D flow such as some surface oceanographic data [74];
- computing a new exact expression for inertial particles fulfilling the complete Maxey-Riley equations in parallel flows; providing a generalized Taylor formula for inertial particle in the complete equations, including Basset term;
- evaluating a new closure for inertial particles.

Bibliography

[1] K. Pearson, The Problem of the Random Walk. *Nature*, **72** (1865), 294 (1905)

[2] G. N. Watson, Three Triple Integrals. *Quart. J. Math., Oxford Ser. 2* **10**, 266-276 (1939).

[3] Ø. Hodnebrog, G. Myhre and B. H. Samset, How shorter black carbon lifetime alters its climate effect. *Nature Communications* **5**, 5065 (2014).

[4] A. J. Majda, I. Timofeyev, E. Vanden Eijnden, A Mathematical Framework for Stochastic Climate Models. *Communications on Pure and Applied Mathematics* **Vol. LIV** , 0891–0974 (2001)

[5] J. Klafter and I. M. Sokolov, Anomalous diffusion spreads its wings. *Physics World* **18** (8), 29–32 (2001)

[6] T. H. Solomon, E. R. Weeks, H. L. Swinney, Observation of anomalous diffusion and Lévy flights in a two-dimensional rotating flow. *Phys. Rev. Lett.*,**71**, 3975 (1993)

[7] H. Scher and E. Montroll, Anomalous transit-time dispersion in amorphous solids. *Physical Review B*, **12**, 2455 (1975)

[8] P.M. Lovalenti, and J.F. Brady, The hydrodynamic force on a rigid particle undergoing arbitrary time-dependent motion at small Reynolds number. *Journal of Fluid Mechanics*, **256**, 561–605 (1993)

[9] J. M. Burgers, On the motion of small particles of elongated form suspended in a viscous fluid (1938). *Selected Papers of J. M. Burgers edited by F. T. M. Nieuwstadt and J. A. Steketee*, 209 , Springer(1995)

[10] F. Langouche, D. Roekaerts, E. Tirapegui, Functional Integration and Semiclassical Expansions. Springer (1982)

[11] F. C. Klebaner, Introduction to stochastic calculus with applications . Imperial College Press (2005)

[12] G. Folland, Real Analysis: Modern Techniques and Their Applications, 2nd ed., Wiley (1999)

[13] R. van Handel, Stochastic Calculus, Filtering, and Stochastic Control. Lecture Notes (2007)

[14] L. Biferale, A. Crisanti, M. Vergassola and A. Vulpiani, Eddy-diffusivity in scalar transport. *Phys. Fluids* **7**, 2725 (1995).

[15] A. Mazzino, Effective correlation times in turbulent scalar transport. *Phys. Rev.* E **56**, 5500 (1997).

[16] P. Castiglione, A. Crisanti, A. Mazzino, M. Vergassola and A. Vulpiani, Resonant enhanced diffusion in time-dependent flow. *J. Phys.* A **31**, 7197 (1998).

[17] A. Mazzino, S. Musacchio and A. Vulpiani, Multiple-scale analysis and renormalization for preasymptotic scalar transport. *Phys. Rev.* E **71**, 011113 (2005).

[18] R. H. Kraichnan, Eddy viscosity and diffusivity: exact formulas and approximations. *Complex Syst.* **1**, 805 (1987).

[19] P. Castiglione, A. Mazzino, P. Muratore–Ginanneschi and A. Vulpiani, On strong anomalous diffusion. *Physica* D **134**, 75 (1999).

[20] M. Avellaneda and A. Majda, Superdiffusion in nearly stratified flows. *J. Stat. Phys.* **69**, 689 (1992).

[21] D. del Castillo Negrete, Asymmetric transport and non-Gaussian statistics of passive scalars in vortices in shear. *Phys. Fluids* **10**, 576 (1998).

[22] T. H. Solomon, E. R. Weeks and H. L. Swinney, Chaotic advection in a two-dimensional flow: Lévy flights and anomalous diffusion. *Physica* D **76**, 70 (1994).

[23] K. H. Andersen, P. Castiglione, A. Mazzino and A. Vulpiani, Simple stochastic models showing strong anomalous diffusion. *Eur. Phys. J.* B **18**, 447 (2000).

[24] G.I. Taylor, Diffusion by continuous movements. *Proc. Lond. Math. Soc. Ser. 2* **20**, 196 (1921).

[25] M. Martins Afonso, Anomalous diffusion for inertial particles under gravity in parallel flows. *Phys. Rev.* E **89**, 063021 (2014).

[26] M. Martins Afonso, A. Mazzino and P. Muratore-Ginanneschi, Eddy diffusivities for inertial particles under gravity. *J. Fluid Mech.* **694**, 426 (2012).

[27] G. A. Pavliotis and A. M. Stuart, Periodic homogenization for inertial particles, *Physica* D **204**, 161 (2005).

[28] M. Holmes, *Introduction to Perturbation Methods*, Springer, 2013.

[29] M. Martins Afonso, The terminal velocity of sedimenting particles in a flowing fluid. *J. Phys.* A **41**, 385501 (2008).

[30] M. R. Maxey and J. J. Riley, Equation of motion for a small rigid sphere in a nonuniform flow. *Phys. Fluids* **26**, 883 (1983).

[31] R. Gatignol, The Faxén formulae for a rigid particle in an unsteady non-uniform Stokes flow. *J. Méc. Théor. Appl.* **1**, 143 (1983).

[32] M. W. Reeks, The relationship between Brownian motion and the random motion of small particles in a turbulent flow. *Phys. Fluids* **31**, 1314 (1988).

[33] J. Bec, Fractal clustering of inertial particles in random flows. *Phys. Fluids* **15**, L81 (2003).

[34] L. Palatella, F. Bignami, F. Falcini, G. Lacorata, A. S. Lanotte and R. Santoleri, Lagrangian simulations and interannual variability of anchovy egg and larva dispersal in the Sicily Channel. *J. Geophys. Res.: Oceans* **119**, 1306 (2014).

[35] G. Lacorata, A. Mazzino and U. Rizza, 3D chaotic model for subgrid turbulent dispersion in large eddy simulations. *J. Atmos. Sci.* **65**, 2389 (2008).

[36] G. Gioia, G. Lacorata, E.P. Marques, A. Mazzino and U. Rizza, Richardson's law in large-eddy simulations of boundary-layer flows. *Bound. Layer Meteorol.* **113**, 187 (2004).

[37] R. L. Honeycutt, Stochastic Runge-Kutta algorithms. I. White noise. *Phys. Rev.* A **45**, 600 (1992).

[38] Z. Warhaft, Passive Scalars in Turbulent Flows. *Annu. Rev. Fluid Mech.* **73**, 203–240 (2000).

[39] M. Germano, U., Piomelli, P. Moin,W. H. Cabot, A dynamic subgrid-scale eddy viscosity model. *Physics of Fluids A* **7**, 1760–1765 (1991).

[40] B. Dubrulle, U. Frisch, Eddy viscosity of parity-invariant flow. *Phys. Rev. A*, **43**, 5355–5364 (1991).

[41] R. Mauri, Heat and mass transport in nonhomogeneous random velocity fields. *Phys. Rev. E*, **68**, 066306 (2003)

[42] G. Boffetta, E. Ecke, Robert, Two-dimensional turbulence. *Annual Review of Fluid Mechanics*, **44** (1), (427–451) (2012)

[43] A. J. Majda and P.R. Kramer, Simplified models for turbulent diffusion: Theory, numerical modelling, and physical phenomena. *Phys. Rep.* , **314**, 237–574 (1999)

[44] G. Falkovich and K. Gawedzki and M. Vergassola, Particles and fields in fluid turbulence. *Rev. Mod. Phys.* , **73**, 913–975 (2001)

[45] N.V. Antonov and Y. Honkonen and A. Mazzino and P. Muratore-Ginanneschi, Manifestation of anisotropy persistence in the hierarchies of magnetohydrodynamical scaling exponents. *Phys. Rev. E*, **62**, R5891–R5894 (2000)

[46] L.Ts. Adzhemyan and N.V. Antonov and A. Mazzino and P. Muratore-Ginanneschi and A.V. Runov, Pressure and intermittency in passive vector turbulence. *Europhys. Lett.* **55**, 801–806 (2001)

[47] G.A. Pavliotis and A.M. Stuart, Multiscale Methods: Averaging and Homogenization, Springer (2007)

[48] A. Bensoussan and J.-L. Lions and G. Papanicolaou, Asymptotic Analysis for Periodic Structures, North-Holland (1978)

[49] M. Vergassola and M. Avellaneda, Scalar transport in compressible flow. *Physica D*, **106**, (148-166) (1997)

[50] M. Cencini and A. Mazzino and S. Musacchio and A. Vulpiani, Large-scale effects on meso-scale modeling for scalar transport. *Physica D* **220** , 146–156, (2006)

[51] A. Crisanti, M. Falcioni, G. Paladin,A. Vulpiani, Lagrangian chaos: Transport, mixing and diffusion in fluids. *Il Nuovo Cimento* **14** (12), 1–80 (1991)

[52] J. C. H. Fung, J. C. R. Hunt, N. A. Malik, R.J. Perkins, Kinematic simulation of homogeneous turbulence by unsteady random fourier modes. *J. Fluid Mech.* **236**, 281–318 (1992)

[53] G. A. Pavliotis and P.R. Kramer, Homogenized transport by a spatiotemporal mean flow with small-scale periodic fluctuations. *Proc. of the IV international conference on dynamical systems and differential equations*, 1–8 (2002)

[54] IPCC: Fifth assessment report – the physical science basis, available at: http://www.ipcc.ch (last access: 14 December 2015), (2013)

[55] P. G. Saffman, On the effect of the molecular diffusivity in turbulent diffusion, *J. Fluid Mech.* **8**, 273-283 (1960)

[56] L.M. Pismen and A. Nir, On the motion of suspended particles in stationary homogeneous turbulence *J. Fluid Mech.* **84**, 193-206 (1978)

[57] U. Frisch, Lecture on turbulence and lattice gas hydrodynamics. In Lecture Notes, NCAR- GTP Summer School June 1987 (ed. J. R. Herring & J. C. McWilliams), 219-371. World Scientific. (1987)

[58] U. Frisch, Turbulence. Cambridge Univ. Press. (1995)

[59] L. C. Biedenharn, J. D. Louck, P. A. Carruthers, Angular momentum in quantum physics: theory and application. Reading, MA: Addison-Wesley (1981)

[60] C. Denjean, F. Cassola, A. Mazzino, S. Triquet, S. Chevaillier, N. Grand, T. Bourrianne, G. Momboisse, K. Sellegri, A. Schwarzenbock, E. Freney, M. Mallet and P. Formenti, Size distribution and optical properties of mineral dust aerosols transported in the western Mediterranean. *Atmos. Chem. Phys.* **16**, 1081-1104 (2016).

[61] P. Tabeling, *Introduction to Microfluidics* (Oxford University Press, 2005).

[62] A.S. Monin and A.M. Yaglom, Statistical Fluid Mechanics. Edited by J. Lumley, MIT Press. Cambridge, Mass (1975)

[63] M.R. Maxey and J.J. Riley, Equation of motion for a small rigid sphere in a nonuniform flow. *Phys. Fluids* **26**, 883–889 (1983)

[64] A. Mazzino and M. Vergassola, Interference between turbulent and molecular diffusion, *Europhys. Lett. 37*, 535-540, 1997.

[65] S. Boi, M. Martins Afonso, and A. Mazzino, Anomalous diffusion of inertial particles in random parallel flows: theory and numerics face to face, *J. Stat. Mech.: Theory and Experiment 10*, P10023, 2015.

[66] N. V. Antonov and N. M. Gulitskiy,, Passive advection of a vector field: Anisotropy, finite correlation time, exact solution, and logarithmic corrections to ordinary scaling, *Phys. Rev. E 92*, 043018, 2015.

[67] Y. Kaneda, T. Ishihara and K. Gotoh, Taylor expansions in powers of time of Lagrangian and Eulerian two-point two-time velocity correlations in turbulence, *Phys. Fluids 11*, 2154-2166, 1999.

[68] S. Boi, A. Mazzino and G. Lacorata, Explicit expressions for eddy-diffusivity fields and effective large-scale advec- tion in turbulent transport, *J. Fluid Mech. 795*, 524-548, 2016.

[69] G. K. Batchelor, and A. A. Townsend, Decay of Turbulence in the Final Period, *of the Royal Society A 194,* 527-543, 1948.

[70] A. Mazzino and P. Castiglione, Interference phenomena in scalar transport induced by a noise finite correlation time, *Europhys. Lett.* **45**, 476-481 (1999)

[71] A. N. Vasilev, The Field Theoretic Renormalization Group in Critical Behavior Theory and Stochastic Dynamics, Chapman & Hall/CRC (2004)

[72] O.A. Druzhinin, L.A. Ostrovsky, The influence of Basset force on particle dynamics in two-dimensional flows, *Physica D* **76**, 34-43 (1994)

[73] S. Boi, A.Mazzino, J. O. Pralits, Minimal model for zero-inertia instabilities in shear-dominated non- newtonian flows. *Physical Review E*, **88**, 033007 (2013)

[74] M. Gatimu Magaldi, T. W. N. Haine, Hydrostatic and non-hydrostatic simulations of dense waters cascading off a shelf: The East Greenland case. *Deep Sea Research Part I: Oceanographic Research Papers* **96**, 89-104 (2015)